Systematic Entomology

Systematic Entomology (2009), **34**, 346–397

Monophyly of Euaesthetinae (Coleoptera: Staphylinidae): phylogenetic evidence from adults and larvae, review of austral genera, and new larval descriptions

DAVE J. CLARKE[1,2] and VASILY V. GREBENNIKOV[3,4]

[1]Department of Zoology, The Field Museum of Natural History, Chicago, Illinois, U.S.A., [2]Department of Biological Sciences, University of Illinois, Chicago, llinois, U.S.A., [3]Entomology Research Laboratory, Ottawa Plant Laboratories, Canadian Food Inspection Agency, Ottawa, Ontario, Canada and [4]Department of Entomology, Institut für Spezielle Zoologie und Evolutionsbiologie, Friedrich-Schiller-Universität Jena, Jena, Germany

Abstract. We develop a morphological dataset for the rove beetle subfamily Euaesthetinae comprising 167 morphological characters (135 adult and 32 larval) scored from 30 terminal taxa including 25 ingroup terminals (from subfamilies Euaesthetinae and Steninae) and five outgroups. Four maximum parsimony analyses using different sets of terminals and character sets were run to test the monophyly of (1) Euaesthetinae, (2) Steninae, (3) Euaesthetinae + Steninae, (4) euaesthetine tribes Austroesthetini, Alzadaesthetini, Euaesthetini, Fenderiini and Stenaesthetini, and (5) the ten currently known austral endemic genera together. Analyses of adult and larval character sets separately and in combination recovered the monophyly of Euaesthetinae, Steninae, and both subfamilies together, with strong support. Analysis of 13 ingroup terminals for which complete data were available suggests that monophyly of Euaesthetinae is supported by 19 synapomorphies (13 adult, six larval), of Steninae by 23 synapomorphies (14 adult, nine larval), and of both subfamilies together by 24 synapomorphies (21 adult, three larval). Within Euaesthetinae, only the tribe Stenaesthetini was recovered as monophyletic based on adult characters, and in no analyses were the ten austral endemic genera recovered as a monophyletic group. Phylogenetic relationships among euaesthetine genera were weakly supported, although analyses including adult characters supported monophyly of *Octavius* and *Protopristus* separately, and of *Octavius* + *Protopristus*, *Austroesthetus* + *Chilioesthetus* and *Edaphus* + *Euaesthetus*. Steninae may include a third genus comprising two undescribed species probably possessing a 'stick–capture' method of prey capture, similar to that in *Stenus*. These two species formed a strongly supported clade recovered as the sister group of *Stenus* based on adult characters. Diagnoses and a key to adults are provided for the 15 euaesthetine genera currently known from the austral region (Australia, New Zealand, South Africa and southern South America). Euaesthetine larvae previously were known only for *Euaesthetus*, and we describe the larvae of nine more genera and provide the first larval identification key for genera of Euaesthetinae.

Correspondence: Dave J. Clarke, Department of Zoology, The Field Museum of Natural History, 1400 S Lake Shore Drive, Chicago, IL 60605, U.S.A. E-mail: dclarke@fieldmuseum.org

Introduction

The enigmatic rove beetle subfamily Euaesthetinae comprises a morphologically diverse assemblage of poorly known, primarily litter- and soil-dwelling predators, all less than 4 mm in length (Fig. 1). Herman (2001) reported 724 species in 26 genera for Euaesthetinae, but since the publication of that catalogue several new (but as yet undescribed) genera have been identified and many new species described (resulting in 762 species in Thayer, 2005). Compared with some of the larger radiations within Staphylinidae, Euaesthetinae is a rather small group (cf. Aleocharinae, 12 851 spp.; Pselaphinae, 9110 spp.; Staphylininae, 6876 spp.; Paederinae, 6101 spp.; Thayer, 2005). However, the extant global species diversity probably is vastly greater than currently known, given their cryptic habits, and the drastically under-sampled south-temperate and tropical rainforests. The rate of new species descriptions is high, particularly in the large and nearly worldwide genera *Edaphus* Motschulsky (e.g. Puthz, 2006a, b) and *Octavius* Fauvel (e.g. Puthz, 2006c), which together contain more than three-quarters of the total described species diversity. Although worldwide in distribution, euaesthetines are encountered in the field rarely because collecting requires specialized techniques, and almost no biological or natural history information is available. This combination of features presents certain challenges to the study of Euaesthetinae, and a lack of monographic and synthetic work on regional faunas, combined with scattered random species descriptions, renders accurate identification extremely difficult. More synthetic taxonomic work on these beetles is badly needed to improve the scope for ecological, phylogenetic and biogeographical studies, to which Euaesthetinae would otherwise be well suited.

Euaesthetinae are placed in the Staphylinine group of Lawrence & Newton (1982), and usually have been considered to be closely related to the subfamily Steninae. In describing *Stenaesthetus*, Sharp (1874) recognized this resemblance and considered his new genus 'intermediate in appearance between *Euaesthetus* Gravenhorst, 1806 and *Stenus* Latreille, 1797'. Steninae is represented by the two genera *Stenus* and *Dianous* Leach and comprises a major staphylinid radiation of more than 2246 species (Thayer, 2005), and by comparison to Euaesthetinae is much better known, largely because of the significant alpha taxonomic efforts of Volker Puthz (with more than 300 papers treating the taxonomy of Steninae, for example Puthz, 1970, 1971, 1972, 2000, 2006d), and of the many studies of the ecomorphological diversity and feeding methods of these beetles (e.g. Jenkins, 1960; Betz, 1996, 1998, 1999, 2002, 2003; Kölsch & Betz, 1998). Moreover, larvae of both genera are known (e.g. Kasule, 1966, *Dianous* in key; Welch, 1966; Weinreich, 1968), and the egg, larval instars and pupae of some *Stenus* species have been described (Weinreich, 1968).

Historically, the relationship of Euaesthetinae to other staphylinid subfamilies has been unclear. One hypothesis advocated by several earlier authors (e.g. Crowson, 1950; Kasule, 1966) was that Euaesthetinae, either separate from or together with Steninae, were related closely to Pselaphidae (now Pselaphinae), another group of litter-dwelling staphylinids, to which some euaesthetines look remarkably similar (e.g. *Edaphus*, *Tamotus* Schaufuss). This relationship was based on many similarities among both adults and larvae of the three subfamilies, including the presence of clubbed antennae in the adults and the external position of the larval antennal sensory appendage. In fact, Crowson (1950, 1960, 1967) considered Steninae (including Euaesthetinae) to be a 'primitive' member of Staphylinidae from

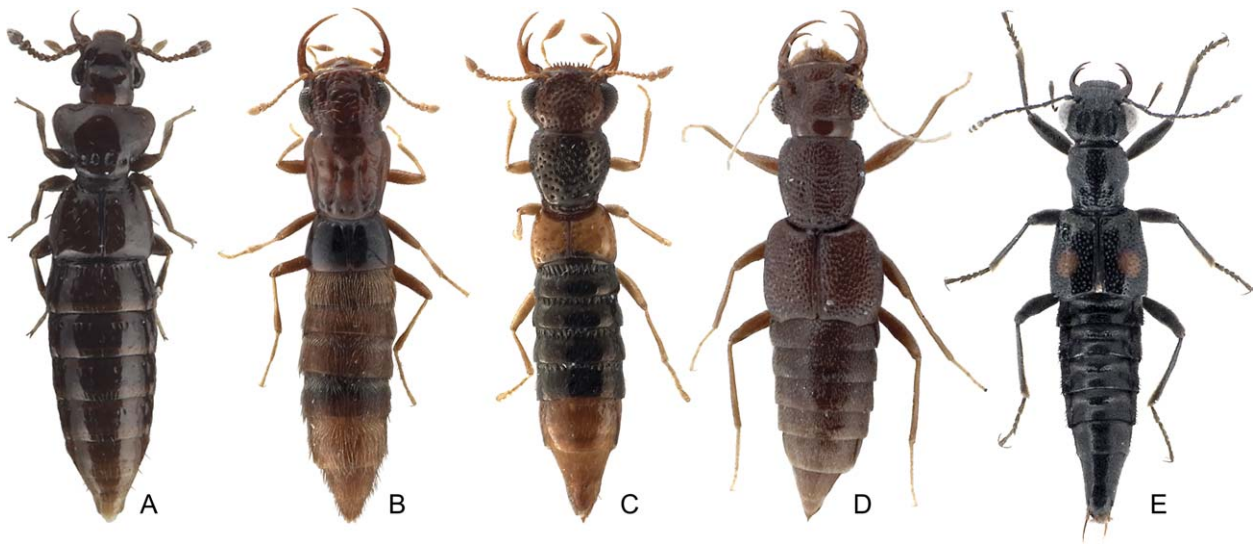

Fig. 1. Euaesthetinae and Steninae adult habitus photos: (A) *Edaphus* sp. (2.0 mm); (B) *Agnosthaetus* sp. (3.3 mm); (C) *Alzadaesthetus furcillatus* Sáiz (3.1 mm); (D) *Stenaesthetus* sp. (2.8 mm); (E) *Dianous nitidulus* LeConte (5.5 mm).

which Pselaphidae could have been derived, and even suggested that the two subfamilies should be transferred to Pselaphidae (see Kasule, 1966: 277). The first explicit phylogenetic hypothesis was advanced by Naomi (1985), who placed Euaesthetinae as the sister group of a clade comprising Pselaphidae (-inae) and Leptotyphlinae, but excluding Steninae. The hypothesis was based on 20 putative synapomorphies, but most of these were rejected as invalid by Newton & Thayer (1988). Pselaphinae later were transferred to the distant Omaliine group (Newton & Thayer, 1995), and many resemblances between Euaesthetinae and Pselaphinae thereby were interpreted as convergences related to a shared leaf litter habitat and mode of predation.

The major problem addressed here is the relationship between the subfamilies Euaesthetinae and Steninae. The monophyly of these two subfamilies together is supported by the unique falciform mandibles and a single pair of parasclerites in the adult, the fusion of the submentum to the gular area in the larvae (Thayer, 2005), and many other synapomorphies identified in Leschen & Newton's (2003) study. Although never tested with an explicit phylogeny, Steninae is supported as monophyletic by several adult and larval putative apomorphies (Hansen, 1997; Thayer, 2005). The monophyly of Euaesthetinae, however, has been doubted: in the only regional multi-genus monograph for the subfamily to date, Orousset (1988) discussed the lack of diagnostic characters for Euaesthetinae but listed the overall small size of these beetles and reductions in tarsomere formula (5-5-5 to 5-5-4, 4-4-4, 3-3-3) and in the number of antennomeres in some (11 to 10 to 9) as general characters of the subfamily. Hansen (1997) suggested the 'dentate' anterior labral edge as possibly the only known autapomorphy of the subfamily, and Naomi (1985) stated a reduced number of metatarsomeres as being the only 'autapomorphic character condition'. However, some genera have a smooth anterior labral edge whereas others have five-segmented tarsi, leaving Euaesthetinae with no known synapomorphies (Thayer, 2005). In Leschen & Newton's (2003) phylogenetic analysis of both adult and larval characters, the monophyly of Steninae + Euaesthetinae was strongly supported, whereas the monophyly of Euaesthetinae was supported only weakly, further indicating the lack of character support and probable paraphyly of Euaesthetinae with respect to Steninae. Based on their results they suggested a case for synonymy of Euaesthetinae with Steninae, but because of the limited euaesthetine taxon sample in their study (*Agnosthaetus* Bernhauer, *Euaesthetus*, *Octavius*) they deferred any taxonomic action.

Further compounding the Euaesthetinae–Steninae problem are the poorly understood relationships among euaesthetine genera (Hansen, 1997). According to Leschen & Newton (2003), the subfamily comprises several distinct generic groupings that conform poorly to the existing suprageneric classification comprising the six tribes Alzadaesthetini, Austroesthetini, Euaesthetini, Fenderiini, Nordenskioldiini and Stenaesthetini (Scheerpeltz, 1974). This system has been criticized as artificial (Newton, 1985; Hansen, 1997) because it was based only on tarsal formula and the presence/absence of a 'margined' abdomen and wings, and because originally it did not include all genera (Newton & Thayer, 1992; Lawrence & Newton, 1995).

At least three significant obstacles have prevented refinement of the current suprageneric classification and hindered progress in understanding the phylogeny of Euaesthetinae and its relationship to Steninae. (1) Most currently valid described genera are very poorly characterized in the adult stage, particularly austral (south-temperate areas: Australia, New Zealand, South Africa and southern South America) endemics, which amount to about one-third of the genera of the subfamily. In addition, several genera do not belong in Euaesthetinae – or even in the Stenine group (sensu Hansen, 1997). (2) No review of generic-level taxa or a broad subfamily-wide survey of adult morphological diversity exists to serve as a knowledge base from which future comparative studies may progress. (3) Knowledge of euaesthetine larvae lags far behind that of adults, and this is a particularly acute case of the more general problem of poorly known immature stages in Staphylinidae (see Newton, 1990a). The only euaesthetine genus known in the larval stage is *Euaesthetus* (Kasule, 1966; Newton, 1990b), but larval characters provide highly informative phylogenetic data (see references in Solodovnikov, 2007) and so descriptions and comprehensive studies of euaesthetine larvae are imperative.

Here we aim to improve our understanding of euaesthetine systematics by providing (1) the first adult morphological character survey, (2) diagnostic descriptions and an identification key for adults of all euaesthetine genera known from the south-temperate region, and (3) the first larval morphological character survey, diagnostic descriptions and an identification key for larvae of 11 euaesthetine genera (plus one of unknown generic status), complete with line illustrations and colour plates. Based on this accumulated morphological information we extend Leschen & Newton's (2003) study and carry out a phylogenetic analysis of Euaesthetinae and Steninae using much broader taxon and character sampling to (1) test the monophyly of Euaesthetinae and identify potential synapomorphies of the subfamily, (2) test the monophyly of Steninae and Euaesthetinae + Steninae, (3) test the monophyly of five of the six euaesthetine tribes, (4) test Newton's (1985) hypothesis that 'all of the austral genera may be more nearly related to one another than to the Holarctic and tropical genera that they are often placed near', and (5) test the monophyly of several genera and some informal generic groupings previously proposed by Newton (1985). We test the monophyly of, and determine the phylogenetic placement of, two undescribed Australian species probably representing an undescribed genus hitherto considered to belong in Euaesthetinae, but which may be a third genus for the subfamily Steninae (Leschen & Newton, 2003; Betz & Kölsch, 2004), and determine the phylogenetic placement of unidentified larvae associated geographically with specimens of this taxon.

Materials and methods

Specimen preparation and examination

Adults. Dry-mounted preparations, alcohol-preserved specimens, and disarticulated or whole slide-mounted specimens were examined under compound and stereoscopic microscopes. Most slide-mounted specimens were prepared and identified by A. Newton, Field Museum of Natural History (FMNH). In addition to standard specimen examination techniques we examined one to several specimens of each taxon under a scanning electron microscope (SEM; LEO EVO 60). Specimens used for SEM study were either alcohol-preserved or dry-mounted. Before being mounted on stubs, specimens were soaked in 2% hydrogen peroxide solution for several hours, sometimes overnight, and placed in an ultrasonic cleaner. Several iterations of soaking and agitation improved specimen cleanliness, but in some cases we could not clean specimens adequately by this method. We tried soaking specimens briefly (1–2 min) in warm KOH solution, which always cleaned specimens perfectly but tended to rupture delicate membranous structures and distort cuticle. Cleaned specimens were transferred to 70% EtOH, followed by 100% EtOH, and transferred to stubs straight from alcohol. Specimens were left to air-dry before being coated with gold and stored long-term in a desiccator. SEM images were taken of all body regions and one of us (DJC) maintains an expanding database of SEM images for Euaesthetinae and other Staphylinidae. Images of whole beetles (Fig. 1) were taken on a Microptics ML Macro XLT digital imaging system. All adult material examined in this study is housed in FMNH, unless indicated otherwise.

Larvae. No Euaesthetinae larvae examined here were reared from adults in the laboratory; all were field-collected, frequently in association with adults, and identified tentatively by A.F. Newton and M.K. Thayer (FMNH) based on the combination of larval morphological characters and the association of larvae with adults. Identifying larvae to species proved difficult, and in most cases the identification is restricted to genus. Larvae stored in 70% ethanol were disarticulated, macerated in hot KOH solution, and mounted in Euparal on microscope slides. Details of larval morphology were observed with a compound microscope under magnification 50–900×, and the morphological drawings were made with the aid of an attached drawing tube. Pencil drawings were scanned and converted to vector files and arranged on plates in the graphical editor program CorelDraw. Larval morphological terms are those explained in Lawrence (1991) with some subsequent modifications (Solodovnikov & Newton, 2005).

Larvae of 11 genera of Euaesthetinae, representing all but one (Nordenskioldiini) of the six currently recognized tribes (Newton & Thayer, 1992), and of the two genera currently recognized of Steninae (*Dianous* and *Stenus*) were available for this study. Larvae of the genera *Edaphosoma* Scheerpeltz and *Nordenskioldia* Sahlberg (Nordenskioldiini) are not known. For nine of the euaesthetine genera, only one species per genus was available in the larval stage; two species of *Octavius* Fauvel were available. One species of an undetermined genus was also available.

Some limitations of our larval study should be noted. Mounting in Euparal slightly deforms the three-dimensional body structure, and it was impossible to observe all details in all specimens examined. However, the characters employed in the description of the Euaesthetinae larvae appear correct for all examined larvae based on the presence of homologous structures in related species. Furthermore, some differences in the presence/absence of small sensilla might be observed on the drawings of the larval heads (Figs 5–8). These differences may be artifacts of the relatively small size of the larvae, which may have resulted in some minute structures being overlooked. In some cases it was impossible to be sure about the number of stemmata, and therefore only two alternative states were noted for each genus in the diagnostic descriptions: either all six stemmata are present and fully developed, or stemmata are reduced in either size or number.

We did not attempt to determine the larval instar in the material available for our study. In staphylinids, certain characters differ between larval instars, particularly between first and second instars, such as the incomplete chaetotaxic patterns and the presence of egg-bursting or -hatching structures in first instars (Ashe & Watrous, 1984). However, we expect that our data would be unaffected by a mix of instars among specimens as we coded no larval chaetotaxic characters, and, judging by the lack of egg-bursting structures from larvae we studied, none appeared to be in the first instar (except possibly *Nothoesthetus* Saiz). Instead we focused on cuticular characters primarily from the head capsule, labrum, mandibles, maxillary mala, labium and urogomphi. Steel (1970) described these structures as being more or less constant among different omaliine larval instars, and we expect them to vary insignificantly among (especially) second and third instars of euaesthetine larvae. We did not calculate mean measurements of head width, but provide individual measurements for each measured larva. Photographic images of larval morphology were taken on a digital camera (Nikon DXM1200F) attached to a dissecting microscope (Nikon SM21500). All larval material examined in this study is housed in FMNH.

Material examined

We examined numerous adult specimens of all genera studied here. For all species-rich genera (see Herman, 2001 for relative species counts) there were multiple species available in the adult stage with which to gain a broad survey of the character variation within genera. However, for many of the adult characters we examined in the phylogenetic analysis it was not possible to survey genera broadly. In most cases only a few specimens of a single exemplar species were examined using SEM. As representative material, we list only data for slide-mounted and SEM material. All euaesthetine material of taxa we treat in the descriptive section is listed there; other euaesthetine

material, and material from other examined subfamilies, is listed in the following paragraph.

Adult slide and SEM material. **Piestinae:** *Siagonium punctatum* (LeConte, 1866). MEXICO: 1♂, 1♀, Nuevo León, Galeana, Cerro Potosí, 10 600 ft, under pine bark, 28.v.1971 (*Newton*); U.S.A.: 2♂, 2♀ (SEM), Tennessee, Sevier Co., 7.9 mi. S Gatlinburg, 3000 ft, under bark of *Liriodendron* in fermenting stage, 21.v.1977 (*Newton & Thayer*). **Oxyporinae:** *Oxyporus lateralis* Gravenhorst, 1802. U.S.A.: 1♀, Massachusetts. *Oxyporus femoralis* Gravenhorst, 1802. U.S.A.: 1♀, Arkansas, Polk Co., Ouachita National Forest, Shady Lake Recreation Area, 1200 ft, on gilled mushrooms, 13.x.1974 (*Newton*). *Oxyporus* sp. U.S.A.: 2♂ (SEM), Maine, N.E. Harbor, 20.viii.1908. **Pseudopsinae:** *Nanobius serricollis* (LeConte, 1875). U.S.A.: California: 1♂, Pomona; 1♀, Amador Co., Tiger Creek, ENE Pioneer, 3500 ft, mossy old conifer log, 26.vi.1975 (*Newton*); 1♂, 1♀ (SEM), Marin Co., Lily Gulch, W side Alpine Lake, 37°57.0′N, 122°38.0′W, 220 m, *Sequoia-Acer* forest near pond, forest leaf & log litter (Winkler extraction; FMHD#93-126), 6.xi.1993 (*Newton, Thayer*). *Pseudopsis arrowi* Bernhauer, 1939. NEW ZEALAND: Nelson Lakes National Park, N slope Mount Robert: 1♂, 1♀, 860 m, *Nothofagus* spp. forest (site ANMT 604), forest litter, 24.iii.1980 (*Newton, Thayer*); 2♂, 2♀ (SEM), Speargrass Track, 880 m, *Nothofagus* spp. forest (site ANMT 704), 14-21.xii.1984 (*Newton, Thayer*). *Pseudopsis minuta* Fall, 1901. U.S.A.: 1♂, 1♀, Arizona, Pima Co., Santa Catalina Mountains, Mount Bigelow, 8300 ft, leaf & log litter, 27.viii.1974 (*Lawrence*). *Pseudopsis montoraria* Herman, 1975. U.S.A.: 1♂, 1♀, California, Amador Co., Peddler Hill, 7000 ft, mixed conifer forest, leaf litter (berlesate), 27.vi.1975 (*Newton*). *Pseudopsis obliterata* LeConte, 1879. U.S.A.: 1♂, Amador Co., Panther Ridge, 6200 ft, forest stream flood debris, 27.vi.1975, (*Newton, Thayer*). *Pseudopsis obtusa* Herman, 1975. U.S.A.: 1♂, 1♀, California, Fresno Co., Sierra National Forest, Hwy. 168, 3.4 mi. SW Mono Springs, 7800 ft, litter (berlesate), 15.v.1976 (*Newton, Thayer*). *Pseudopsis subulata* Herman, 1975. U.S.A.: 1♂, New Hampshire, Coos Co., White Mountains National Forest, Jefferson Notch, 3000 ft, sparse fir forest, leaf litter (berlesate), 27.vii.1974 (*Newton*). **Megalopsidiinae:** *Megalopinus* sp. nr. *madecassa* Puthz, 1992. MADAGASCAR: 1♂, Prov. Fianarantsoa, 29 km SSW Ambositra, Ankazomivady, 20°46.6′S, 47°9.9′E, 1700 m, disturbed montane rainforest, sifted leaf mould and rotten wood (50 mini Winkler samples; FMHD#98-350; B.L. Fisher#1590), 7.i.1998 (*Fisher*). *Megalopinus* spp. BRAZIL: 1♀, Santa Catarina, Nova Teutônia, iv-v.1977 (*Plaumann*); 1♂, 1♀ (SEM), same data; AUSTRALIA: 1♂, 1♀, New South Wales, Unumgar State Forest (near Woodenbong), Pole Bridge Road, 28°14.4′S 152°24.0′E, 430 m, dry *Araucaria–Eucalyptus* rainforest (site ANMT 788), flight intercept (window) trap (FMHD#87-172), 2-11.i.1987 (*Newton, Thayer*). **Steninae:** *Dianous aurichalceus* (Champion, 1920). INDIA: 1♂, Chakrata District, Sainj Khud, 6500 ft, 29.v.1922 (*Cameron*). *Dianous chalybaeus* LeConte, 1863. U.S.A.: 1♀, New Hampshire, Coos Co., 0.7 mi. S Jefferson Notch, 880 m, forest stream flood debris and wet moss, 31.vii.1982 (*Newton, Thayer*). *Dianous nitidulus* LeConte, 1874. U.S.A.: 1♂, 1♀, New Mexico, Lincoln Co., S. Fork Bonito Creek, 75–8000 ft, moss and debris along stream, 7.vii.1972 (*Newton*); 1♂, 1♀ (SEM), New Hampshire, Coos Co., 1 mi. S Jefferson Notch, 2700 ft, flood debris and wet moss along forest stream (berlesate), 7.ix.1975 (*Newton, Thayer*). *Stenus* spp. U.S.A.: 1♂, 1♀, Massachusetts, Middlesex Co., Bedford, Pickman Area, flood debris (berlesate), 2.iv.1977 (*Newton, Thayer*); 1♂, 1♀ (SEM), same data. TRINIDAD AND TOBAGO: 1♂, 1♀, Port of Spain, beaten from leaves of trees and shrubs; 1♂, 1♀ (SEM), same data. 'SteNovAUS1W'. AUSTRALIA: Queensland: Lamington National Park: 1♀, near O'Reillys, leaf & log litter (berlesate; ANIC 655), 22-27.x.1978 (*Lawrence, Weir*); 1♂, 1♀ (SEM), Binna Burra, sifted bark (Endrödy-Younga70a), 15.xi.1982 (*Endrödy-Younga*). 'SteNovAUS2F'. AUSTRALIA: Tasmania: 1♂, 1♀, Florentine Valley, 22 km NW Maydena, 700 ft, berlesate 247, 15.ii.1977 (*Kethley*); 1♀ (SEM), Derwent Valley, 7 km NW Maydena, sassafrass litter (FMHD#77-150; berlesate #249), 16.ii.1977 (*Kethley*). **Euaesthetinae:** *Stictocranius puncticeps* LeConte, 1866. U.S.A.: Tennessee: 1♂, 1♀, Gatlinburg, 5 mi. S on US 441, 2200 ft, forest floor litter (berlesate), 7.x.1973 (*Newton*); 1♀ (SEM), Cumberland Co., 1.8 mi. E Ozone, 1300 ft, mixed hardwood-fir-pine forest near stream, litter (berlesate), 6.x.1973 (*Newton*). North Carolina: 2♂, 2♀ (SEM), Macon Co., 4 mi. N Franklin, pine duff around rotten logs (berlesate), 21.iii.1976 (*Watrous*). *Gerhardia africana* (Bernhauer, 1915). DEMOCRATIC REPUBLIC OF THE CONGO: Kivu: 1♂, riv. Musosa (env. Butembo), t. Lubero, 1630 m, vii-viii.1955 (*Célis*); 1♀, Terr. Lubero, Mulo, 1880 m, dans terreau au berlese, 3.vii.1954 (*Célis*). RWANDA: 1♀, Forêt de la Rugege, 2150 m, recolté dans l'humus, iv.1951 (*Leleup*). TANZANIA: 1♂ ('e550'), 1♀ ('e556') (SEM), S slope Mount Hanang, 2500 m, high brush with *Protea*, 26.v.1957 (*Basilewsky, Leleup*).

Larval slide material. **Oxyporinae:** *Oxyporus rufipennis* LeConte, 1863. U.S.A.: 1 larva, Michigan, Berrien Co., 6.vi.1990 (*Newton, Thayer*). **Megalopsidiinae:** *Megalopinus* sp. MEXICO: 1 larva, Chiapas, Palenque, 27-29.vii.1983 (*Peck, Kukalová-Peck*). **Pseudopsinae:** *Pseudopsis montoraria* Herman, 1975. U.S.A.: 2 larvae**,** Oregon, Curry Co., 12 mi. N Brookings, vicinity of Cape Ferrelo, litter, 2.iv.1983 (*Johnson*). *Nanobius serricollis* (LeConte, 1875). U.S.A.: 1 larva, California, Los Angeles Co., Angeles Crest highway, mile 49.06, 34°18.1′N, 118°0.1′W, 1635 m, *Quercus-Pinus coulteri-Pseudotsuga macrocarpa-Calocedrus decurrens* forest, leaf & log litter (berlesate; FMHD#95-36), 14.iii.1995 (*Newton, Thayer*). **Piestinae:** *Siagonium punctatum* (LeConte, 1866). U.S.A.: 2 larvae, Arizona, Pima Co., Mt. Lemmon, 5.ix.1974 (*Lawrence*).

Terminal taxa

The ingroup taxon sample included species of *Stenus* and *Dianous* (Steninae) and representative species and genera of Euaesthetinae (Table 1). Two undescribed Australian

species possibly belonging to a new genus in Steninae were included as the terminals 'SteNovAUS1W' (winged species) and 'SteNovAUS2F' (wingless species). Hereafter, both species together will be referred to with the abbreviation 'SteNovAUS'. Ten euaesthetine genera are endemic to the south-temperate region and all ten genera are represented in our analyses. One of these austral genera is undescribed and is referred to here as 'EuaAUS' (endemic to Australia with one known undescribed species); see 'Descriptive Part' for discussion of the generic status of this species. The terminal taxon we refer to as 'Eua?LTAS' is the only terminal lacking adult data and comprises two larvae of an undetermined genus and (possibly new) species. Although no adults were associated with these larvae, they may belong to a SteNovAUS species. We include them as a separate terminal in order to test this possibility phylogenetically. The following genera not endemic to the south-temperate region were included in the ingroup: *Fenderia* Hatch and *Stictocranius* LeConte (Fenderiini), *Edaphus*, *Euaesthetus* and *Octavius* (Euaesthetini), and *Gerhardia* Kistner and *Stenaesthetus* (Stenaesthetini). Several South African specimens of the genus *Schatzmayrina* Koch were seen too late to be included here.

Most terminals in Table 1 are genera, but several euaesthetine genera were split into infrageneric terminal taxa including individual species: *Alzadaesthetus* Kistner (includes two species) was split into the terminals *A. furcillatus* Saiz and *A. chilensis* Kistner because the genus may not be monophyletic (each species has different states for tarsal formula and abdominal margination), and available larvae could be assigned reliably to *A. furcillatus*. The genera *Austroesthetus* Oke and *Chilioesthetus* Saiz, 1968 should probably be combined (see Newton, 1985) but were maintained as separate terminals because species assigned to each genus differ in the structure of the labium. *Octavius* was split into '*Octavius*SA' and '*Octavius*PAN' because available *Octavius* larvae could be associated with adults from the same region or collection event (and thus each of these terminals probably represents adult and larval data from a single species). *Protopristus* Broun was split into '*Protopristus*NZ' and '*Protopristus*TAS' because larvae were available only from New Zealand. These two terminals represent infrageneric groupings that are possibly monophyletic clades endemic to each region: *Protopristus* from Australia and New Zealand differ in female genital characters and therefore it is most appropriate to combine the New Zealand *Protopristus* larval characters with New Zealand *Protopristus* adult characters. Although terminal taxa representing more than a single species entail the assumption of monophyly for the included species, those terminals aggregate numerous morphologically similar species that were uniform for the easily observable external characters we score. Dividing the ingroup into more terminal taxa is a method (Nixon & Davis, 1991) to remove polymorphism from the data matrix. This also permitted some tests of generic monophyly. The result is only a few cells in the data matrix coded as polymorphic. Prendini (2001) argues for an exemplar approach to coding supraspecific terminal taxa, and in principle we agree that this method is superior to other methods. However, euaesthetine alpha taxonomy is so poorly developed that not only would using individual species be very difficult to achieve because of the practical difficulties associated with identification, but in most cases we could not associate larvae with species – a critical aspect of our decision to code genera instead of species. Furthermore, we were constrained to coding genera because most of the criteria for exemplar selection offered by Prendini (2001) could not be met. However, we met the maximal diversity criterion by examining geographically diverse exemplars for widespread genera.

We included four outgroup taxa, namely Megalopsidiinae: *Megalopinus* Eichelbaum, Pseudopsinae: *Pseudopsis* Newman and *Nanobius* Herman, Oxyporinae: *Oxyporus* Fabricius (all in Staphylinine group, sensu Lawrence & Newton, 1982) and one outgroup outside the Staphylinine group, Piestinae: *Siagonium* Kirby & Spence (Oxyteline Group, sensu Lawrence & Newton, 1982). All except *Nanobius* were studied by Leschen & Newton (2003).

Character sampling and coding for phylogenetic analysis

One hundred and thirty-five adult and 32 larval morphological characters were coded into a taxon × character data matrix (Table 1) using the program Nexus Data Editor (NDE) version 0.5.0 (Page, 2001a). In this data matrix, a '?' refers to actual missing data; no characters were inapplicable to any taxa. All multistate characters were treated as unordered and all characters were weighted equally in all analyses. As this is the first comprehensive phylogenetic analysis of this group, with many new characters introduced, we have little a priori justification for proposing any transformational or polarity assumptions. Consequently, character state polarity was interpreted in the context of the analysis and no ancestral states were designated. We included most characters analysed by Leschen & Newton (2003), and used various publications as sources of characters and guides to defining our own characters, including, but not limited to, Newton (1982a); Naomi (1987a, b, 1988a–d, 1989a–d, 1990); Newton & Thayer (1995); Hansen (1997); Solodovnikov & Newton (2005); and Thayer (2005). This literature provided the starting point for character analysis, but all characters were checked in every terminal taxon, and multiple species exemplars were examined for speciose genera, including species from different biogeographic regions for widespread genera (e.g. *Edaphus*, *Stenaesthetus*). However, we doubt that some of our characters are constant within each genus or infrageneric subgroup, particularly for the large genera *Stenus*, *Megalopinus*, *Edaphus*, *Octavius* and others, and especially because larvae are so poorly known within Euaesthetinae.

We define and code some characters differently from Leschen & Newton (2003) and other authors for four reasons: (1) our larger euaesthetine taxon sample, (2) differing interpretation of structures (character definition and state delimitation) and primary homology assessments, (3) our use of a reductive coding strategy (see Wilkinson,

1995), and (4) our incorporation of scanning electron microscopy in conjunction with light microscopy to aid in adult morphological character discovery and interpretation. Where our character and state definitions deviate from those of previous studies, justification is provided in the character list (Appendix 1).

One adult and seven larval characters used by Leschen & Newton (2003) are relevant to the phylogenetic problems studied here but were excluded because we were unable to score some or all of our taxa for them. These included their characters 15 (adult metacoxae length relative to width), 34 (structure of larval apical maxillary palpomere), 35 (ventral sclerite of larval prementum divided or entire), 37 (larval transhypopharyngeal bracon present or absent), 38 (larval epipharyngeal plate present or absent), 42 (structure of larval tentorial bridge), 45 (larval abdominal sternites divided or entire), and 48 (relative length of larval urogomphal seta(e) to length of urogomphus or abdominal segment IX). For some other characters, in our study we assigned the alternative state, or both states (polymorphism), to the same terminal taxa studied by Leschen & Newton (2003). For notes on all differences from Leschen & Newton's state assignments (not character or state definitions), see our characters 2 (location of antennal insertion), 64 (procoxal mesial surface), 70 (elytral epipleural keel presence or absence), 78 (mesothoracic anapleural suture presence or absence), 101 (posterior face of metacoxae oblique or vertical), 130 (female tergite IX not or completely divided by X), 133 (first and second gonocoxites articulated or fused ipsilaterally) and 135 (gonostyle presence or absence). We also defined several of their characters and/or states differently; for notes on major alternative character and state definitions see our characters 92–95 (number of apparent pro-, meso-, and metatarsomeres in adult), 118–121 (adult abdominal 'margination' on segments III–VI), 137 (larval labrum separation from frons), 138 (anterior edge of larval labrum or nasale toothed or smooth), 143 (larval maxillary foramen open or closed mesially), 144 (stem of larval ventral ecdysial lines), 150 (larval mandibular teeth presence or absence), 152 (size of larval mala) and 162 (sub-basal carinae on abdominal tergites II–VIII presence or absence).

Phylogenetic analyses

Tree searches were carried out in PAUP*4.0b10 (Swofford, 2002). Prior to phylogenetic analyses, the incongruence length difference (ILD) test of Farris *et al*. (1994) was performed to test for a difference in phylogenetic signal between adult and larval character sets. The ILD was performed in PAUP* (as the partition homogeneity test) by first designating adult and larval character sets (commands: charset adults = 1–135; charset larvae = 136–167) and then executing the following commands: charpartition adultslarvae = 1: adults, 2: larvae; exclude uninf; hompart partition = adultslarvae nreps = 1000 seed = 123;). All other default settings were followed. A *P*-value greater than 0.05 indicates that both character sets have congruent phylogenetic signal and that combining them should increase phylogenetic accuracy (Cunningham, 1997). We performed this test only on our reduced dataset (see description of Analysis 3, below) owing to excessively long computation time, presumably caused by missing data for 12 of the terminals included in Analysis 1 (see below).

Most parsimonious trees (MPTs) were obtained by heuristic searching and employing all default settings (addition sequence = simple; #trees held at each step = 1; swapping algorithm = TBR; collapse option in effect = yes(max); multrees option = yes; steepest descent = no; multistate taxa interpreted as uncertainty). For all tree searches the maximum trees held at each addition-sequence replicate was set to increase automatically by 100. Resulting trees were rooted on *Siagonium*. Parsimony-uninformative characters were excluded from all analyses and do not contribute to tree length nor to other statistics; they are included in the character list (Appendix 1) and data matrix (Table 1), and are optimized onto Fig. 3. All phylogenetic trees were examined and manipulated in TreeView 1.6.6 (Page, 2001b). Four analyses were run:

Analysis 1 (30 terminal taxa; 167 adult and larval characters). This was the most inclusive analysis and included all the taxa and characters in Table 1. Eleven terminal taxa had no larval data (SteNovAUS1W, SteNovAUS2F, *Alzadaesthetus chilensis*, *Mesoaesthetus*, *Tasmanosthetus* Puthz, *Kiwiaesthetus*, *Protopristus*TAS, *Stictocranius*, *Gerhardia*, *Stenaesthetus*, EuaAUS), and therefore the data matrix for this analysis had many missing data entries (12.7%). One terminal taxon had no adult data (Eua?LTAS). Characters 56, 64, 73, 97 and 131 were parsimony-uninformative.

Analysis 2 (29 terminal taxa; 135 adult characters only). The terminal taxon Eua?LTAS has no associated adult data and was excluded from this analysis. Larval characters (136–167) were excluded from this analysis and the same five characters as in Analysis 1 were parsimony-uninformative.

Analysis 3 (18 terminal taxa; 167 adult and larval characters). This analysis was based on a reduced taxon sample comprising only those terminals with complete adult and larval data. The 11 adult-only terminal taxa listed under Analysis 1, plus Eua?LTAS, were excluded. Twenty characters were parsimony-uninformative in this analysis, including six that were constant (19, 43, 51, 61, 74, 90) and 14 that were variable (35, 40, 44, 45, 50, 52, 56, 64, 71, 73, 97, 99, 110, 131) (Table 1).

Analysis 4 (19 terminal taxa; 32 larval characters only). The final analysis included the 19 terminal taxa with larval data. Adult characters 1–135 were excluded from this analysis and all larval characters were parsimony-informative. The 11 adult-only terminal taxa listed under Analysis 1 were excluded.

Clade robustness was assessed by bootstrap analysis (Felsenstein, 1985) using 1000 replicates (nreps = 1000) and all default settings (but with MaxTrees set to autoincrease by 100), and Bremer support values (Bremer, 1988) were calculated using AUTODECAY (Eriksson, 2001). Support values are plotted on consensus trees for all analyses except Analysis 3, for which we report support values with one of two equally parsimonious trees. In all cladograms, only bootstrap proportions >49% are reported.

Character optimization

Character state changes were examined in WINCLADA (Nixon, 2002). The data matrix was transferred from NDE to WINCLADA using MESQUITE (Maddison & Maddison, 2007). This enabled transfer of the data complete with character and character state names (Agnarsson, 2004), which are lost in export from NDE in HENNIG86 (.ss) format (readable by WINCLADA). To present and discuss character support for the major clades described in this study we considered only unambiguously optimized character state changes, as reported by WINCLADA, and mapped these onto one of two most parsimonious trees resulting from Analysis 3 (Fig. 3). We used the results from Analysis 3 because they were not affected by the large amount of missing larval data, and the underlying matrix represents the most complete taxon × character data set currently available for Euaesthetinae. Other analyses produced many equally parsimonious trees, making selection of the best hypothesis highly subjective. The alternative tree differed from the one in Fig. 3 only in the placement of *Fenderia* as the sister group of *Agnosthaetus*, but we prefer Fig. 3 because *Fenderia* + (*Protopristus*, *Octavius*) is supported by a unique synapomorphy (modified setae of protarsomeres 1 and 2 of males, 92-1) and three reversals (absence of tentorial bridge, 8-1; stem of metendosternite, 88-0; intersegmental membrane attached to apex of preceding segment, 106-0) that seem more plausible than reversal to five tarsomeres in the pro- and mesotarsi (i.e. two changes that support *Fenderia* + *Agnosthaetus*). Several other clades recovered in this study involved terminal taxa that were excluded from Analysis 3. To discuss the synapomorphies of those clades we refer to the unambiguously optimized character state changes recovered in Analysis 1 (results not shown; only character state changes occurring on all 132 MPTs were considered). The 14 variable parsimony-uninformative characters in Analysis 3 have their apomorphic character states mapped onto Fig. 3, but these characters do not contribute to tree length or other statistics.

When discussing character support for clades (see 'Discussion') we refer to character state changes that occur on a single branch or on more than one branch as 'unique' and 'non-unique' synapomorphies, respectively, and these are interpreted as such only in the context of the present study unless otherwise indicated. Character states were optimized according to the default option in WINCLADA – homoplasy/homology is mapped by state, such that only discontinuous states are mapped as homoplasy. In Fig. 3, then, black squares represent 'unique synapomorphies' and white squares indicate 'non-unique synapomorphies' (i.e. homoplastic states). An important consequence of this distinction is that a character with a state optimized as a unique synapomorphy (black square) on a branch in Fig. 3 also may show a reversal to a plesiomorphic state above the node in question. Furthermore, if the character was a multistate character, another apomorphic state may be recovered as a non-unique synapomorphy (i.e. show homoplasy). In both cases, therefore, the character itself may have a consistency index lower than 1.0. Because of this distinction, we highlight the consistency indices of characters when discussing proposed synapomorphies (character states).

Results of phylogenetic analysis

The incongruence length difference test was performed only for Analysis 3, producing a *P*-value of 0.558, and therefore demonstrated no significant difference in phylogenetic signal between adult and larval character sets. The following results of Analyses 1–4 are presented sequentially, following the order described in 'Materials and Methods'. Cladograms are presented in Figs 2–4 and major clades are indicated with letters A–H, which are referred to in the text. Hereafter, Bremer support (= decay index) and bootstrap support values will be abbreviated with DI and BS, respectively. Ensemble tree statistics are indicated in capitals: TL = tree length, CI = consistency index, RI = retention index. Statistics for individual characters are indicated in lowercase.

Analysis 1: All taxa, simultaneous analysis of adult and larval characters

Simultaneous analysis of 162 informative adult and larval characters and 30 terminal taxa produced 132 most parsimonious trees (TL = 331 steps; CI = 0.57; RI = 0.80), the strict consensus of which is shown in Fig. 2. This tree recovers Euaesthetinae (B) as monophyletic with very strong bootstrap and Bremer support (BS = 98%; DI = 7). Phylogenetic relationships within the subfamily Euaesthetinae, however, were not established with strong support (Fig. 2). The austral endemic euaesthetine genera (terminal taxa underlined in Fig. 2) did not form a monophyletic group, and of the five currently valid tribes represented in this analysis (Alzadaesthetini, Austroesthetini, Euaesthetini, Fenderiini, Stenaesthetini) only Stenaesthetini (H) was recovered as monophyletic, although this result was only moderately supported (BS = 69%; DI = 1). The four included genera of Stenaesthetini formed a series of less-inclusive sister groups, with strong bootstrap support (98%) recovered for *Stenaesthetus* + *Gerhardia* (Fig. 2). A somewhat surprising result was the non-monophyly of Alzadaesthetini. This monogeneric tribe is represented only by the species *Alzadaesthetus furcillatus* and *A. chilensis*, and in Fig. 2 the latter species is the sister group of *Stictocranius* (Fenderiini), although this result is weakly supported. Only

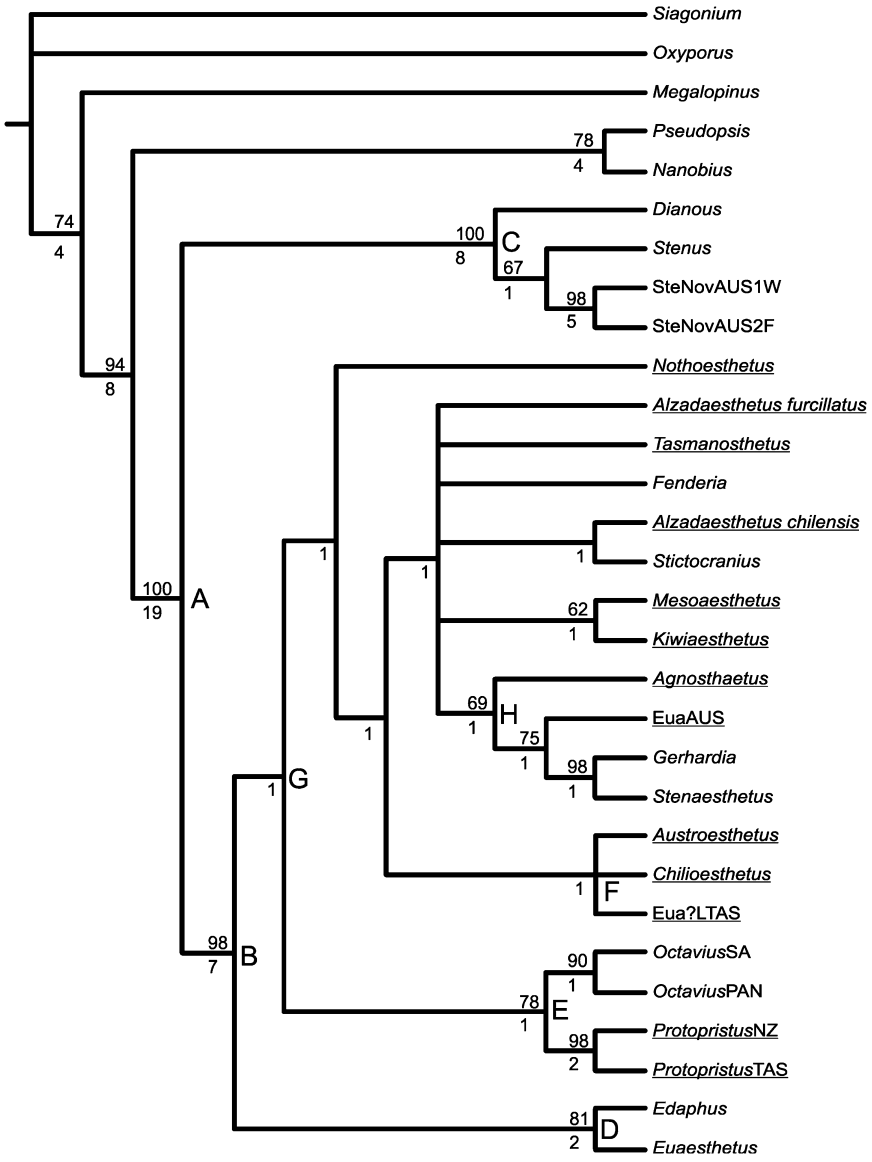

Fig. 2. Strict consensus tree from Analysis 1 (30 terminal taxa and 167 adult and larval characters). Analysis of all data produced 132 most parsimonious trees (TL = 331 steps; CI = 0.57; RI = 0.80). Bootstrap proportions (>49%) are listed above branches, decay index values below branches. Clades A–G are referred to in the text; clade B = Euaesthetinae, clade C = Steninae. Southern temperate endemic euaesthetine terminal taxa are underlined.

weak to moderate support was recovered for sister-group relationships between *Euaesthetus* + *Edaphus* (D) (BS = 81%; DI = 2), *Octavius* + *Protopristus* (E) (BS = 78%; DI = 1), and *Mesoaesthetus* + *Kiwiaesthetus* (BS = 62%; DI = 1). The genera *Octavius* and *Protopristus* were each recovered as monophyletic, and each was strongly supported by bootstrap analysis, but weakly supported by decay analysis. The Eua?LTAS terminal was placed within Euaesthetinae in this analysis, and, furthermore, the larvae were placed in a trichotomy containing *Austroesthetus* and *Chilioesthetus* (Fig. 2; F), supporting the identity of this taxon as a species of one of these genera (both occur in Australia). In Table 1, *Austroesthetus* and Eua?LTAS share identical states for all 32 larval characters. This trichotomy was, however, only weakly supported by character data (BS $\leq$ 49%; DI = 1), and Eua?LTAS was not included in the bootstrap 50% majority rule consensus tree, which instead recovered *Austroesthetus* and *Chilioesthetus* as a clade (BS = 70%) to the exclusion of Eua?LTAS.

Based on morphological characters, our study firmly establishes that the two undescribed Australian species SteNovAUS1W and SteNovAUS2F belong in the subfamily Steninae, and not in Euaesthetinae. The strict consensus tree in Fig. 2 recovers subfamily Steninae (C), together with

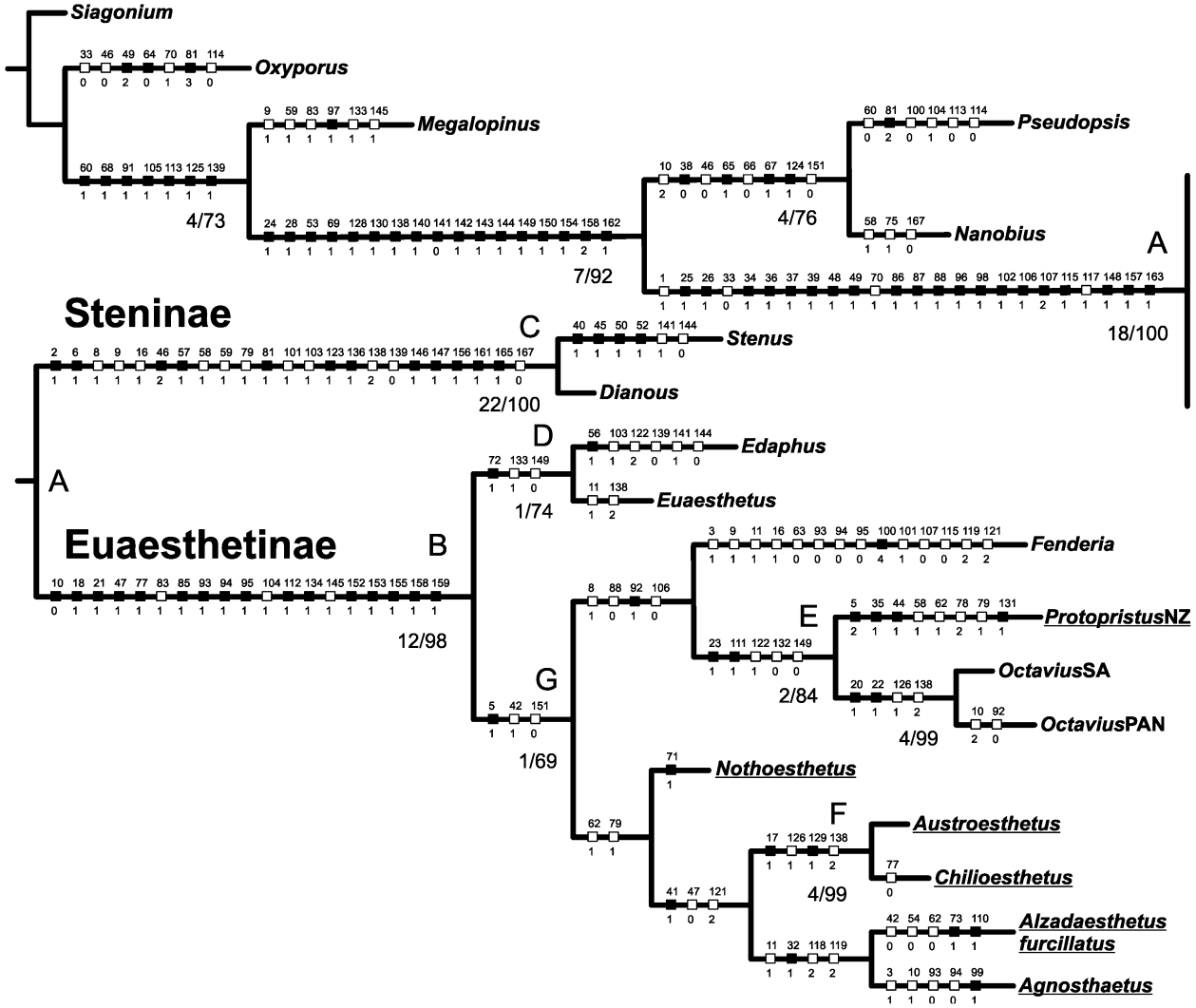

Fig. 3. One of two most parsimonious trees from Analysis 3 (18 terminal taxa and 147 adult and larval characters; TL = 281 steps; CI = 0.60; RI = 0.79) with unambiguously optimized character state changes mapped. Characters 1–135 are adult characters; 136–167 are larval characters. Character numbers appear above squares, state numbers below squares. Filled squares represent unique synapomorphies, unfilled squares represent homoplastic – or discontinuous – states. Decay index values/bootstrap proportions (>49%) are listed below branches. Clades A–G are referred to in the text; clade B = Euaesthetinae, clade C = Steninae. Southern temperate endemic euaesthetine terminal taxa are underlined.

SteNovAUS, as a very strongly supported monophyletic group (BS = 100%; DI = 8). Monophyly of SteNovAUS also was strongly supported (BS = 98%; DI = 5), but the placement of this clade as the sister group of *Stenus* was supported only weakly (BS = 67; DI = 1).

Euaesthetinae + Steninae (A) was recovered as a strongly supported monophyletic group (BS = 100%; DI = 19), solidly establishing the sister-group relationship of these two staphylinid subfamilies and corroborating the results of previous morphological studies (Hansen, 1997; Leschen & Newton, 2003; Thayer, 2005) that collectively proposed a long list of synapomorphies for this clade. One notable result is the placement of Pseudopsinae as the sister group of Euaesthetinae + Steninae, which is strongly supported (BS = 94%; DI = 8), and of Megalopsidiinae as the sister group of these (BS = 74%; DI = 4).

Analysis 2: All taxa (except Eua?LTAS), separate analysis of adult characters

Separate analysis of 130 informative adult characters and 29 terminal taxa (Eua?LTAS excluded, no adult data) produced 44 most parsimonious trees (TL = 273 steps; CI = 0.55; RI = 0.80), the strict consensus of which was nearly identical to that in Fig. 2. There were only two

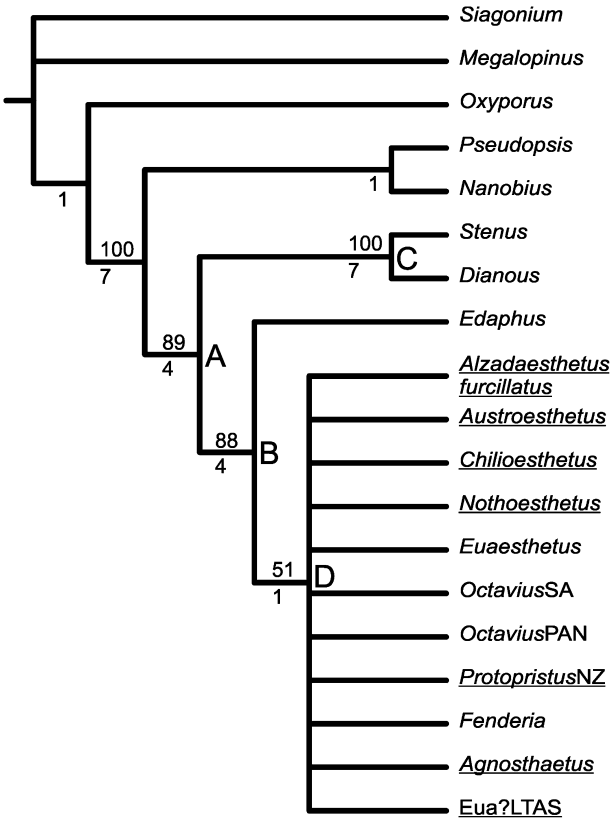

Fig. 4. Strict consensus tree from Analysis 4 (19 terminal taxa and 32 larval characters). Analysis of larval data produced 35 most parsimonious trees (TL = 54 steps; CI = 0.69; RI = 0.85). Bootstrap proportions (>49%) are listed above branches, decay index values below branches. Clades A–D are referred to in the text; clade B = Euaesthetinae, clade C = Steninae. Southern temperate endemic euaesthetine terminal taxa are underlined.

topological differences between it and the one shown in Fig. 2: Megalopsidiinae was placed as an alternative sister group of Steninae + Euaesthetinae (BS = 66%; DI = 2), and Pseudopsinae was the sister group of these (BS = 71%; DI = 2). Moreover, Eua?LTAS was absent from the analysis and hence from the consensus tree of Analysis 2. That consensus tree did, however, recover *Austroesthetus* + *Chilioesthetus* as a strongly supported clade (BS = 97%; DI = 3) compared with the same clade including Eua?LTAS (F in Fig. 2) that was only weakly supported (BS < 50%; DI = 1). In terms of support for other major clades, some had more or less identical bootstrap and/or Bremer support values in both Analyses 1 and 2. A major difference between the two analyses, however, was that where support values differed, there was a nearly uniform increase in support for the lettered ingroup clades in Analysis 2 (Euaesthetinae, B – BS = 93%, DI = 9; Steninae, C – DI = 10; *Edaphus* + *Euaesthetus*, D – BS = 93%; *Octavius* + *Protopristus*, E – BS = 85%, DI = 2; Stenaesthetini, H – BS = 72%; compare these values with Fig. 2). Other clades within Euaesthetinae were not supported in Analysis 2. One possible explanation for this general increase in support with exclusion of larval data is the effect of missing data on clade support measures. The data matrix used for Analysis 2 had only a few unfilled cells compared with nearly 13% missing data in Analysis 1. Reducing the amount of missing data reduced the number of equally parsimonious trees in Analysis 2 (44) compared to Analysis 1(132).

Analysis 3: Reduced taxon sample, simultaneous analysis of adult and larval characters

Simultaneous analysis of 147 informative adult and larval characters and 18 terminal taxa produced two most parsimonious trees (TL = 281 steps; CI = 0.60; RI = 0.79), which differed only in the placement of *Fenderia* as the sister group of either *Protopristus* + *Octavius* (E), as in Fig. 3, or of *Agnosthaetus*. The strict consensus tree (not shown) of these two trees therefore collapsed all unlettered euaesthetine clades in Fig. 3 (except *Octavius*) to a polytomy at clade G. Outgroup relationships were congruent with those in Analysis 1 (Fig. 2), in which Megalopsidiinae was the sister group of Pseudopsinae + (Steninae, Euaesthetinae).

With respect to clades A through F recovered in Analyses 1 and 2 (Fig. 2), the results of Analysis 3 were topologically congruent. As in Analysis 2, Eua?LTAS was not included in the analysis and hence is absent from Fig. 3. *Austroesthetus* + *Chilioesthetus* (F) was again recovered as a clade, but more strongly supported than in Analysis 2 (BS = 99%; DI = 4). In terms of support, some clades had more or less identical bootstrap and/or Bremer support values in Analyses 1 and 3. But like Analysis 2, where support values differed from those in Analysis 1 there was again a nearly uniform – and more dramatic – increase in support for the lettered ingroup clades in Analysis 3, particularly for Bremer support values (Euaesthetinae, B – DI = 12; Steninae, C – DI = 22; *Edaphus* + *Euaesthetus*, D – BS = 74%, DI = 1; *Octavius* + *Protopristus*, E – BS = 84%, DI = 2; compare these values with Fig. 2). Additional clades recovered within Euaesthetinae were not supported in Analysis 3.

This apparent inverse relationship between taxon sample size and statistical support for Euaesthetinae, Steninae and some other clades demonstrates the significant influence that a smaller taxon sample together with complete data can have on inflating the statistical support for major clades in our analyses. As more taxa and data are added, so the amount of missing data increases, which may result in an increasing influence of homoplasy, as missing characters from the larval character set cannot contribute to resolving conflict that may exist among specific groups defined by different individual characters, or by different character sets. Stated another way, statistical support – particularly Bremer support – for some clades recovered in Analysis 3 (e.g. Euaesthetinae – B, Steninae – C, and *Austroesthetus* + *Chilioesthetus* – F) seems particularly sensitive to increases in both taxon sampling and missing data, whereas other clades (e.g. Steninae + Euaesthetinae – A) do not. Unambiguously optimized character states mapped onto Fig. 3 are described in the 'Discussion'.

Analysis 4: Reduced taxon sample, separate analysis of larval characters

Separate analysis of 32 informative larval characters and 19 terminal taxa produced 35 most parsimonious trees (TL = 54 steps; CI = 0.69; RI = 0.85), the strict consensus of which is shown in Fig. 4. Consistent with the three previous analyses, the strict consensus tree maintained Euaesthetinae + Steninae (A), Euaesthetinae (B) and Steninae (C) each as strongly supported monophyletic groups (Fig. 4). However, in contrast to Analyses 1–3, only one weakly supported clade (D) was recovered within Euaesthetinae. The genus *Euaesthetus* was placed within this clade, rather than as the sister group of *Edaphus* as recovered in other analyses. Examination of all 35 most parsimonious trees revealed that none was completely resolved, and the lack of resolution therefore reflects the absence of larval characters informative below the subfamily level, rather than the presence of conflicting groups among the most parsimonious trees. A notable result of this analysis was the recovery of Pseudopsinae as the sister group of Euaesthetinae + Steninae, which was strongly supported (BS = 100%; DI = 7), confirming the dominant influence of larval characters in recovering this relationship when adult and larval characters were analysed together.

Discussion

Monophyly of Euaesthetinae (clade B)

In this study we provide a strong case for the monophyly of the rove beetle subfamily Euaesthetinae and propose at least 19 synapomorphies from adult and larval character sets. In separate and combined analyses of adult and larval characters the monophyly of Euaesthetinae was consistently strongly supported in both bootstrap and decay analyses. Our results contrast with Leschen & Newton's (2003) earlier study, in which a combined analysis of adult and larval characters recovered only weak support for the monophyly of Euaesthetinae, compared with strong support recovered for the monophyly of Steninae + Euaesthetinae. Their results formally indicated the possibility of euaesthetine paraphyly with respect to Steninae (Thayer, 2005). Although the primary objectives of Leschen & Newton's phylogenetic study were to test the phylogenetic placement of *Megalopinus* and the identification of *Megalopinus* larvae, their study is the only other one that has addressed the question of Euaesthetinae monophyly using phylogenetic methods, and their conclusions argue for sinking Euaesthetinae as a junior synonym of Steninae. It is therefore appropriate to contrast our study with theirs.

The results of the two studies were different for at least three reasons. First, we used a much larger (>3×) character sample (135 vs 28 adult; 32 vs 20 larval; 167 vs 48 total characters). We focused on obtaining new data that could be informative for the question of Euaesthetinae monophyly and relationships among a much larger euaesthetine taxon sample than was analysed by Leschen & Newton (2003). Several other aspects of our study probably contributed to the greater number of accessible characters. For example, the reciprocal illumination between scanning electron microscopy and traditional light microscopy should be underscored, as the two techniques used together greatly aided the discovery and proper interpretation of previously unknown or intractable structural features. We focused on different character systems, such as the endoskeleton (tentorium and internal muscle attachment points), included >50% more larval characters, and employed reductive coding for characters such as 'tarsal formula', all of which greatly increased the number of informative characters. Our results recovered the dentate labrum (21-1) and four metatarsomeres (95-1) as synapomorphies of Euaesthetinae, as was previously suggested by Hansen (1997) and Naomi (1985), respectively, although Leschen & Newton (2003) did not use the labrum character. Second, if we implement changes to some of Leschen & Newton's characters in their dataset (see our characters 2, 64, 70, 78, 101, 130, 133 and 135 – other changes described in 'Materials and Methods' were inapplicable to their study), we recover ~75% bootstrap support for the monophyly of Euaesthetinae (analysis of each character set separately, and combined, each resulted in a single most parsimonious tree). Two of the three synapomorphies in their original analysis supported this clade when the data were modified (spiracles placed in tergite 1, c.i. = 1.0; ventral sclerite of larval prementum divided along midline, c.i. = 0.5). However, a third synapomorphy was four metatarsomeres (c.i. = 1.0), which differed from their original analysis (see Appendix 1, note to characters 93–95). The result of these changes therefore suggests that the lack of statistical support for euaesthetine monophyly in Leschen & Newton's study was caused not necessarily by a lack of character support in their dataset. Third, we used a much larger euaesthetine taxon sample in all our analyses (17 genera in Analyses 1 and 2, 10 in Analyses 3 and 4), and five out of the six tribes were represented. Leschen & Newton (2003) noted that Euaesthetinae is in 'need of critical review', although they used three genera possibly representing 'basal divisions within the subfamily'. By adding a much greater number of euaesthetine terminal taxa in this analysis, we could survey the previously hypothesized synapomorphies (e.g. dentate labrum, four metatarsomeres, spiracles on abdominal segment I) more widely and assess a larger pool of characters. However, as we discuss below, it is likely that we did not include the most plesiomorphy-rich euaesthetine genera in this study, and probably these will be critical both for any analysis of the Steninae–Euaesthetinae problem, and for higher-level analyses within the Staphylinine group.

Character support for Euaesthetinae (clade B)

The monophyly of Euaesthetinae is supported by 19 unambiguously optimized synapomorphies, 13 of which

derive from the adult character set (Fig. 3). In Analysis 3, the following five unique synapomorphies (each with c.i. = 1.0) supported Euaesthetinae monophyly. (1) A group of differentiated setae asymmetrically distributed around the apex of antennomere X (and usually IX) (18-1; Fig. 11G, H, arrows) was discovered using SEM. These setae are clearly differentiated from other antennal setae (Fig. 11G). The presence of similar setae could not be confirmed in the stenines we examined, but further study may prove this character to be a synapomorphy of Euaesthetinae + Steninae. (2) The denticulate or serrate anterior labral margin (21-1; Fig. 11C, I, M) was identified previously as a possible autapomorphy for Euaesthetinae (Hansen, 1997), and within the Staphylinine group it may be unique to Euaesthetinae. Therefore we consider this character to be strong evidence for Euaesthetinae monophyly, but note that several genera have a smooth labrum (e.g. reversed in *Stenaesthetus* and *Gerhardia*). (3) An apical disc on each mesothoracic apodeme (85-1; Orousset, 1988: fig. 299) presumably is a site of muscle attachment within the mesothorax and is possibly present in all euaesthetine genera. However, the shape of this disc is variable – in some genera it is distinctly circular (e.g. *Edaphus*), whereas in others it is not (e.g. *Fenderia*). Such muscle discs may be present also in some Leptotyphlinae. (4) The placement of the spiracles in the tergite of abdominal segment I (112-1) was recovered as a synapomorphy of Euaesthetinae also by Leschen & Newton (2003). (5) The structure of the second gonocoxite, with the mesal edge produced to an apical spine (134-1; Fig. 15A, arrow) might be a character state shared by all euaesthetine genera and is independent of both the shape of the second gonocoxite (which can be broad and flattened, or narrow and acute), and the ipsilateral (same-side) fusion of the first and second gonocoxites (as in *Edaphus* and *Euaesthetus*).

In Analysis 3, another six unique adult synapomorphies (each with c.i. < 1.0) supported Euaesthetinae monophyly but were reversed subsequently to the plesiomorphic state on at least one branch within Euaesthetinae (Fig. 3). (1) The corporotentorium (character 10, c.i. = 0.4) is a three-state character. A split corporotentorium (10-0) is reversed subsequently in *Agnosthaetus* (absence of corporotentorium, 10-1), and a fused corporotentorium (10-2) is optimized independently as a synapomorphy of Pseudopsinae and an autapomorphy of *Octavius*PAN. (2) On the branch leading to *Austroesthetus–Agnosthaetus*, the relative length of the first labial palpomere (character 47, c.i. = 0.5) is reversed from very short (47-1; Fig. 12C) to at least half as long as palpomere 2 (47-0; Figs 11M; 12A, B). In Analysis 1, 47-1 was homoplastic; after reversal to 47-0 within Euaesthetinae, 47-1 was regained independently twice in *Tasmanosthetus* and *Fenderia*. With the addition of more taxa to the analysis, this character may require quantification and splitting into multiple states. (3) The mesothoracic pleural suture (character 77, c.i. = 0.5) is obliterated and not visible externally as a suture or carina in Euaesthetinae (77-1; Fig. 13D, F), and was reversed in *Chilioesthetus* (77-0). Naomi (1985) identified 77-1 as an 'underlying autapomorphy' of Euaesthetinae + Leptotyphlinae + Pselaphidae. Pselaphidae (-nae) is now placed in the Omaliine group (Newton & Thayer, 1995), leaving 77-1 as an autapomorphy of Euaesthetinae and possibly of Leptotyphlinae. The next two characters (93 and 94), each with a consistency index of 0.33, include the articulation of the basal two (4) protarsomeres, and (5) mesotarsomeres. In both characters those tarsomeres are indistinguishably fused in Euaesthetinae (93-1, 94-1, e.g. Fig. 13H, J), but with subsequent reversal to five tarsomeres in *Fenderia* and *Agnosthaetus*. (6) The basal two metatarsomeres (character 95, c.i. = 0.5) are reversed from being fused (95-1) to articulated (95-0) in *Fenderia*. The varying degrees of fusion among different euaesthetine genera demonstrate that this transformation has occurred multiple times within Euaesthetinae, as it has in Oxytelinae (Herman, 1970; Newton, 1982b; cited in Newton & Thayer, 1988), and probably happens independently on each pair of legs. Therefore we consider character states 93-1, 94-1 and 95-1 as spurious support for Euaesthetinae monophyly.

The following two non-unique adult synapomorphies (c.i. = 0.5) supported monophyly of both Euaesthetinae and one of the outgroups (Fig. 3). (1) Straight mesothoracic apodemes (83-1; Orousset, 1988: fig. 299) occur also in Megalopsidiinae, but in this taxon they are directed anterodorsally and are partly fused to the pleural phragma (82-1). Given this additional structural difference it is likely that the straight mesothoracic apodemes of Euaesthetinae are not homologous to those of Megalopsidiinae. (2) The presence of a distinct row of macrosetae on the posterior margin of the metacoxae (104-1; Fig. 14C, left arrow; E, bottom left arrow) also was optimized as an autapomorphy of *Pseudopsis*, and based on preliminary investigation this character may be present in all euaesthetine genera.

Six larval synapomorphies of Euaesthetinae demonstrate the importance of this character set. Five of these were unique synapomorphies (c.i. = 1.0) (Fig. 3). (1) A markedly reduced maxillary mala (152-1; Fig. 6, cf. Fig. 16G, right arrow) was used also by Leschen & Newton (2003) but defined differently. In our taxon sample, some taxa completely lack a mala, whereas in others it is extremely reduced, raising a question as to whether these two sets of taxa actually share a state. Nevertheless, no euaesthetines examined had a well-developed mala. Similarly, (2) the cardo in euaesthetine larvae is markedly reduced and much narrower than the base of the stipes (153-1; Figs 7D–F; 8; 10I, arrow, cf. Fig. 16G, bottom left arrow), and (3) the stipes is also markedly narrowed distally (155-1; Figs 7C–F; 8). (4) The mentum sclerite is narrow and transverse, also bisetose (158-1). (5) The fact that the location of the longest leg seta is on the tibia (159-1; Fig. 16H, arrow) may constitute weak evidence of monophyly as we did not determine if the longest setae in all taxa are homologous setae. (6) One non-unique synapomorphy was the attachment of the antennae (character 145, c.i. = 0.5) to a markedly developed membranous ring (145-1, Figs 5C–F; 6), which also was optimized as an autapomorphy of *Megalopinus*.

Phylogenetic relationships within Euaesthetinae (clade B)

The dataset presented in this study was insufficient for proposing a robust hypothesis of euaesthetine generic relationships because of significant conflict among adult characters and a lack of informative larval characters. The tribes Alzadaesthetini, Austroesthetini, Euaesthetini and Fenderiini were not recovered as monophyletic; hence the available morphological data does not support Scheerpeltz's (1974) suprageneric classification of Euaesthetinae, which although thought to be artificial was never tested phylogenetically. Newton's (1985: 206) hypothesis that all the austral endemic euaesthetine genera form a monophyletic group also was unsupported in this study. However, several clades were recovered consistently and will be mentioned briefly here.

A basal split within Euaesthetinae separated clades D and G (Fig. 3). The monophyly of *Euaesthetus* + *Edaphus* (D) was supported by one unique (72-1; basal spine of elytral marginal ridge; Fig. 13B, arrow) and two non-unique synapomorphies, and the monophyly of the rest of Euaesthetinae (G) was supported also by one unique (5-1; gular sutures united along most of length) and two non-unique synapomorphies. Within this clade (G), and based on Analysis 1, Stenaesthetini was the only tribe recovered as monophyletic, and this included the undescribed genus from Australia, EuaAUS (Fig. 2, clade H). Based on Analysis 1, Stenaesthetini was supported by one unique synapomorphy, the mesocoxal mesal surface with carina-delimited groove (99-1; Fig. 13D, right arrow). Within Stenaesthetini, the monophyly of *Stenaesthetus* and *Gerhardia* was strongly supported by seven synapomorphies, three of which were unique: (1) each of antennomeres 9–11 > 3× as long as wide (19-1), (2) presence of a depigmented callosity on the prosternum (61-1; Fig. 12I, top arrow), and (3) obliquely deflected anteprocoxal carinae (62-2; Fig. 12I, bottom arrow). *Gerhardia* was erected by Kistner (1960), who distinguished it from all other genera by the smooth labral margin, the filiform antennae, the absence of hind wings, and tarsal formula 5-5-4 (all characters shared with species of *Stenaesthetus*), and from *Stenaesthetus* by the absence of wings, shorter elytra, and extremely coarse punctation. *Gerhardia* later was synonymized with *Stenaesthetus* by Puthz (1980), who reinstated it subsequently based on some derived male sexual characters (Puthz, 1995). However, based on Kistner's original characters, none of which is unique to species of *Gerhardia*, combined with strong support for the monophyly of these two genera and the observation that the two terminals are identical for all characters, we consider that *Gerhardia* and *Stenaesthetus* probably should be combined.

Among the austral endemic genera, several previously hypothesized relationships were recovered in Analyses 1 (Fig. 2) and 3 (Fig. 3). Newton's (1985) '*Austroesthetus* Group', comprising the genera *Austroesthetus* and *Chilioesthetus* (Fig. 3, F), was supported by four synapomorphies, two of which appear to be unique within Euaesthetinae: (1) apex of antennomere 10 concave to receive 11 (17-1), and (2) aedeagus with bilobed parameres (129-1). We did not survey exhaustively the full range of characters supporting this relationship, but nonetheless our results support Newton's (1985) view that the two genera should be combined. The undetermined larva (Eua?LTAS) also was placed in this clade (F) in Analysis 1 and probably represents the larva of an *Austroesthetus* species. This relationship was supported in all primary trees of Analysis 1 by the larval nasale having an odd number of teeth, including a distinct central tooth (138-2; Fig. 16A, arrow). Newton's (1985) '*Nothoesthetus* Group', comprising the genera *Nothoesthetus* and *Tasmanosthetus*, was not recovered in any analysis. These genera share a characteristic elytral epipleural fold (71-1; Fig. 13A, arrow), as pointed out by Newton (1985), but we could not find any other characters supporting this group. In Analysis 1 (Fig. 2), the New Zealand genus *Kiwiaesthetus* was recovered consistently as the sister group of the Australian genus *Mesoaesthetus*, and this clade was supported by one unique synapomorphy (tergum and sternum of segments IV–VI separated by distinct suture, 121-1). The genus *Protopristus* is restricted to New Zealand and south eastern Australia and Tasmania. Newton (1985) considered it closely related to the species-rich genus *Octavius*, and our results support this view. The clade *Protopristus* + *Octavius* (E) was supported by five synapomorphies (Fig. 3), two of which were unique: (1) presence of epipharyngeal marginal setae (23-1; Fig. 11J, right arrow), (2) apicolateral spine of abdominal tergites III–VI (111-1; Fig. 14I, arrow).

The genera *Octavius* and *Protopristus* were each recovered as monophyletic based on adult characters (Figs 2; 3). The monophyly of *Octavius* was supported by four synapomorphies, two of which were unique: (1) antennomeres 10 and 11 partly fused, not separated by antennal stem (20-1; Fig. 11G), (2) epipharynx longitudinally furrowed (22-1; Fig. 11J, bottom arrow). Monophyly of *Protopristus* was supported in Analysis 1 by six synapomorphies, three of which were unique: (1) gular sutures united anteriorly, diverging posteriorly (5-2), (2) pair of papillate setae at apex of maxillary palpomere III (35-1; Fig. 11O, arrow), (3) presence of median overlapping teeth on the ligula (44-1; Fig. 12C, arrow). The papillate maxillary palpomere setae are present also in *Euaesthetotyphlus* Coiffait & Decou (not analysed here) and may be synapomorphic for these two genera, whereas the median ligula teeth appear to be a unique autapomorphy of *Protopristus*, as recognized previously (Puthz, 1980; Newton, 1985).

Monophyly of Steninae and the systematic position of SteNovAUS (Clade C)

The subfamily Steninae previously had been hypothesized to be monophyletic based on several derived adult and larval characters (e.g. Hansen, 1997; Leschen & Newton, 2003; Thayer, 2005), but our study presents the first phylogenetic test of this hypothesis using morphological characters. Recovering Steninae as a monophyletic group (including a possibly new genus) when adult characters were analysed either together with or separately from larval characters is

a significant result, especially given the potential for larval characters to alter tree topology dramatically (as in Ashe, 2005). It is clear from our study that an increased knowledge of euaesthetine larvae has contributed significantly to the questions of Euaesthetinae and Steninae monophyly.

The monophyly of Steninae is supported by 23 unambiguously optimized synapomorphies (Fig. 3). Because the focus of this study is on the subfamily Euaesthetinae, we highlight here only those six adult and six larval (12 total) characters with a consistency index of 1.0 (except character 46; c.i. = 0.66), and states uniquely optimized in Analysis 3. (1) Location of antennal insertion on frons between eyes (2-1; Fig. 11E). This character has been used traditionally to diagnose the subfamily (e.g. Thayer, 2005), although in Analysis 1 it was reversed to 2-0 in SteNovAUS2F. (2) Presence of apodemes arising from interantennal pits (6-1). (3) Labial palps inserted close together and near anterior margin of labium (46-2; Fig. 12A). (4) Pronotal marginal carina meeting pronotosternal suture anterolaterally (57-1; Fig. 12G, left arrow). (5) Apex of mesoventral intercoxal process abutting apex of metaventral process (81-1; Fig. 13E, middle arrow). (6) Paired pygidial defence glands opening into rectum (123-1, see Dettner, 1993, for illustration). These glands are worth highlighting because they are present also in SteNovAUS. The six larval synapomorphies are as follows: (7) setae on cranium and tergites differentiated in length into long and thick versus short and thin (136-1; Figs 5A; 17E, F), (8) antennomere 1 constricted transversely in basal part, antennae appearing 4-segmented (146-1; Fig. 5A, top arrow), (9) antennomeres 1 and 2 markedly elongate (147-1; Fig. 5A), (10) second maxillary palpomere markedly bent and at least 5× as long as wide (156-1; Fig. 16G, top arrow), (11) tibia with four to six apical setae exceeding length of claw (161-1; Fig. 16I, J, arrow), and (12) abdominal segment IX with latero-ventral projection on each side (165-1; Fig. 17I, far right arrow). The markedly elongate larval antenna and (after Kasule, 1966) larval spiracles placed on conical projections were mentioned by Thayer (2005) as autapomorphies of Steninae. However, in our analysis the latter character was recovered as a synapomorphy of Steninae + Euaesthetinae.

SteNovAUS had been referred to previously as an undescribed genus of Euaesthetinae that may actually belong in Steninae (Leschen & Newton, 2003; Betz & Kölsch, 2004). Indeed, the two known species look remarkably similar externally to some euaesthetines. The presence of an eversible prementum in these species with similarly modified 'paraglossae' (see comments relating to characters 38–41 for discussion of application of labial morphological terms in staphylinid systematics) led these authors to raise the possibility that a method of prey capture 'possibly homologous' to that of *Stenus* had evolved in Euaesthetinae (if the two species were euaesthetines). These undescribed species therefore were of particular relevance to the problems addressed in this study, as the derived mouthparts of SteNovAUS and apparently similar modifications in the euaesthetine genus *Tyrannomastax* Orousset, 1988 would have implications for potential sister-group relationships among individual genera of Steninae and Euaesthetinae if these modifications are indeed homologous. We included both species of SteNovAUS in Analyses 1 and 2, in which they were nested within Steninae as the sister group of *Stenus*. Based on Analysis 1, this relationship was supported by four unique adult synapomorphies: (1) presence of adhesive cushions on the sides of labium (40-1; Figs 11L, right arrow; 12A, left arrow), (2) absence of lateral rows or combs of setae on the hypopharynx (45-1), (3) prementum elongated into eversible rod-like structure (50-1; Fig. 11L, middle arrow), (4) palpomere rests on mentum divided by a medial longitudinal carina (Fig. 11K, arrow). Based on our results we interpret the external resemblance of SteNovAUS to some euaesthetines as convergence resulting from a shared forest leaf litter habitat, which also may explain the reduction in eye size, the appearance of long interfacetal ocular setae, and the obscured condyle of antennomere 1 in these two species. The monophyly of SteNovAUS was supported by five synapomorphies, four of which were unique: (1) presence of a mesal mound at the apex of the labium, on which the apical labial setae are placed (43-1; Fig. 12A, right arrow), (2) mentum with the anterior part deflected vertically such that the mentum sclerite is not completely in the same plane (51-1; Fig. 11L, left arrow), (3) presence of distinctly circular mesoventral procoxal rests (74-1; Fig. 13E, top arrow), (4) protibia distinctly expanded posteriorly, with the internal face excavate (90-1; Fig. 13I, arrow).

Monophyly of Euaesthetinae + Steninae (clade A)

The monophyly of the subfamilies Euaesthetinae + Steninae has been suggested by previous studies (Hansen, 1997; Leschen & Newton, 2003; Thayer, 2005) and is supported here. Naomi (1985) did not identify a sister-group relationship between Steninae and Euaesthetinae, but his study is rather anomalous among the more modern morphological literature on staphylinid systematics in using a questionable method of phylogenetic analysis (see Newton & Thayer, 1988). However, two analyses that included molecular data to explore relationships within Staphyliniformia (Caterino *et al*., 2005) and Staphylinoidea (Ballard *et al*., 1998) did not recover Euaesthetinae + Steninae as monophyletic. In our study, the monophyly of Euaesthetinae + Steninae is strongly supported by 24 unambiguously optimized morphological synapomorphies, 21 adult and three larval, which we do not list here (see Fig. 3). Based on this accumulated morphological evidence it may be concluded that Euaesthetinae and Steninae are almost certainly monophyletic, and future phylogenetic analyses should focus on elucidating the placement of this group within the larger Staphylinine group of subfamilies and the relationships among genera of Euaesthetinae.

Future morphological studies

In this study we introduce a new character set containing many novel adult and larval characters, and analyse the phylogenetic relationships of previously unstudied euaesthetine

taxa. Nevertheless, some problems with our analyses stand out and suggest new directions for the study of Euaesthetinae + Steninae and of the more inclusive Staphylinine group in which they are placed (Lawrence & Newton, 1982). For example, the strongly supported basal nodes (outgroups, and Euaesthetinae, Steninae, and these two together) contrast with the weakly supported terminal nodes within Euaesthetinae. Moreover, the euaesthetine genus *Fenderia* consistently is a highly derived terminal branch, as in Fig. 3, and has several alternative placements in our different analyses. These results suggest significant character conflict as a source of ambiguity. Character conflict and lack of supporting apomorphies are suggested also by the weakly supported relationships within Euaesthetinae (Figs 2–4), which may in part result from 'problem' taxa such as *Fenderia*. These problems will be best addressed with more complete taxon sampling and further morphological character sampling (see below).

The conclusion of Euaesthetinae monophyly or paraphyly will be most robust when all genera, and preferably multiple species-level exemplars, are included in a phylogenetic analysis of the entire Staphylinine group. Based on a preliminary survey of very limited material, and examination of primary literature for all euaesthetine genera, we predict that certain genera will be critical for a robust assessment of Euaesthetinae monophyly. The genus *Libanoeuaesthetus* Lefebvrea *et al*. (2005) was described from a late Cretaceous fossil – the oldest known euaesthetine fossil – but seems indistinguishable from the extant genus *Nordenskioldia*. Both extant genera *Nordenskioldia* and *Edaphosoma* (Nordenskioldiini) are known only from type material but will be critical additions to future analyses of the Euaesthetinae–Steninae problem because, although both genera have the denticulate or serrate labral margin (21-1), they may be the most plesiomorphy-rich genera in Euaesthetinae. Both have the primitive 5-5-5 tarsal formula, a single pair of abdominal parasclerites per segment, and lack derived labial structures of other euaesthetines (e.g. 41-1). Our analyses could have been improved by the addition of other outgroups from within the Staphylinine group, such as Leptotyphlinae and Solieriinae, which may shorten some long branches in our study.

The present study represents a fairly exhaustive survey of the major external and internal features of these beetles, but four notable morphological character systems remain poorly or completely unrepresented, namely (1) adult and (2) larval chaetotaxy, and (3) male and (4) female internal genitalia. Larval chaetotaxy – the number and distribution of macrosetae and other external cuticular sensory structures – is widely known as a useful source of morphological characters in phylogenetic studies (e.g. see review in Solodovnikov, 2007), but adult chaetotaxy has yet to be applied widely in phylogenetic analyses of rove beetles (D. J. Clarke, in preparation, and see Ashe (2005), for use of mouthpart chaetotaxy in Tachyporinae and Aleocharinae). We did not include larval chaetotaxic characters here because of the limited material available to us, and an in-depth study of adult chaetotaxic characters was beyond the scope of our present goal. However, preliminary studies suggest strikingly uniform adult macrosetal patterns within Euaesthetinae that may prove highly informative for resolving generic relationships. In addition, if larval chaetotaxy is so informative then it is likely that adult chaetotaxy holds similar promise. Of particular interest for future comparative studies is the morphology of the male aedeagus but also the highly unusual internal male genitalic structures present in certain euaesthetine genera. For example, some *Edaphus*, *Stenaesthetus*, *Schatzmayrina* and *Tamotus* species possess what has been termed a 'sperm pump' (Puthz, 1973), a highly characteristic but variably shaped structure continuous with the ejaculatory duct, which in *Tamotus* is associated with other unusual structures (see Puthz, 1973: fig. 24). Outside of Euaesthetinae, possibly the only other staphylinoid taxon known to have a structure comparable to the sperm pump in Euaesthetinae is the scydmaenid genus *Clidicus* Laporte, 1832 (Besuchet, 1970), and it is noteworthy that Scydmaenidae may actually belong in Staphylinidae, within the Staphylinine group (Lawrence & Newton, 1982). The shape and structure of the female spermatheca is widely used in taxonomic studies of Euaesthetinae (e.g. Orousset, 1990), Steninae (e.g. Naomi, 2006a, b), and other staphylinid groups. While coding characters for this analysis, we discovered numerous unusual sclerotized and unsclerotized internal structures associated with the female genitalia. Both male and female internal structures will no doubt be highly informative in phylogeny, especially at lower levels, but determining the homology of these structures must await specialized anatomical studies and a broader survey of the species within relevant genera.

Conclusions

We have contributed the first broad morphology-based phylogenetic analysis of the subfamily Euaesthetinae and paved the way for future advances in the systematics of a poorly known group of rove beetles. Based on a data matrix of 167 adult and larval characters, most of which are new, we conclude that Euaesthetinae are monophyletic, and that there is a strong case for maintaining them as a separate staphylinid subfamily. In spite of the large dataset, phylogenetic relationships among genera of Euaesthetinae remain uncertain as a result of rampant homoplasy within the adult dataset and a lack of informative variation within the larval dataset. The current system of six tribes is not supported by morphological characters, and only Stenaesthetini stands out as a potentially monophyletic group. The austral genera of Euaesthetinae do not form a monophyletic group, and several distinct evolutionary scenarios may be required to account for the presence of endemic genera in each of Australia, New Zealand and southern South America. We demonstrate that the widespread genera *Octavius* and *Protopristus* are strongly supported as monophyletic, but the genus

Alzadaesthetus, restricted to temperate South America, is possibly not monophyletic. The austral endemic genera *Austroesthetus* and *Chilioesthetus* form a strongly supported monophyletic group, corroborating Newton's (1985) view that they should be combined, whereas *Tasmanosthetus* and *Nothoesthetus* (the *Nothoesthetus* Group) were not recovered as monophyletic. The tribe Stenaesthetini contains a fifth, presently undescribed, monotypic genus, whereas *Gerhardia* should probably be combined with *Stenaesthetus*. We provide the first quantitative phylogenetic support for the monophyly of subfamily Steninae, and our preliminary study suggests that it contains a third, as yet undescribed genus, comprising two undescribed species that are phenetically considerably different from typical species of *Stenus*, but which together are the sister group of *Stenus*. In agreement with most previous morphological phylogenetic studies, the monophyly of Euaesthetinae and Steninae together is unambiguously supported by morphological characters.

Descriptive part

Key to genera of austral Euaesthetinae based on adults

The following key is to adults of all euaesthetine genera currently known from the austral region (Australia, New Zealand, Chile/Argentina and South Africa). In the final stages of completing this manuscript, South African *Schatzmayrina* (Euaesthetini) specimens were discovered in FMNH, so this genus was added to the key but is excluded from our phylogenetic study. The key has been constructed to emphasize characters observable with a stereo microscope, and which can be seen in dry- or alcohol-preserved specimens. Within couplets, characters are arranged subjectively by increasing difficulty of observation, not by relative diagnostic importance. Figure references illustrate specific characters that can be present in many genera, and therefore may not refer to an image of the reference taxon. *Alzadaesthetus* keys out in two different couplets; *Stenaesthetus* and *Gerhardia* key out together.

1. Abdominal segments IV–VI with parasclerites (abdomen margined laterally, e.g. Fig. 14F–I) 2
– Abdominal segments IV–VI without parasclerites (abdomen unmargined laterally, e.g. Fig. 14J) 7
2. Antennae 9-segmented, with large 1-segmented club; lateral pronotal carina absent; mesoventrite with two subcircular procoxal rests anteriorly (e.g. Fig. 13E, top arrow) ..... *Schatzmayrina*
– Antennae 11-segmented with 2- or 3-segmented club (e.g. Fig. 11G); lateral pronotal carina present (e.g. Fig. 12F, arrow); mesoventrite without subcircular procoxal rests anteriorly (e.g. Fig. 13D) 3
3. Head dorsally with deep furrows, ventrally with gular sutures separated; pronotum strongly constricted basally and with basolateral longitudinal carinae and basal foveae; metacoxae with mesal edges widely separated ..... *Edaphus* (Fig. 1A)
– Head dorsally without deep furrows, ventrally with gular sutures united at least anteriorly; pronotum not strongly constricted basally, basolateral longitudinal carinae and foveae absent; metacoxae with mesal edges contiguous or very closely spaced (e.g. Fig. 14E, arrow) 4
4. Intersegmental membranes of abdominal segments attached apically to preceding segments (e.g. Fig. 14G, I); antennae with compact club (antennomeres 10 and 11 closely spaced, Fig. 11G); head and neck distinctly separated dorsally by nuchal groove; abdominal segments III–VII each with two pairs of parasclerites ... 5
– Intersegmental membranes of abdominal segments attached preapically to preceding segments (e.g. Fig. 14 H, J); antennae with loose club (antennomeres 10 and 11 well separated; head and neck distinguished only by faintly impressed nuchal line; abdominal segments III–VI each with one pair of parasclerites, segment VII without parasclerites 6
5. Antennomeres 10 and 11 distinctly separated by antennal stem; mesothoracic anapleural carina absent; male tergite IX separated from tergite X by distinct suture (Fig. 14L, arrow); left mandible with small tooth on ventral side; labium with medial overlapping teeth (Fig. 12C, arrow) ..... *Protopristus*
– Antennomeres 10 and 11 partly fused (Fig. 11G); mesothoracic anapleural carina distinct at least anteriorly (e.g. Fig. 13F, top left arrow); male tergite IX indistinguishably fused to tergite X (Fig. 14M); left mandible without tooth on ventral side; labium without medial tooth (Fig. 11I) ..... *Octavius*
6. Total body length 3–4 mm; head, pronotum, and elytra deeply punctate, each puncture large and setiferous; eyes very large, more than half head length (measured from frontal margin of head to nuchal groove); elytra without epipleural fold (most similar to Fig. 13B); tarsal formula 5-5-5 ..... *Alzadaesthetus chilensis*
– Total body length 1.5–2.5 mm; head, pronotum, and elytra impunctate; eyes small, less than half head length (measured from frontal margin of head to nuchal groove); elytra with distinct epipleural fold (Fig. 13A, arrow); tarsal formula 4-4-4 ..... *Nothoesthetus*
7. Abdominal tergite III separated from sternite by suture or parasclerite (Fig. 14J, top arrow) 8
– Abdominal tergite III fused with sternite to form solid ring 10
8. Anterior margin of labrum smooth (Fig. 11A); antennae much longer than head, filiform, with indistinct club, apex of antennomere 10 not concave to receive 11; paramedial carinae of abdominal sternite III present (Fig. 14J, bottom left arrow); tarsal formula 5-5-4 ..... *Stenaesthetus* (Fig. 1D)/*Gerhardia*
– Anterior margin of labrum serrate (Fig. 11C); antennae subequal in length to head, not filiform, with large distinct club, apex of antennomere 10 concave to receive 11; paramedial carinae of sternite III absent; tarsal formula 4-4-4 9

9. Antennae with loose 2-segmented club; pronotum and elytra smooth or shallowly punctate; elytral disc without lateral groove ..... *Austroesthetus*
– Antennae with compact 2-segmented club (similar to Fig. 11G); pronotum and elytra heavily sculptured (Fig. 12L); elytral disc with distinct lateral groove (Fig. 12L, arrow) ..... *Chilioesthetus*
10. Tarsal formula clearly 5-5-4; basal tarsomere of hind leg distinctly elongate and much longer than combined length of succeeding two tarsomeres 11
– Tarsal formula 4-4-4 or 5-5-5 (may be difficult to see); basal tarsomere of hind leg subequal to length of, or shorter than combined length of succeeding two tarsomeres 12
11. Pronotum distinctly longitudinally grooved laterally and/or dorsally; eyes large, more than half head length (measured from frontal margin of head to nuchal groove); mesoventrite not carinate near middle (e.g. Fig. 13D); lateral margin of galea with large cuticular projection (Fig. 11M, left arrow); labium with pair of sclerotized spines (Fig. 11M, middle arrow) ..... *Agnosthaetus* (Fig. 1B)
– Pronotum entirely smooth, without grooves; eyes small, less than half head length (measured from frontal margin of head to nuchal groove); mesoventrite with paired arcuate carinae at middle; lateral margin of galea smooth, without cuticular projection (Fig. 12B); labium with pair of small membranous digitiform processes ..... Stenaesthetini: EuaAUS
12. Eyes tiny or absent; elytra with epipleural fold (similar to Fig. 13A, arrow); prosternal intercoxal process sharp apically (Fig. 12E, H, K); intermesocoxal process of metaventrite carinate ..... *Tasmanosthetus*
– Eyes larger, distinct (Fig. 11A, C, E); elytral epipleural fold absent (most similar to Figs 12O; 13B); prosternal intercoxal process rounded apically (Fig. 12I, J); intermesocoxal process of metaventrite spiniform 13
13. Bicoloured, elytra and terminal abdominal segments distinctly citrine, rest of body dark brown to black; head, pronotum, and elytra distinctly punctate, each puncture large and setiferous; margin of labrum with large teeth ..... *Alzadaesthetus furcillatus* (Fig. 1C)
– Unicoloured, brownish; head, pronotum, and elytra impunctate; labrum only finely serrate 14
14. Eyes less than half head length (measured from frontal margin of head to nuchal groove); pronotum setose, with deep basolateral depressions; mesocoxal acetabula delimited posteriorly by carina; mesoventral intermesocoxal process rounded, projecting between coxae, contacting intermesocoxal process of metaventrite (Fig. 13D, middle arrow); labium with pair of elongate membranous digitiform processes (Fig. 12B, top arrow) ..... *Mesoaesthetus*
– Eyes occupying nearly whole side of head; pronotum glabrous, basolateral depressions absent; mesocoxal acetabula not delimited posteriorly by carina; intermesocoxal process of mesoventrite sharp, projecting obliquely away from body, distinctly separated from intermesocoxal process of metaventrite; digitiform labial processes absent ..... *Kiwiaesthetus*

Key to all known larvae of the genera of Euaesthetinae

Larvae of *Octavius* have very slight mandibular serration visible only at 500× magnification so this genus is keyed as both with and without mandibular serration.

1. Mandibles with serration along mesal edge (Fig. 5B, top arrow, C, arrow) 2
– Mandibles without serration along mesal edge (e.g. Fig. 5D–F) 4
2. Nuchal carina absent (Figs 5C; 7D); serration on mesal edge of mandibles arranged in two parallel rows of teeth (Fig. 5C, arrow); nasale without medial tooth (Fig. 5C); tentorial pits located at posterior edge of ventral surface of head capsule adjacent to occipital foramen (Fig. 7D, left arrow); ventral surface of head capsule with two anteriorly divergent sutures originating from posterior tentorial pits (Fig. 7D, right arrow) ..... *Edaphus*
– Nuchal carina present (e.g. Fig. 5B, arrow); serration on mesal edge of mandibles arranged in one row of teeth (Fig. 5B, top arrow); nasale with medial tooth (Figs 5B, 6D, 9M, N); tentorial pits located at about middle of ventral surface of head capsule (Figs 7C, arrow, 8E); ventral surface of head capsule with single suture extending between posterior tentorial pits (Figs 7C, 8E, arrow) 3
3. Mandibular serration consisting of 10 or more teeth visible in dissecting microscope (Fig 5B, arrow), with paramedial teeth on nasale markedly wider than medial tooth (Figs 9D, 16E); mala wider than long; apical antennomere not reduced in size (Fig 16C, left arrow) ..... *Euaesthetus*
– Mandibular serration consisting of about 5 teeth visible on cleared slide preparations under magnification of about 500×; paramedial teeth on nasale about as wide as medial tooth (Figs 6D, 9M, N); mala longer than wide; apical antennomere much reduced in size (Fig. 6 D) ..... *Octavius*
4. Nasale with medial tooth (Figs 5F, 9F, I, J, M, N, 16A, left arrow) 5
– Nasale without medial tooth (e.g. Figs 5D, E, 6A, C, E) 8
5. Antennal sensorium (Fig. 6D, arrow) not longer than maximal width of penultimate antennomere, bulbous; mandibular serration consisting of about 5 very small teeth along mesal edge, visible on cleared slide preparations under magnification of about 500×; nasale with paramedial teeth not longer than medial tooth (Figs 5 D; 9M, N) ..... *Octavius*
– Antennal sensorium 1.2–1.5× as long as maximal width of penultimate antennomere, parallel-sided along most of its length (Fig. 16A, right arrow); mandibles not serrate along mesal edge (e.g. Figs 5 D-F; 6B); nasale with paramedial teeth markedly longer than medial tooth (Figs 6B; 9F, I, J; 16A) ... 6

6. Stemmata reduced in size and number, hardly visible in dorsal view (Fig. 5F); nasale as in Figs 5F; 9J ..... *Chilioesthetus*
– Stemmata well developed, easily visible in dorsal view (Figs 6B; 16A); nasale different 7
7. Nasale as in Fig. 16A, with 7 teeth along margin ..... *Austroesthetus*
– Nasale as in Fig. 6B, with 5 teeth along margin ..... Eua?LTAS
8. Central part of nasale almost straight and without teeth (Fig. 5E); basal labial palpomere originating from mesal part of anterior edge of markedly developed palpiger, with lateral part of palpiger forming a lobe (Figs 5E, arrow, 9H) *Alzadaesthetus furcillatus*
– Central part of nasale with markedly developed teeth (Figs 5D; 6A, C, E); labial palpiger reduced 9
9. Nasale with all teeth large and of about equal size, each side of nasale bearing 3 large teeth forming a crown-with medial 2 teeth of each crown equally shaped and smaller than the lateral tooth (Figs 6E; 9O); posterior tentorial pits surrounded by minute teeth visible with compound microscope (Fig. 8F, bottom arrow) ..... *Protopristus*
– Nasale with paramedial teeth markedly larger than others (Figs 5D; 6A, C; 9G, K, L); teeth of nasale not forming crowns and differently shaped; posterior tentorial pits not surrounded by minute teeth 10
10. Paramedial teeth of nasale about 3× as long as any other teeth (Figs 5D; 9G) ..... *Agnosthaetus*
– Paramedial teeth of nasale not more than 2× as long as any other teeth (Figs 6A, C; 9K, L) 11
11. Nasale with deep and narrow notch between paramedial teeth (Figs 6A; 9K); sides of head capsule subparallel to slightly convergent posteriorly (Fig. 6A); mentum with one long and one short seta on each side (Fig. 8B, right arrow) ..... *Fenderia*
– Nasale barely notched between paramedial teeth (Figs 6C; 9L); sides of head capsule converging posteriorly (Fig. 6C); mentum with one short seta on each side (Fig. 8D, arrow) ..... *Nothoesthetus*

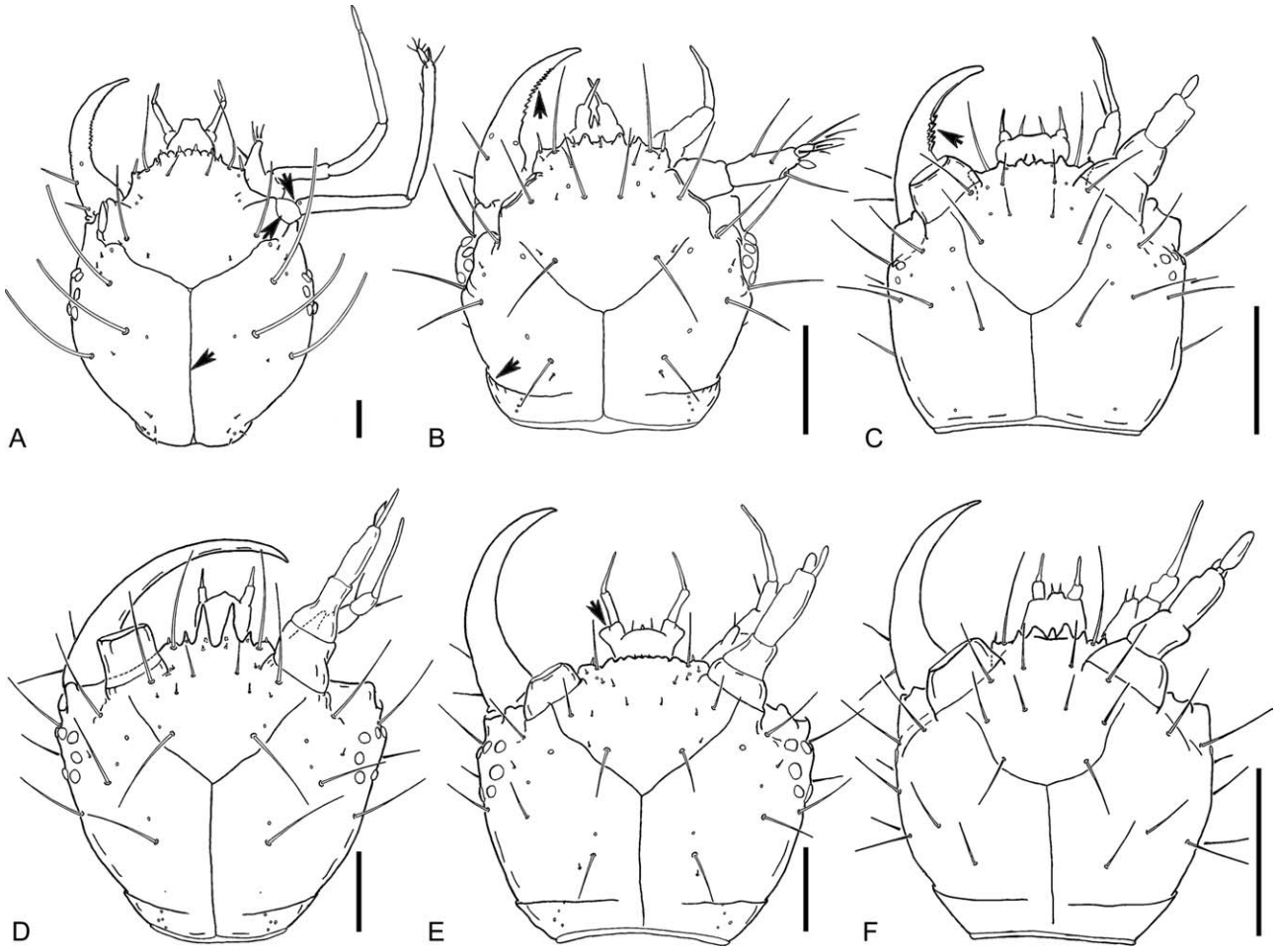

Fig. 5. Larvae of Steninae and Euaesthetinae, heads, dorsal view (right mandible, left maxilla and left antenna omitted): (A) *Dianous* sp.; (B) *Euaesthetus* sp.; (C) *Edaphus* sp.; (D) *Agnosthaetus* sp.; (E) *Alzadaesthetus furcillatus* Sáiz; (F) *Chilioesthetus* sp. Scale bars: 100 μm. Arrows indicate structures referred to in the text.

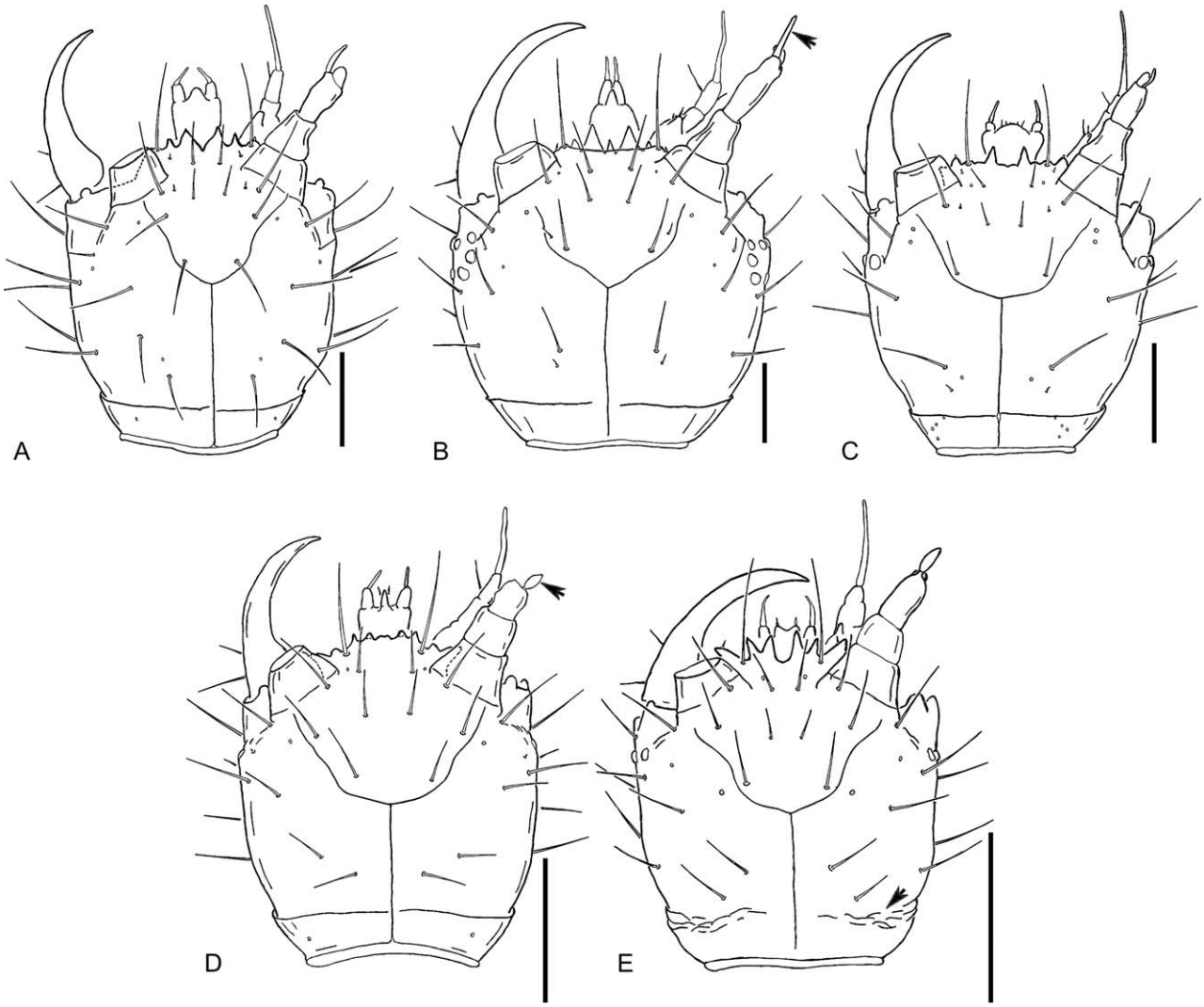

Fig. 6. Larvae of Euaesthetinae, heads, dorsal view (right mandible, left maxilla and left antenna omitted): (A) *Fenderia* sp.; (B) Eua?LTAS; (C) *Nothoesthetus* sp.; (D) *Octavius* sp. (*Octavius*PAN); (E) *Protopristus* sp. (*Protopristus*NZ). Scale bar: 100 μm. Arrows indicate structures referred to in the text.

Diagnostic descriptions of adults and larvae of selected Euaesthetinae genera

In this section we provide adult diagnostic descriptions for all euaesthetine genera currently known from the south-temperate region (Australia, New Zealand, Chile/Argentina and South Africa), including the South African genus *Schatzmayrina* (Euaesthetini), which, however, was excluded from our phylogenetic study. We cannot distinguish *Stenaesthetus* and *Gerhardia* (Stenaesthetini) and so provide a diagnosis only for *Stenaesthetus*. We also provide larval diagnostic descriptions for all genera of Euaesthetinae known from larvae. Matching adult diagnoses are provided for non-south-temperate genera for which we describe the larvae (*Fenderia*, *Euaesthetus* and *Edaphus*). The genera are grouped alphabetically into their respective current tribes, which are arranged alphabetically. With the possible exception of Stenaesthetini, these tribes probably are not monophyletic. Figure references illustrate specific characters that can be present in many genera, and therefore may not refer to an image of the diagnosed taxon.

Tribe Alzadaesthetini Scheerpeltz, 1974

Alzadaesthetus Kistner, 1961 (Figs 5E; 7F; 9H; 11N; 13C, H, L)

Type species. *Alzadaesthetus chilensis* Kistner, 1961

Adult diagnosis. Head, pronotum and elytra punctate; gular sutures united; eyes large, occupying most of side of head; labium with pair of digitiform membranous processes

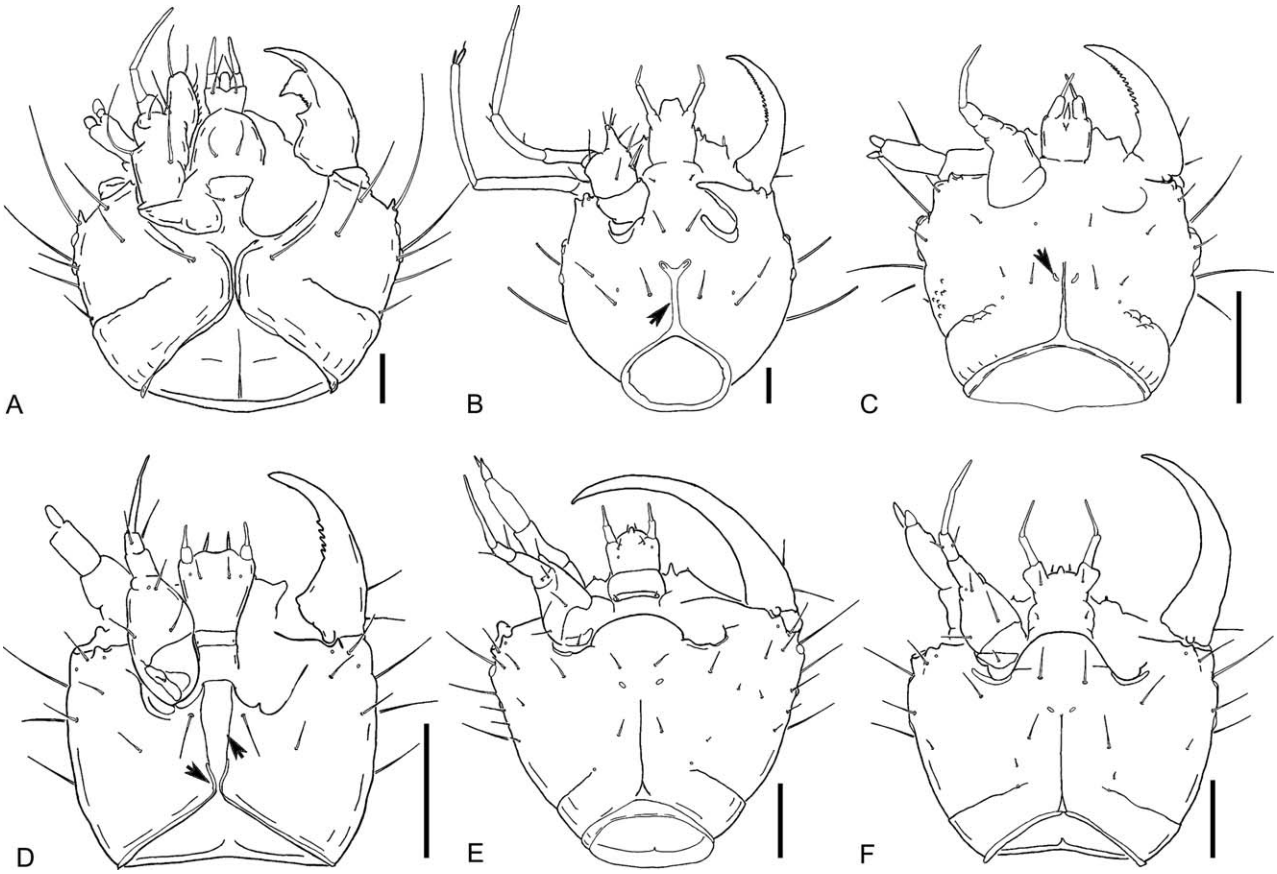

Fig. 7. Larvae of Megalopsidiinae, Steninae and Euaesthetinae, heads, ventral view (right mandible, left maxilla and left antenna omitted): (A) *Megalopinus* sp.; (B) *Dianous* sp.; (C) *Euaesthetus* sp.; (D) *Edaphus* sp.; (E) *Agnosthaetus* sp.; (F) *Alzadaesthetus furcillatus* Sáiz. Scale bars: 100 μm. Arrows indicate structures referred to in the text.

(Fig. 12B, top arrow); lateral margin of galea with small cuticular projection (Fig. 11M, left arrow); wings absent or vestigial; mesothoracic anapleural carina present only posteriorly (Fig. 13D, left arrow); tarsal formula apparently 5-5-5, but with the two basal tarsomeres partly to entirely fused; base of abdominal segments with arcuate carinae (Fig. 14H, right arrow); abdominal segments III–VI each with or without one pair of parasclerites, VII without parasclerites; sternite III with lateral carina (Fig. 14J, middle arrow) obsolete before apex of sternite; tergite IX of male entire, moderately elongate in front of tergite X; female with tergite IX divided dorsally or reduced to thin strip in front of tergite X (Fig. 15C, arrow), gonocoxites I and II articulated ipsilaterally (Fig. 15D, right arrow).

Adult material examined. *Alzadaesthetus furcillatus* Sáiz, 1972. CHILE: 1♂, 1♀, Osorno Prov., Parque Nacional Puyehue, 4.1 km E Anticura, 430 m, Valdivian rainforest (trap site 662), leaf and log litter (berlesate), 19-26.xii.1982 (*Newton, Thayer*). Chiloé Pr.: 1♂, 1♀ (SEM), Miraflores, road to, 0.6 km W Ruta 5, 42°46.7′S, 73°47.7′W, 130 m, secondary Valdivian rainforest with few conifers (site ANMT 1063), leaf and log litter (berlesate; FMHD#2002-077), 12.xii.2002 (*Newton, Thayer*); 1♀ (SEM), Quemchi, 11 km W of (11 km E Hwy 5), 42°10.4′S, 73°35.7′W, 140 m, Valdivian rainforest remnant with thick bamboo understorey (site ANMT1060), leaf and log litter (berlesate; FMHD#2002-068), 10.xii.2002 (*Newton, Solodovnikov*). *Alzadaesthetus chilensis* Kistner, 1961. CHILE: 1♂, 1♀, Chiloé, Piruquina, 23.i.1970 (*Cekalovic*); 2♂, 2♀ (SEM), Reg. Los Lagos, Antillanca, 40°23.4′S, 72°9.6′W, 700 m, *Nothofagus–Podocarpus* forest (CHI-84), 29.x.1990 (*Endrödy-Younga*) (TMSA).

Larval diagnosis. Nuchal carina present, linear; stemmata fully developed, not or slightly protruding laterally (Fig. 5 E); teeth of nasale small and indistinct (Fig. 9H); ventral surface of head capsule with posterior tentorial pits located at about midlength of head, without anteriorly divergent ridges (Fig. 7F); mesal edges of mandibles smooth; apical antennomere two-thirds length of antennal sensorium, length to width ratio 1.5; antennal sensorium elongate and narrow, parallel-sided along much of its length, subequal in length to width of penultimate antennomere; mala small but clearly recognizable, as long as wide, with one long and one short seta; labial palpiger present, basal labial palpomere originating from its mesal part with lateral part flattened

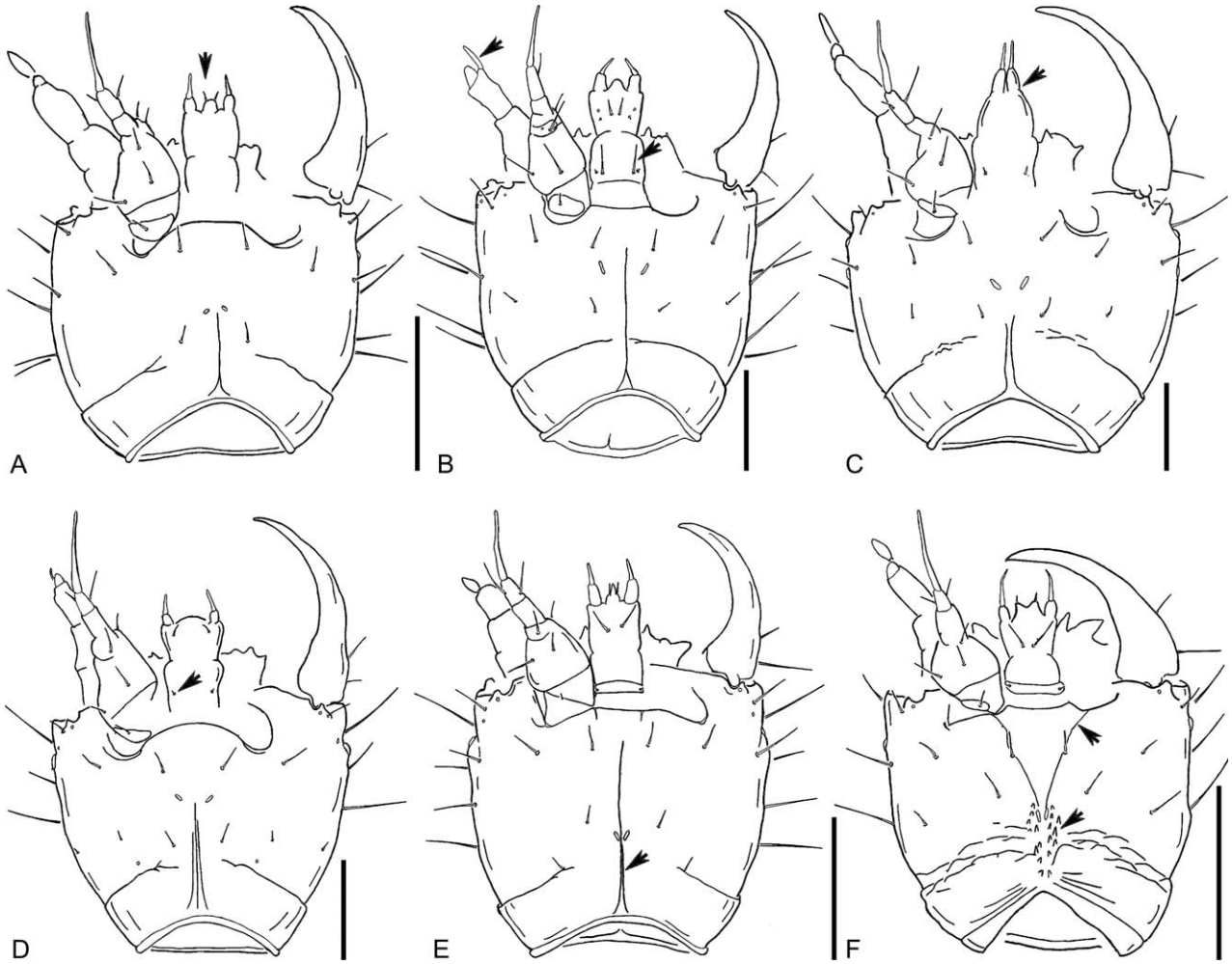

Fig. 8. Larvae of Euaesthetinae, heads, ventral view (right mandible, left maxilla and left antenna omitted): (A) *Chilioesthetus* sp.; (B) *Fenderia* sp.; (C) Eua?LTAS; (D) *Nothoesthetus* sp.; (E) *Octavius* sp. (*Octavius*PAN); (F) *Protopristus* sp. (*Protopristus*NZ). Scale bars: 100 μm. Arrows indicate structures referred to in the text.

and modified as lobes (Fig. 5E, arrow); ligula half as wide as basal labial palpomere, no more than half of length of basal labial palpomere, rounded at apex; tibia abruptly styliform in apical half; urogomphi evenly narrowed towards apices.

Larval material examined. *Alzadaesthetus furcillatus* Sáiz, 1972. CHILE: 1 larva (HW = 1.00 mm), 1 associated ♀, Osorno Prov., Parque Nacional Puyehue, Antillanca road, 490 m, Valdivian rainforest, leaf & log litter (berlesate), 20-25.xii.1982 (*Newton, Thayer*).

Tribe Austroesthetini Cameron, 1944

Austroesthetus Oke, 1933 (Figs 9I; 12D; 13M; 15A; 16A, H; 17C)

Type species. *Austroesthetus passerculus* Oke, 1933

Adult diagnosis. Head, pronotum, and elytra smooth or very finely sculptured; gular sutures united; eyes large, more than half head length (measured from frontal margin of head to nuchal line); left mandible with minute subapical tooth below preapical tooth; labium with small pair of digitiform membranous processes (Fig. 12D, left arrow); antennae with loose 2-segmented club, antennomere 10 concave to receive 11; pronotum with small basolateral impression on each side; mesothoracic anapleural carina present only posteriorly (Fig. 13D, left arrow), or absent; metaventrite carinate anteriorly; tarsal formula 4-4-4; abdominal segment III with one pair of parasclerites, IV–VI each with tergite and sternite fused into solid ring, VII without parasclerites; sternite III with lateral carina (Fig. 14 J, middle arrow) reaching middle of sternite; tergites IX and X of male indistinguishably fused (Fig. 14M); female with tergite IX divided dorsally or reduced to thread-like strip in front of tergite X (Fig. 15A, left arrow), gonocoxites I and II

Fig. 9. Larvae of Megalopsidiinae, Steninae and Euaesthetinae, anterior part of head showing nasale (dorsal view): (A) *Megalopinus* sp.; (B) *Dianous* sp.; (C) *Stenus* sp.; (D) *Euaesthetus* sp.; (E) *Edaphus* sp.; (F) Eua?LTAS; (G) *Agnosthaetus* sp.; (H) *Alzadaesthetus furcillatus*; (I) *Austroesthetus* sp.; (J) *Chilioesthetus* sp.; (K) *Fenderia* sp.; (L) *Nothoesthetus* sp.; (M) *Octavius* sp: (*Octavius*PAN); (N) *Octavius* sp. (*Octavius*SA); (O) *Protopristus* sp. (*Protopristus*NZ). Scale bars: 100 μm. Arrows indicate structures referred to in the text.

Fig. 10. Larvae of Megalopsidiinae, Steninae and Euaesthetinae, heads, details of morphology: (A) *Megalopinus* sp., head capsule (ventral); (B) *Dianous* sp., head capsule (ventral); (C) *Agnosthaetus* sp., tentorial pits, maxillae and labrum (ventral); (D) *Agnosthaetus* sp., head (dorsal); (E) *Agnosthaetus* sp., head (ventral); (F) *Agnosthaetus* sp., prementum and mentum (ventral); (G) *Agnosthaetus* sp., submentum (ventral); (H) *Agnosthaetus* sp., tentorial pits and posterior arms of tentorium (ventral); (I) *Agnosthaetus* sp., cardo, stipes and part of submentum (ventral); (J) Eua?LTAS, abdominal segments VIII, IX (with urogomphi) and X (pygopod) (dorsal); (K) *Fenderia* sp., abdominal segments VIII, IX (with urogomphi) and X (pygopod) (lateral); (L) *Fenderia* sp., thorax (lateral). Scale bars: 100 μm. Arrows indicate structures referred to in the text.

articulated ipsilaterally (Fig. 15D, right arrow); aedeagus of male with bilobed parameres.

Adult material examined. Austroesthetus passerculus Oke, 1933. AUSTRALIA: Victoria: 1♂, 1♀, Acheron Gap, near Warburton, 750 m, debris under bark of *Eucalyptus regnans*, 30.iv.1978 (*Peck, Kukalová-Peck*); 2♂, 3♀ (SEM), Warburton, Cement Creek, 670 m, *Nothofagus cunninghamii* etc. forest, leaf and log litter (berlesate), 10-17.i.1980 (*Newton, Thayer*). *Austroesthetus* sp. Queensland: 1♀,

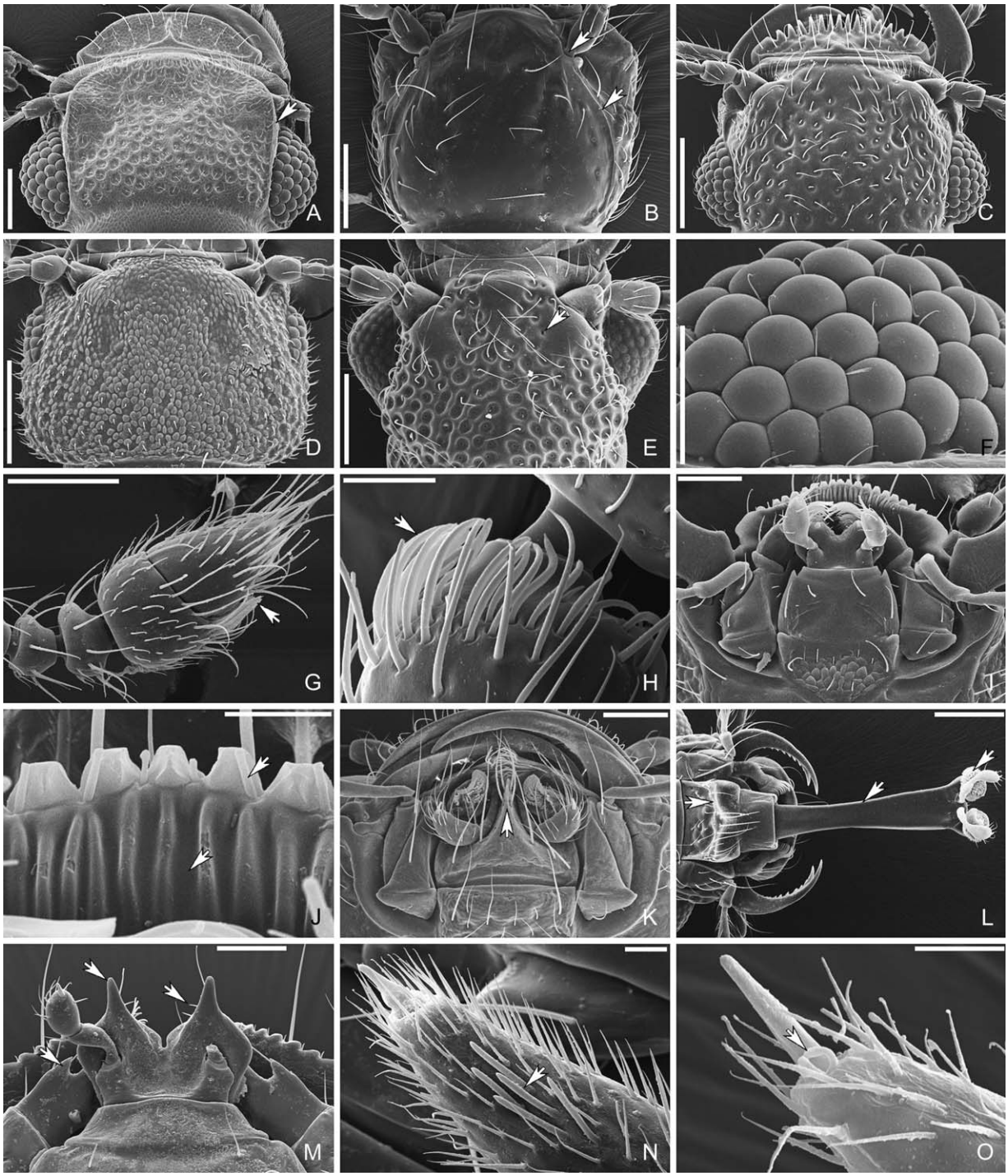

Fig. 11. Scanning electron micrographs of head and mouthpart structures of Euaesthetinae and Steninae: (A) *Stenaesthetus* sp.; (B) *Fenderia* sp.; (C) *Euaesthetus* sp.; (D) *Octavius* sp. (*Octavius*SA); (E) SteNovAUS1W; (F) *Stenaesthetus* sp., ommatidia with interfacetal setae; (G) *Octavius* sp. (*Octavius*SA), antennal club; (H) *Kiwiaesthetus* sp., antennomere 9; (I) *Octavius* sp. (*Octavius*SA), mouthparts; (J) *Octavius* sp. (*Octavius*SA), detail of epipharynx; (K) *Stenus* sp., mouthparts; (L) SteNovAUS1W, mouthparts; (M) *Agnosthaetus* sp., mouthparts; (N) *Alzadaesthetus furcillatus* Sáiz, maxillary palpomeres 3 and 4; (O) *Protopristus* sp. (*Protopristus*NZ), maxillary palpomeres 3 and 4. Scale bars for H, J, N, O: 10 μm; F, G, I, M: 50 μm; and A–E, K, L: 100 μm. Arrows indicate structures referred to in the text.

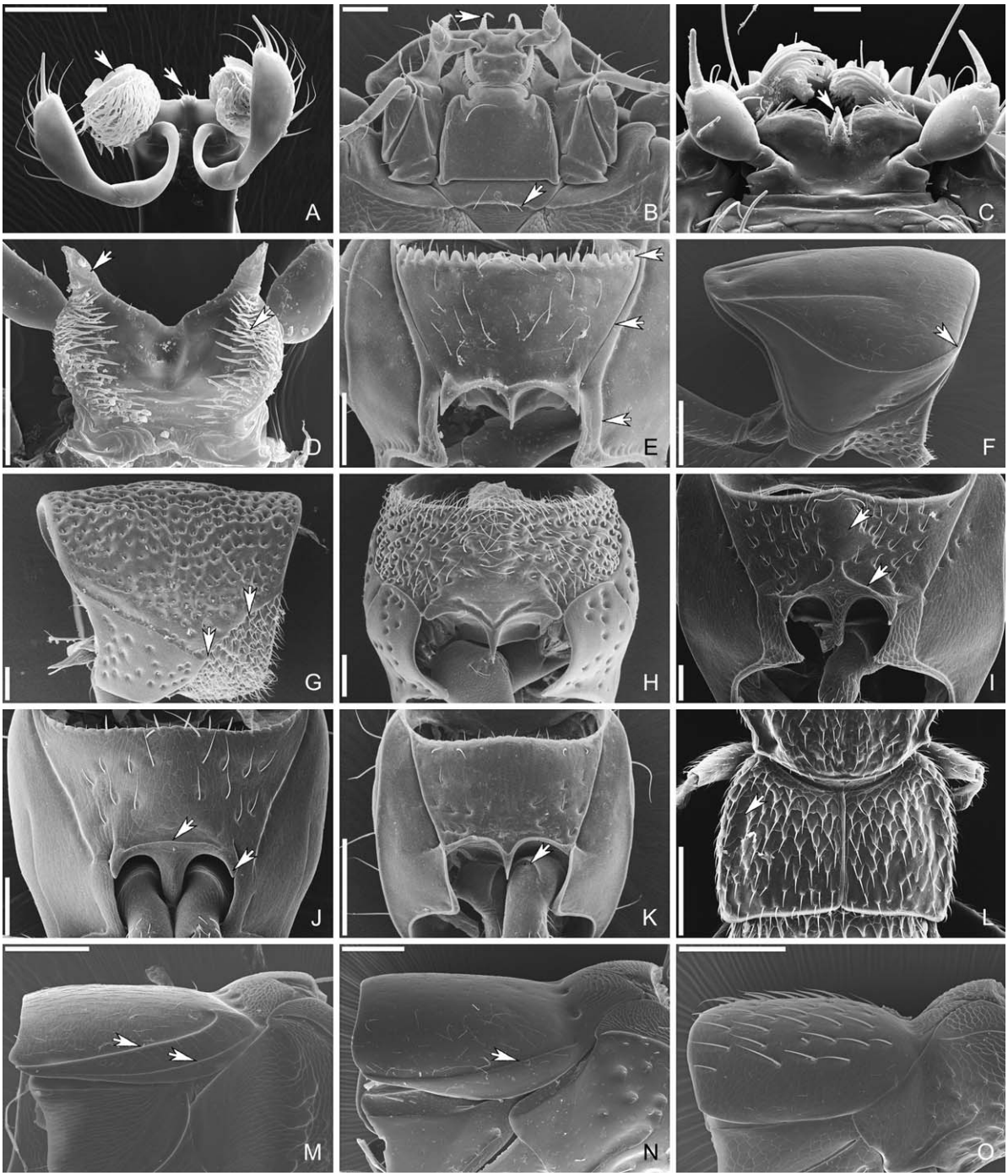

Fig. 12. Scanning electron micrographs of mouthpart and thoracic structures of Euaesthetinae and Steninae: (A) SteNovAUS1W, labial structures; (B) *Stenaesthetus* sp., mouthparts; (C) *Protopristus* sp. (*Protopristus*TAS), mouthparts; (D) *Austroesthetus* sp., labium (dorsal); (E) *Edaphus* sp., prothorax (ventral); (F) *Stenaesthetus mrazi* Rambousek, 1915, prothorax (right lateral); (G) *Stenus* sp., prothorax (right lateral); (H) *Stenus* sp., prothorax (ventral); (I) *Stenaesthetus mrazi*, prothorax (ventral); (J) *Kiwiaesthetus* sp., prothorax (ventral); (K) *Fenderia* sp., prothorax (ventral); (L) *Chilioesthetus* sp., elytra; (M) *Stenaesthetus mrazi*, pterothorax (right lateral); (N) *Agnosthaetus* sp., pterothorax (right lateral); (O) *Kiwiaesthetus* sp., pterothorax (right lateral). Scale bars for C: 10 μm; A, B, D, E, I, J: 50 μm; F–H, K–O: 100 μm. Arrows indicate structures referred to in the text.

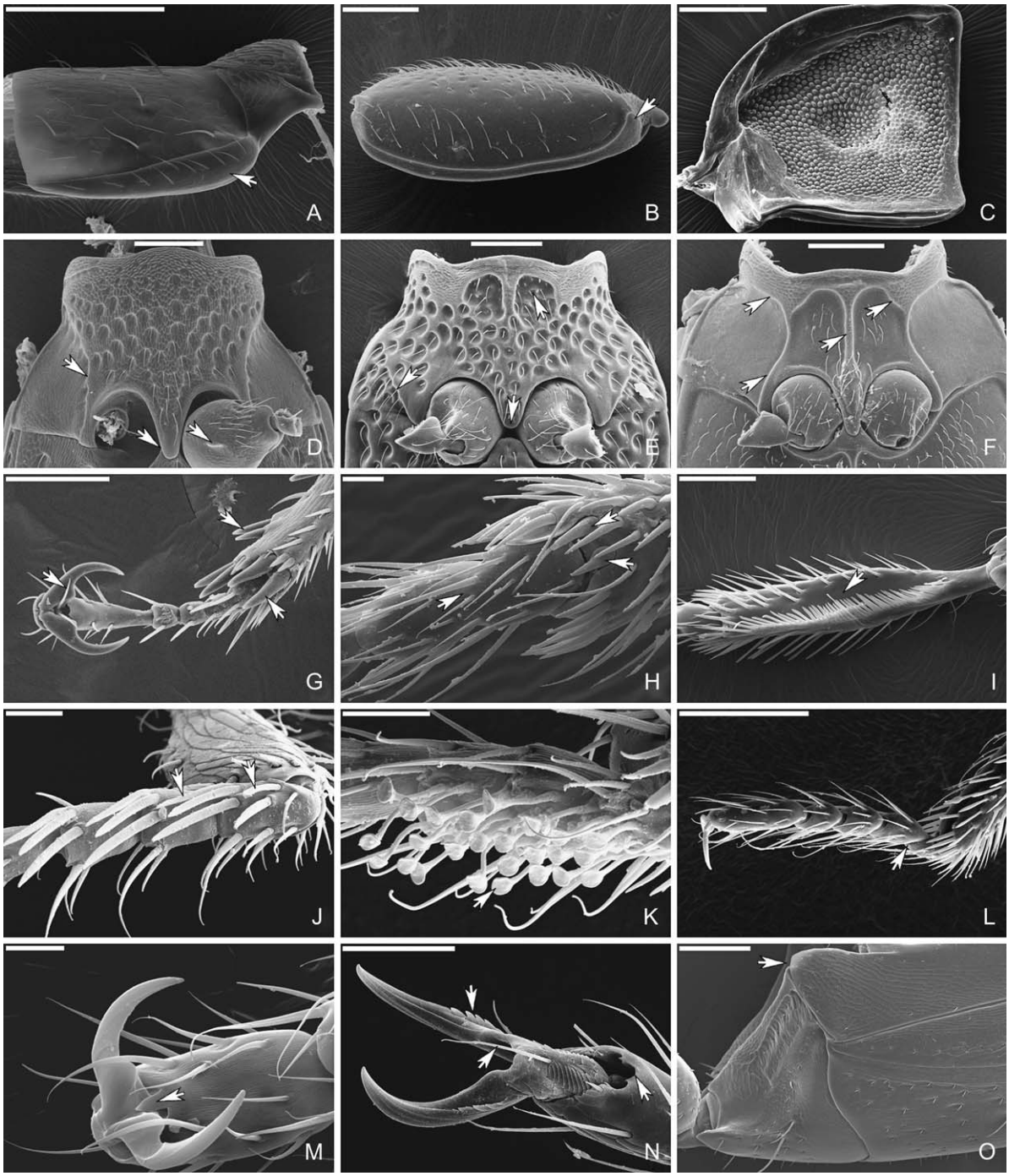

Fig. 13. Scanning electron micrographs of Euaesthetinae, Steninae, *Megalopinus* (Megalopsidiinae) and *Siagonium* (Piestinae): (A) *Nothoesthetus* sp., elytra (right lateral); (B) *Euaesthetus* sp., elytra (right lateral); (C) *Alzadaesthetus furcillatus* Sáiz, left elytron (ventral); (D) *Stenaesthetus* sp., pterothorax (ventral); (E) SteNovAUS1W, pterothorax (ventral); (F) *Euaesthetus* sp., pterothroax (ventral); (G) *Siagonium punctatum* LeConte, mesotarsus; (H) *Alzadaesthetus furcillatus* Sáiz, protarsus (ventral); (I) SteNovAUS2F, protibia (ventral); (J) *Protopristus* sp. (*Protopristus*TAS), metatarsus (ventral); (K) *Protopristus* sp. (*Protopristus*TAS), protarsus of male (ventral); (L) *Alzadaesthetus chilensis* Kistner, protarsus (dorsal); (M) *Austroesthetus* sp., protarsal claws (ventral); (N) *Megalopinus* sp., protarsal claws (ventral); (O) *Siagonium punctatum* LeConte, pterothorax (right lateral). Scale bars for H, J, K, M: 10 μm; I, N: 50 μm; A–G, L, O: 100 μm. Arrows indicate structures referred to in the text.

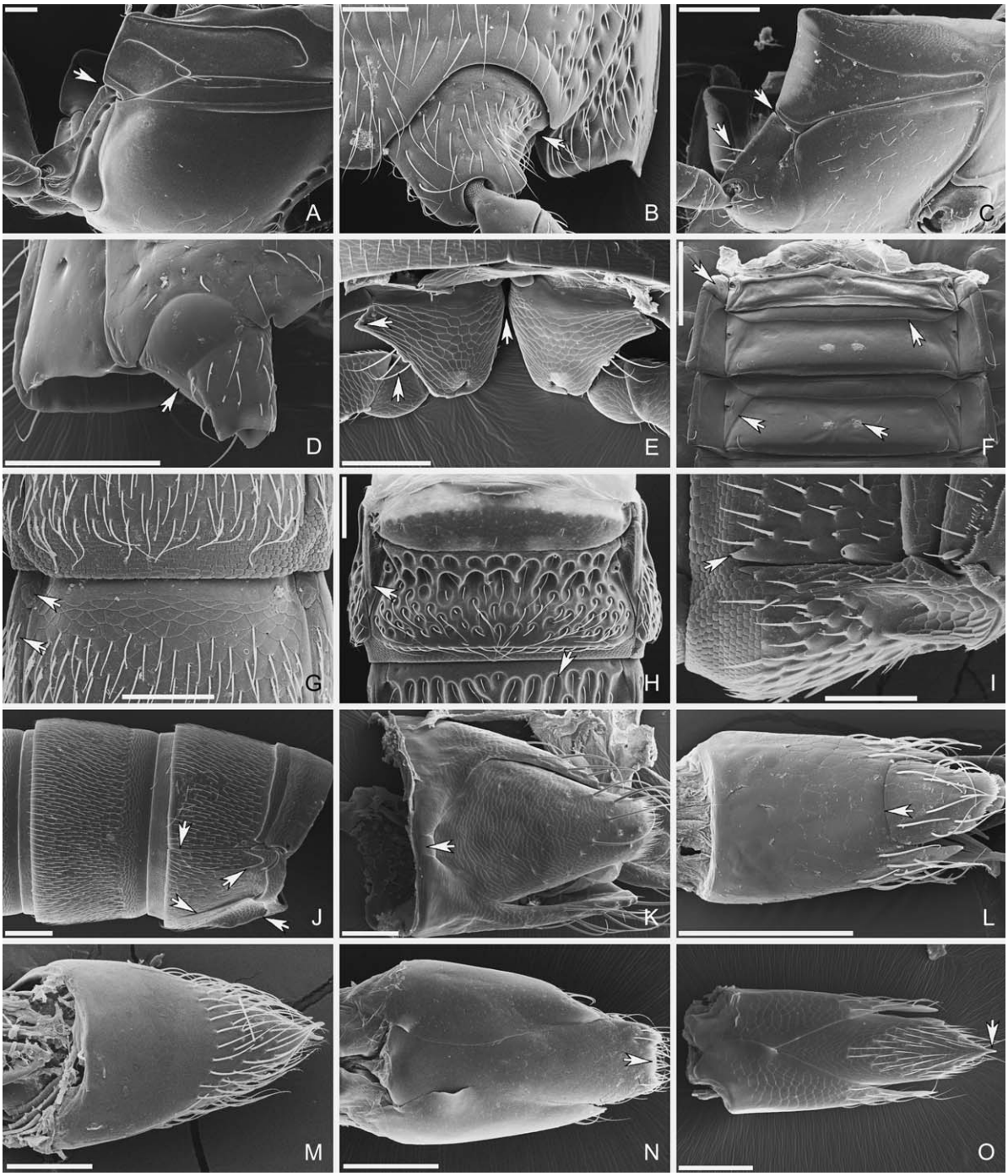

Fig. 14. Scanning electron micrographs of Euaesthetinae, Steninae, *Megalopinus* (Megalopsidiinae) and *Oxyporus* (Oxyporinae): (A) *Megalopinus* sp., pterothorax (right lateral); (B) *Stenus* sp., metaventrite and left metacoxa (ventral); (C) *Euaesthetus* sp., pterothorax and right metacoxa (right lateral); (D) *Fenderia* sp., metaventrite and right metacoxa (ventral); (E) *Stenaesthetus mrazi* Rambousek, 1915, metacoxae (dorsal); (F) *Oxyporus* sp., abdominal segments II–IV; (G) *Protopristus* sp. (*Protopristus*TAS), abdominal segments VI and VII (dorsal); (H) SteNovAUS1W, abdominal segments II–IV (dorsal); (I) *Octavius* sp. (*Octavius*SA), abdominal segment III (right lateral); (J) *Stenaesthetus mrazi*, abdomen (right lateral); (K) *Oxyporus* sp., male genital segment (dorsal); (L) *Protopristus* sp. (*Protopristus*TAS), male genital segment (dorsal); (M) *Octavius* sp. (*Octavius*SA), male genital segment (dorsal); (N) SteNovAUS1W, male genital segment (ventral); (O) *Nothoesthetus* sp., male genital segment (ventral). Scale bars for I, G: 50 μm; A–E, H, J–O: 100 μm; F: 500 μm. Arrows indicate structures referred to in the text.

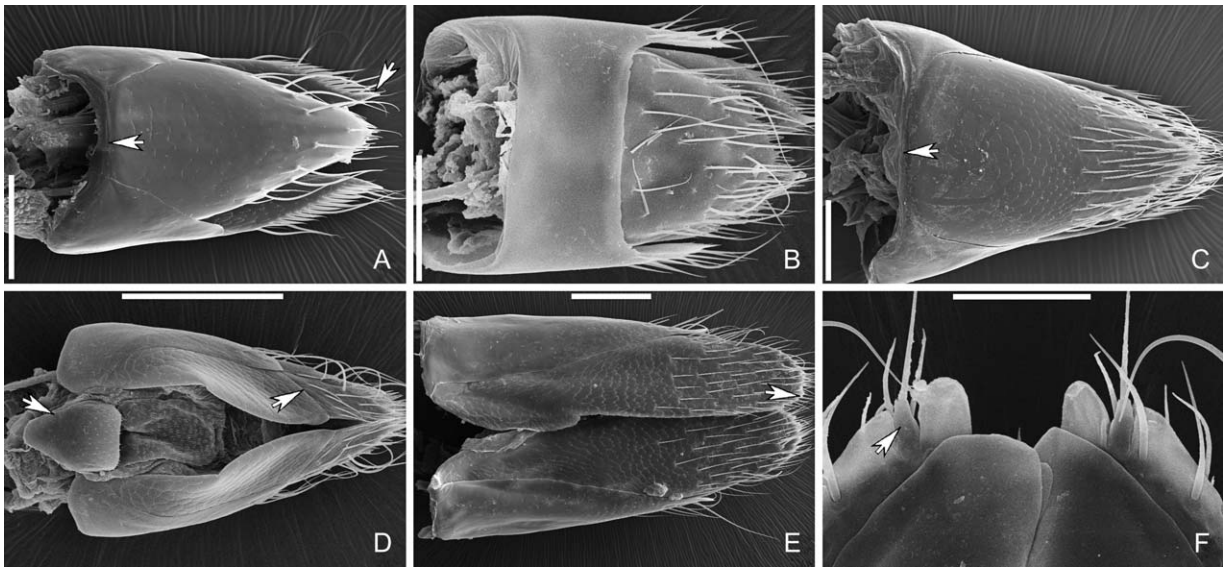

Fig. 15. Scanning electron micrographs of Euaesthetinae, Steninae and *Siagonium* (Piestinae): (A) *Austroesthetus* sp., female genital segment (dorsal); (B) *Edaphus* sp., female genital segment (dorsal); (C) *Agnosthaetus* sp., female genital segment (dorsal); (D) *Protopristus* sp. (*Protopristus*TAS), female genital segment (ventral); (E) *Stenus* sp., female genital segment (ventral); (F) *Siagonium punctatum* LeConte, apex of female gonocoxites. Scale bars for F, B: 50 μm; A, C–E: 100 μm. Arrows indicate structures referred to in the text.

Mount Bellenden Ker (summit), 1560 m, moss forest, berlesate (ANIC 367), 7.vii.1971 (*Taylor, Feehan*).

Larval diagnosis. Nuchal carina present, linear; stemmata fully developed, not or slightly protruding laterally; nasale with medial tooth (Fig. 16A, left arrow), paramedial teeth slightly longer than others (Figs 9I; 16A); ventral surface of head capsule with posterior tentorial pits located at about midlength of head, without anteriorly divergent ridges; mesal edges of mandibles smooth; apical antennomere less than half length of antennal sensorium, length to width ratio 1.5; antennal sensorium elongate and narrow, parallel-sided along much of its length, about 1.5× as long as width of penultimate antennomere (Fig. 16A, top arrow); mala small but clearly recognizable, as long as wide, with 3 subequal setae; labial palpiger absent; ligula as wide as basal labial palpomere, about as long as basal labial palpomere, rounded at apex; tibia abruptly styliform in apical half (Fig. 16H); urogomphi evenly narrowed towards apices.

Larval material examined.
Austroesthetus sp. AUSTRALIA: 2 larvae (HW = 0.90 mm; 1 larva measured), 1 associated ♂, Victoria, Mount Worth National Park, Trevorrows Mill, 38°17.0′S, 146°0.0′E, 300 m, wet sclerophyll forest, window trap (FMHD #87-238), 7.ii.1987 (*Newton, Thayer*).

Chilioesthetus Sáiz, 1968 (Figs 5F; 7A; 9J; 12L)

Type species. *Chilioesthetus lorenae* Sáiz, 1968

Adult diagnosis. Head, pronotum, and elytra heavily sculptured (Fig. 12L); gular sutures united; eyes not more than half head length (measured from frontal margin of head to nuchal line), or absent; left mandible with distinct subapical tooth below preapical tooth; labium bilobed (Fig. 11I); antennae with compact 2-segmented club, antennomere 10 concave to receive 11; pronotum with median fovea and distinct elongate basolateral impression on each side; elytral disc distinctly grooved laterally (Fig. 12L, arrow); wingless; mesothoracic anapleural carina absent; metaventrite carinate in anterior half; tarsal formula 4-4-4; abdominal segment III with one pair of parasclerites, IV–VI each with tergite and sternite fused into solid ring, VII without parasclerites; sternite III with lateral carina (Fig. 14 J, middle arrow) obsolete beyond middle of sternite; tergites IX and X of male indistinguishably fused (Fig. 14M); female with tergite IX divided dorsally or reduced to thread-like strip in front of tergite X (Fig. 15A, arrow), gonocoxites I and II articulated ipsilaterally (Fig. 15D, right arrow); aedeagus of male with bilobed parameres.

Adult material examined.
Chilioesthetus sp.1. AUSTRALIA: 1♂, 1♀, Western Australia, Walpole National Park, 6 km NE Coalmine Beach, sand and fungus under litter under Red Tingle, (berlesate #130B; FMHD#76-496), 13.xii.1976 (*Kethley*). *Chilioesthetus* sp.2. CHILE: 1♂, 1♀, Osorno Prov., Parque Nacional Puyehue, Antillanca Road, 720 m, *Nothofagus* spp. forest (trap site 659), leaf & log litter (berlesate), 18-24.xii.1982 (*Newton, Thayer*). *Chilioesthetus* sp. 3. CHILE: 1♂, 1♀, Malleco Prov., Parque Nacional Contulmo, 10 km W Purén, 240 m, mixed hardwood forest with *Chusquea*, leaf & log litter (berlesate), 12.xii.1982 (*Newton, Thayer*). *Chilioesthetus* sp. 4. CHILE: 2♂, 2♀ (SEM), Osorno Prov., Parque Nacional Vicente Pérez Rosales, N slope Volcan Osorno, road to Ref. La Picada,

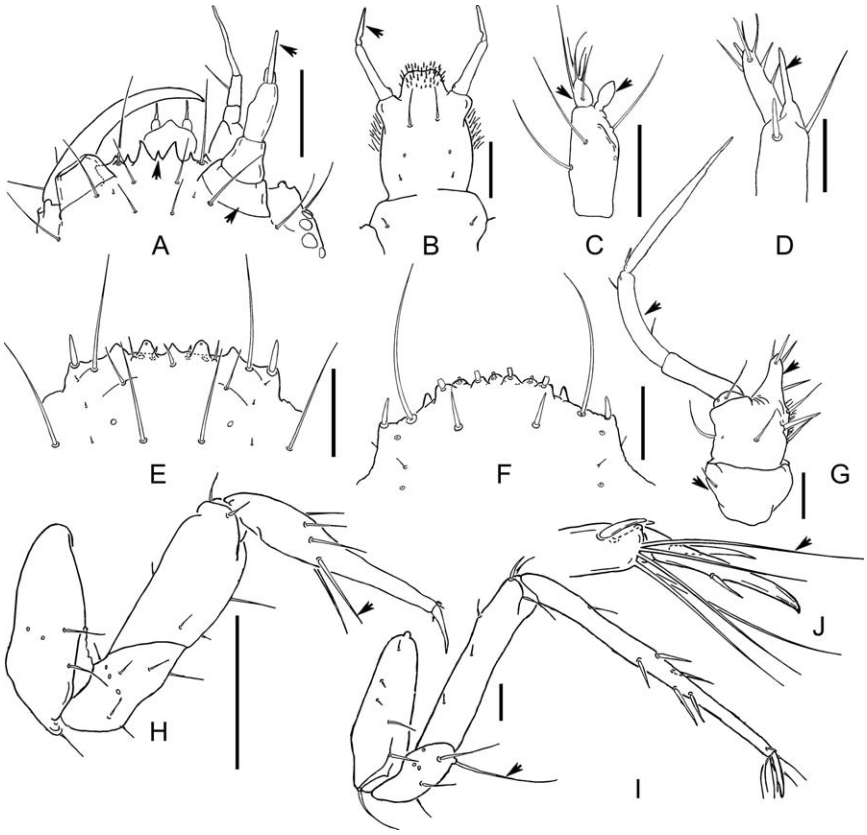

Fig. 16. Larvae of Steninae and Euaesthetinae, details of morphology: (A) *Austroesthetus* sp., anterior part of head (dorsal; right mandible, left maxilla and left antenna omitted); (B) *Dianous* sp., labium (ventral); (C) *Euaesthetus* sp., right antennomeres II and III (dorsal); (D) *Dianous* sp., apical part of right antennomere II and antennomere III (dorsal); (E) *Euaesthetus* sp., nasale (dorsal); (F) *Dianous* sp., nasale (dorsal); (G) *Dianous* sp., right maxilla (ventral); (H) *Austroesthetus* sp., left middle leg (anterior); (I) *Dianous* sp., left middle leg (anterior); (J) *Dianous* sp., left middle tarsus and claw (anterior). Scale bars: 100 μm. Arrows indicate structures referred to in the text. Scale bars for C–E: 50 μm; A, B, F–I: 100 μm. Arrows indicate structures referred to in the text.

41°3.3′S, 72°30.2′W, 660 m, *Nothofagus dombeyi* with conifers, dense *Chusquea* bamboo understorey, flat area (site ANMT 1067), leaf and log litter (berlesate; FMHD#2002-082), 16.xii.2002 (*Solodovnikov, Thayer, Newton*).

Larval diagnosis. Nuchal carina present, linear; stemmata reduced in size and/or number, not protruding laterally (Fig. 5F); nasale with medial tooth and paramedial teeth slightly longer than others (Fig. 9J); ventral surface of head capsule with posterior tentorial pits located at about mid-length of head, without anteriorly divergent ridges (Fig. 8A); mesal edges of mandibles smooth; apical antennomere less than one-third length of antennal sensorium, length to width ratio 1.0; antennal sensorium elongate and narrow, along much of its length parallel-sided, about as long as width of penultimate antennomere; mala small but clearly recognizable, 1.5× as long as wide, with 3 subequal setae; labial palpiger absent; ligula as wide as basal labial palpomere, no more than half length of basal labial palpomere, concave at apex; tibia abruptly styliform in apical half; urogomphi bottle-shaped with distal part abruptly narrowing at about middle.

Larval material examined. *Chilioesthetus* sp. CHILE: 3 larvae (HW = 0.55, 0.50 and 0.489 mm), 1 associated male, Arauco Prov., 16 km N Tres Pinos, 170 m, *Cupressus–Eucalyptus* forest, litter (berlesate; FMHD# 82-716), 12. xii.1982 (*Newton, Thayer*).

Kiwiaesthetus Puthz, 2008 (Figs 11H; 12J, O)

Type species. *Kiwiaesthetus kuscheli* Puthz, 2008

Adult diagnosis. Head, pronotum and elytra (Fig. 12O) smooth or finely microsculptured; head sparsely setose, gular sutures united; eyes large, greater than two-thirds head length (measured from frontal margin of head to nuchal line); labrum with medial pair of thick spines; labium sub-bilobed, minutely notched at middle and with subtriangular anterolateral lobes; pronotum glabrous (excluding macrosetae), without basolateral depressions; elytra sparsely setose (Fig. 12O), fused at least to mesothorax; elytral basal ridge absent; wingless; mesothoracic anapleural carina present only posteriorly (Fig. 13D, left arrow);

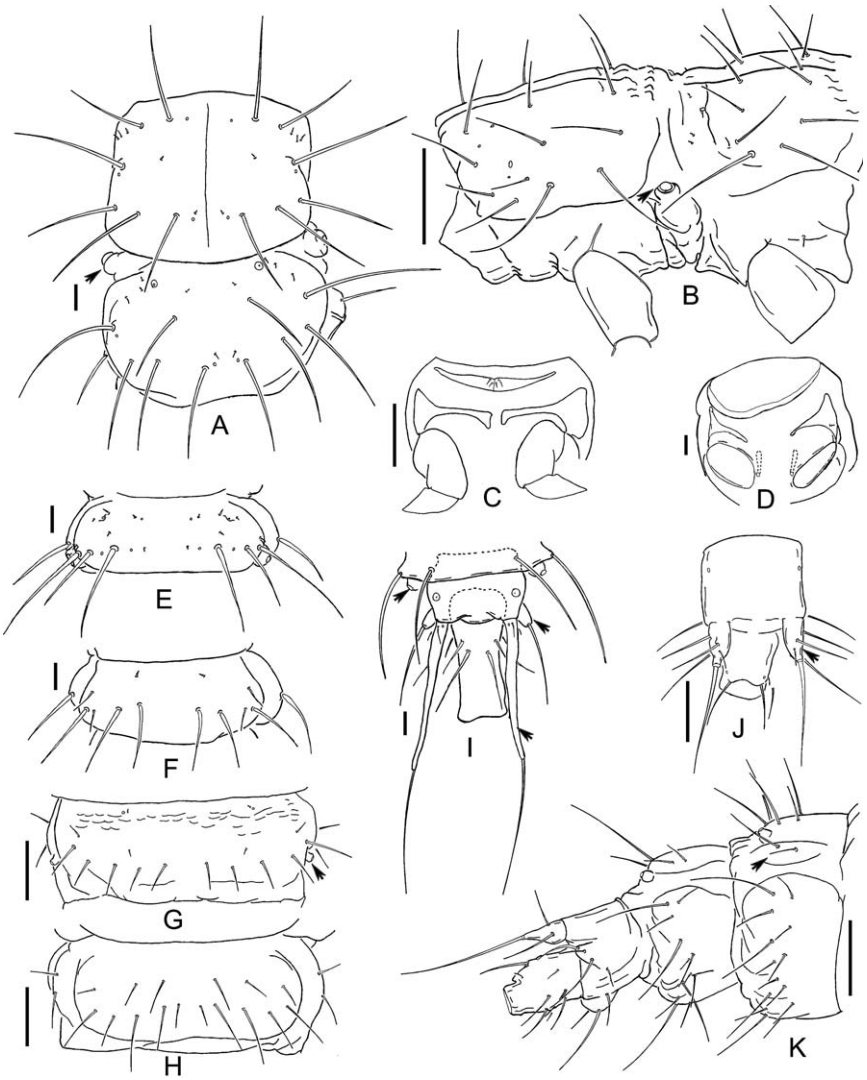

Fig. 17. Larvae of Steninae and Euaesthetinae, details of morphology: (A) *Dianous* sp., pro- and mesothorax (dorsal; legs omitted); (B) *Fenderia* sp., pro- and mesothorax (lateral; legs omitted); (C) *Austroesthetus* sp., prothorax (ventral; legs omitted); (D) *Dianous* sp., prothorax (ventral; legs omitted); (E–F) *Dianous* sp., abdominal segment IV, dorsal (E) and ventral (F); (G–H) Eua?LTAS, abdominal segment VI, dorsal (G) and ventral (H); (I) *Dianous* sp., abdominal segments IX and X (dorsal); (J) Eua?LTAS, abdominal segments IX and X (dorsal); (K) *Fenderia* sp., abdominal segments VII–X (lateroventral). Scale bars: 100 μm. Arrows indicate structures referred to in the text.

mesoventral intermesocoxal process oblique, with apex widely separated from metaventral intermesocoxal process; mesocoxal acetabula not delimited posteriorly by carina; tarsal formula 4-4-4; metacoxae with posterior faces nearly vertical; abdominal segments III–VII without parasclerites (Fig. 14J), III–VI each with suture separating tergite and sternite; sternite III with lateral carina (Fig. 14 J, middle arrow) reaching slightly beyond middle of sternite; tergite IX of male forming thick bridge in front of tergite X; female with tergite IX divided dorsally or reduced to thin strip in front of tergite X (Fig. 15A, left arrow), gonocoxites I and II articulated ipsilaterally (Fig. 15D, right arrow).

Adult material examined. *Kiwiaesthetus* spp. NEW ZEALAND: 1♂, 1♀, Arthur's Pass National Park, Bealey Valley Track, 840 m, subalpine *Nothofagus* forest, leaf & log litter (berlesate), 18-21.iii.1980 (*Newton, Thayer*); 3♂, 3♀ (SEM), Loop Line Road Scenic Reserve, SSE Kumara, 160 m, podocarp–hardwood forest (site ANMT 730), leaf and log litter (berlesate), 8-19.i.1985 (*Newton, Thayer*).

Larvae. Unknown.

Mesoaesthetus Cameron, 1944

Type species. *Mesoaesthetus wilsoni* Cameron, 1944

Adult diagnosis. Head, pronotum, and elytra finely sculptured and setose; gular sutures united, laterally with postocular semicircular carina; eyes small, no more than half head length (measured from frontal margin of head to nuchal line); labium with pair of digitiform membranous processes (Fig. 12B, top arrow); pronotum with a deep basolateral depression on each side; elytral basal ridge present; wings vestigial or absent; mesothoracic anapleural carina present only posteriorly (Fig. 13D, left arrow); mesocoxal acetabula delimited posteriorly by carina; tarsal formula 4-4-4; metacoxae with posterior faces oblique; abdominal segments III–VII without parasclerites (Fig. 14J), III–VI each with suture separating tergite and sternite; sternite III with lateral carina (Fig. 14J, middle arrow) reaching slightly beyond middle of sternite; tergite IX of male forming narrow bridge in front of tergite X; female with tergite IX divided dorsally or reduced to thin strip in front of tergite X (Fig. 15A, left arrow), gonocoxites I and II articulated ipsilaterally (Fig. 15D, right arrow).

Adult material examined. *Mesoaesthetus tasmanicus* Puthz, 1978. AUSTRALIA: 1♂, 1♀, Tasmania, Cradle Mountain National Park, Cradle Mountain, 4500 ft, litter under shrubs (berlesate 231; FMHD#77-131), 4.ii.1977 (*Kethley*). *Mesoaesthetus* spp. AUSTRALIA: 1♂, 2♀, Victoria, Mount Donna, Buang, near Warburton, 37°25.8′S, 145°24.6′E, 1200 m, *Nothofagus cunninghamii*-wet sclerophyll forest (site ANMT 811), leaf and log litter (berlesate; FMHD#87-221), 1.ii.1987 (*Newton, Thayer*); 1♂, 1♀ (SEM), Tasmania, Southwest National Park, Scotts Peak Road (21 km S Gordon River Road), Creepy Crawly Nature Trail, 42°50.0′S, 146°29.0′E, 600 m, *Nothofagus cunninghamii* with tree ferns (very mossy) (site ANMT 904), leaf and log litter (berlesate; FMHD#93-53), 24.i.1993 (*Newton, Thayer*).

Larvae. Unknown.

Nothoesthetus Sáiz, 1970 (Figs 6C; 8D; 9L; 13A; 14O)

Type species. *Nothoesthetus coiffaiti* Sáiz, 1970

Adult diagnosis. Head, pronotum, and elytra smooth or very finely microsculptured; gular sutures united; eyes small, less than half head length; left mandible with minute subapical tooth below preapical tooth; labium deeply bilobed (Fig. 11I); pronotum oblong, with faint basolateral impression on each side; elytra with distinct epipleural ridge (Fig. 13A, arrow); wingless; mesothoracic anapleural carina present only posteriorly (Fig. 13D, left arrow); tarsal formula 4-4-4; abdominal segments III–VI each with one pair of parasclerites, VII without parasclerites; sternite III with lateral carina (Fig. 14J, middle arrow) reaching slightly beyond middle of sternite; tergite IX of male entire, moderately elongate in front of tergite X; female with tergite IX divided dorsally or reduced to thread-like strip in front of tergite X (Fig. 15A, left arrow), gonocoxites I and II articulated ipsilaterally (Fig. 15D, right arrow).

Adult material examined. *Nothoesthetus scitulus* Sáiz, 1970. CHILE: 1♂, 1♀, Concepcion Prov., Agua de la Gloria, 10.iv.1972 (*Cekalovic*). *Nothoesthetus* spp. CHILE: 1♂, 2♀ (SEM), Malleco Prov., Parque Nacional Contulmo, 10 km W Purén, 240 m, mixed hardwood forest with *Chusquea*, leaf & log litter (berlesate), 12.xii.1982 (*Newton, Thayer*); 1♂, 1♀ (SEM), Valdivia Prov., 35 km WNW La Union, 700 m, mixed forest, berlesate (FMHD#85-997; P#85-114), 7.ii.1985 (*Peck, Kukalová-Peck*).

Larval diagnosis. Nuchal carina present, linear; stemmata reduced in number, not protruding laterally (Fig. 6C); nasale with paramedial teeth markedly longer than remaining teeth, without medial tooth (Fig. 9L); ventral surface of head capsule with posterior tentorial pits located at about midlength of head, without anteriorly divergent ridges (Fig. 8D); mesal edges of mandibles smooth; apical antennomere two-thirds length of antennal sensorium, length to width ratio 1.2; antennal sensorium elongate and narrow, parallel-sided along much of its length, slightly shorter than width of penultimate antennomere; mala small but clearly recognizable, as long as wide, with one long and one short seta; labial palpiger absent; ligula 3× as wide as basal labial palpomere, no more than half length of basal labial palpomere, rounded at apex; tibia abruptly styliform in apical half; urogomphi bottle-shaped with distal part abruptly narrowing at about middle.

Larval material examined. *Nothoesthetus* sp. CHILE: 1 larva (HW = 0.76 mm), 1 associated male, Cautín Prov., Parque Nacional, Ñielol, near Temuco (site 652), ~250 m, native forest remnants with *Nothofagus*, leaf litter (berlesate), 14-30.xii.1982 (*Newton, Thayer*).

Tasmanosthetus Puthz, 1978

Type species. *Tasmanosthetus okei* Puthz, 1978

Adult diagnosis. Head, pronotum, and elytra finely sculptured; gular sutures united; eyes reduced or absent; labium bilobed (Fig. 11I); pronotum narrowly grooved basolaterally; elytra with distinct epipleural fold (Fig. 13A, arrow); wingless; mesothoracic anapleural carina absent; mesoventral intermesocoxal process spiniform, widely separated from carinate metaventral intermesocoxal process; tarsal formula 4-4-4; abdominal segments III–VII without parasclerites (Fig. 14J), III–VI each with tergite and sternite fused into solid ring; sternite III with lateral carina (Fig. 14J, middle arrow) not reaching beyond anterior one-quarter of sternite; tergite IX of male forming thick bridge in front of tergite X; female with tergite IX divided dorsally or reduced to thin strip in front of tergite X (Fig. 15A, left arrow), gonocoxites I and II articulated ipsilaterally (Fig. 15D, right arrow).

Adult material examined. *Tasmanosthetus* spp. AUSTRALIA: 1♂, 1♀, Tasmania, Florentine Valley, 22 km NW Maydena, 700 ft, berlesate 247, 15.ii.1977 (*Kethley*); 3♂, 3♀ (SEM), Murchison Highway State Reserve, Murchison Highway at Que River Mine Road, 41°36.0′S, 145°41.0′E, 680 m, *Nothofagus cunninghamii* rainforest with *Atherosperma*, *Eucalyptus*, tree ferns (site ANMT 907), leaf & log litter (berlesate; FMHD#93-24), 11.i.1993 (*Newton, Thayer*).

Larvae. Unknown.

Tribe Euaesthetini Thomson, 1859

Edaphus Motschulsky, 1857 (Figs 5C; 7D; 9E; 12E; 15B)

Type species. *Edaphus nitidus* Motschulsky, 1857

Adult diagnosis. Head with deep furrows uniting dorsal tentorial pits, gular sutures separated; neck expanded behind eyes, dorsal nuchal groove absent; labrum minutely to finely serrate; labium without medial notch; labial palpi appearing 2-segmented, first palpomere extremely reduced or absent (Fig. 12C); mentum with strong apicolateral spines; transverse submental carina absent; pronotum strongly constricted basally, with basolateral longitudinal carinae and basal foveae; anterior prosternal margin usually deeply notched (Fig. 12E, top arrow); anteprocoxal prosternal carina absent; elytral marginal ridge distinctly toothed near humerus (Fig. 13B, arrow); mesothoracic anapleural carina present, continuous with transverse carina on side of mesothorax (Fig. 13F, top and bottom left arrows); mesoventrite with midlongitudinal, transverse and anterior oblique carinae (Fig. 13F, middle arrow, top left and right arrows, respectively); meso- and metaventral intermesocoxal processes with apices narrowly truncate; tarsal formula 4-4-4; metacoxae with mesal edges widely separated; abdominal segments III–VII with basal transverse carina (Fig. 14F, top arrow), III–VII each with one pair of parasclerites; sternite III with lateral carina (Fig. 14J, middle arrow) reaching from middle to apex of sternite; tergite IX of male and female (Fig. 15B) forming thick bridge in front of tergite X; female with gonocoxites I and II fused ipsilaterally (Fig. 15E).

Adult material examined. *Edaphus americanus* Puthz, 1974. U.S.A.: 1♂, 1♀, Tennessee, Cumberland Co., 1.8 mi. E. Ozone, 1300 ft, forest, litter (berlesate), 6.x.1973 (*Newton*). *Edaphus* spp. VENEZUELA: 1♂, 1♀, Aragua Rancho Grande, 15 km N Maracay, 1000–1400 m, forest litter, 19-27.ii.1971 (*Peck*); JAPAN: 1♂, 1♀, Shikoku Ishizuchi Mountain National Park, Tsuchigoya, Mt. Tsutsujo, 1600 m, *Betula–Fagus* log, stump, moss litter (berlesate), 11-18.viii.1980 (*Peck, Kukalová-Peck*); AUSTRALIA: New South Wales: 1♂, 1♀, Dorrigo National Park, E end Blackbutt Track, 710 m, subtropical rainforest, in and under rotting fruits of *Endiandra introsa*, 28.ii-5.iii.1980 (*Newton, Thayer*); 2♂, 3♀ (SEM), Unumgar State Forest (near Woodenbong), Pole Bridge Road, 28°14.4′S, 152°24′E, 430 m, dry rainforest, *Araucaria–Eucalyptus* (site ANMT 788), leaf & log litter (berlesate; FMHD#87-174), 2.i.1987 (*Newton, Thayer*).

Larval diagnosis. Nuchal carina absent; stemmata fully developed, not or slightly protruding laterally (Fig. 5C); nasale with all teeth approximately similar in size, without medial tooth (Fig. 9E); ventral surface of head capsule with posterior tentorial pits located at posterior margin adjacent to occipital foramen, and with anteriorly divergent ridges arising from posterior tentorial pits (Fig. 7D, arrows); mesal edges of mandibles with 2 rows of serration (Fig. 5C); apical antennomere minute, length to width ratio <0.3; antennal sensorium bulbous, with convex sides and constricted base, slightly shorter than width of penultimate antennomere; mala very small and hardly recognizable, twice as long as wide, asetose; labial palpiger absent; ligula 3× as wide as basal labial palpomere, no more than half length of basal labial palpomere, straight or slightly concave at apex; tibia entirely styliform; urogomphi deformed and not characterizable on the single available larva.

Larval material examined. *Edaphus* sp. AUSTRALIA: 1 larva (HW = 0.58 mm), New South Wales, Pole Bridge Road, 28°24.0′S 152°40.0′E, 430 m, dry *Araucaria–Eucalyptus* rainforest (ANMT 788), litter (berlesate; FMHD #87-174), 2.i.1987 (*Newton, Thayer*).

Euaesthetus Gravenhorst, 1806 (Figs 5B; 7C; 9D; 11C; 13B, F; 14C; 16C, E)

Type species. *Euaesthetus scaber* Gravenhorst, 1806

Adult diagnosis. Head with gular sutures narrowly separated; neck expanded behind eyes, dorsal nuchal groove absent; mandibles with serration along mesal edges (Fig. 11C); labium without medial notch; labial palpi 3-segmented, first palpomere less than one-quarter length of second palpomere (Fig. 12C); mentum with strong apicolateral spines; transverse submental carina absent; anteprocoxal prosternal carina absent; elytral marginal ridge distinctly toothed near humerus (Fig. 13B, arrow); mesothoracic anapleural carina present (Fig. 13F, bottom left arrow), continuous with transverse carina on side of mesothorax (Fig. 13F, top left arrow); mesoventrite with midlongitudinal and anterior oblique carinae (Fig. 13F, middle and right arrows, respectively); meso- and metaventral intercoxal processes with apices rounded (Fig. 13F); tarsal formula 4-4-4; metacoxae slightly longer than wide, contiguous mesially; abdominal segments III–VII with basal transverse carina (Fig. 14F, top right arrow), III–V each with one pair of parasclerites, VI and VII in males with tergite and sternite fused into solid ring, VI of females with one pair of parasclerites, VII without parasclerites; sternite III with lateral carina (Fig. 14J, middle arrow) curved dorsally to contact dorsal margin; tergite IX of male and female

forming thick bridge in front of tergite X; female with gonocoxites I and II fused ipsilaterally (Fig. 15E).

Adult material examined. *Euaesthetus americanus* Erichson, 1840. U.S.A.: Massachusetts: Middlesex Co.: 1♂, 1♀, Bedford Pickman Area, flood debris along river edge (berlesate), 2.iv.1977 (*Newton, Thayer*); 1♂, 1♀, Estabrook Woods near Concord, wet sticks (berlesate), 2.viii.1974 (*Newton*). Illinois: 2♂, 3♀ (SEM), Mason Co., Sand Ridge State Forest, 40°23.3′N, 89°52.8′W, 500 ft, small permanent pond in oak woods with river birch, wet debris at pond edge and leaf & log litter in vicinity of pond (berlesate; FMHD#2001-44), 18.viii.2001 (*Newton*).

Larval diagnosis. Nuchal carina present, linear; stemmata fully developed, clearly protruding laterally (Fig. 5B); nasale with paramedial teeth longer than others, medial tooth present (Figs 9D; 16E); ventral surface of head capsule with posterior tentorial pits located at about midlength of head, and without anteriorly divergent ridges (Fig. 7C); mesal edges of mandibles with one row of serration (Fig. 5B); apical antennomere (Fig. 16C, left arrow) approximately half width of penultimate antennomere, length to width ratio 1.2; antennal sensorium bulbous, with convex sides and constricted base, about half as long as width of penultimate antennomere (Fig. 16C, right arrow); mala very small and hardly recognizable, wider than long, with one long and one short seta; labial palpiger absent; ligula half as wide as basal labial palpomere, slightly more than half length of basal labial palpomere, pointed at apex; tibia abruptly styliform in apical half; urogomphi evenly narrowed towards apices.

Larval material examined. *Euaesthetus* sp. U.S.A.: 3 larvae (HW = 0.75 and 0.69 mm), 1 associated ♂, Massachusetts, Pickman area, Bedford, viii.1975, 1-year-old straw pile with black mould (*Lawrence*).

Octavius Fauvel, 1873 (Figs 6D; 8E; 9M, N; 11D, G, I, J; 14I, M)

Type species. *Octavius pyrenaeus* Fauvel, 1873

Adult diagnosis. Head (e.g. Fig. 11D), pronotum and elytra granulate to coarsely and irregularly punctate; gular sutures united; neck distinctly narrower than head, delimited dorsally by nuchal groove; eyes approximately half head length (measured from frontal margin of head to nuchal groove), or shorter, or absent; antennae with bulbous 2-segmented club, antennomeres 10 and 11 partly fused (Fig. 14 G); labium bilobed (Fig. 14I); transverse submental carina absent; anteprocoxal prosternal carina absent; mesothoracic anapleural carina present at least anteriorly; mesoventrite with midlongitudinal and anterior oblique carinae (Fig. 13F, middle and right arrows, respectively), side of mesothorax with transverse carina (Fig. 13F, top left arrow); tarsal formula 4-4-4; abdominal segments III–VII each with two pairs of parasclerites, VII with one parasclerite more anterior to other (e.g. Fig. 14G, arrows); sternite III with lateral carina (Fig. 14J, middle arrow) obsolete beyond middle of sternite, paramedial carina (Fig. 14J, bottom left arrow) present; tergite IX of male indistinguishably fused to X (Fig. 14M); female with tergite IX elongate in front of X, with intergonopodal sclerite (Fig. 15D, left arrow), and gonocoxites I and II articulated ipsilaterally (Fig. 15D, right arrow).

Adult material examined. *Octavius* spp. (*Octavius*PAN). PANAMA: 1♂, 1♀, and 2♂, 2♀, 2 sex indet. (SEM), Panamá, Canal Zone, Barro Colorado Island, litter under fungusy logs, 4.ii.1976 (*Newton*). *Octavius* spp. (*Octavius*SA). SOUTH AFRICA: 2♂, 2♀, and 3♂, 3♀, 3 sex indet. (SEM), Kwazulu-Natal, Cathedral Peaks Forest Station, 75 km WSW Estcourt, 1500 m, podocarp forest, ravine litter x/hyphae (berlesate 3), 12.xii.1979 (*Peck, Kukalová-Peck*).

Larval diagnosis. Nuchal carina present, linear; stemmata fully developed or reduced in size and/or number, not or slightly protruding laterally (Fig. 6D); nasale with all teeth approximately similar in size, medial tooth present (Fig. 9 M, N); ventral surface of head capsule with posterior tentorial pits located at about midlength of head, without anteriorly divergent ridges (Fig. 8E); mesal edges of mandibles with one row of extremely fine serration, only visible with magnification >500×; apical antennomere minute, length to width ratio 1.0; antennal sensorium bulbous, with convex sides and constricted base, about as long as, or markedly shorter than, width of penultimate antennomere (Fig. 6D, arrow); mala small but clearly recognizable, as long as wide, with one long seta at midlength; labial palpiger absent; ligula half as wide as basal labial palpomere, about as long as or slightly longer than half length of basal labial palpomere, pointed at apex; tibia abruptly styliform in apical half; urogomphi bottle-shaped with distal part abruptly narrowing at about middle.

Larval material examined. *Octavius* sp. (*Octavius*PAN). PANAMA: 2 larvae (HW = 0.55 and 0.51 mm), 1 associated ♀, Canal Zone, Barro Colorado Island, forest stream, wet leaves & debris, 12.ii.1976 (*Newton*). *Octavius* sp. (*Octavius*SA). SOUTH AFRICA: 3 larvae (HW = 0.75, 0.73 and 0.73 mm), 1 associated ♂, Kwazulu Natal, 75 km WSW Estcourt, Cathedral Peaks Forest Station, 7-31.xii. 1979 (*Peck, Kukalová-Peck*).

Protopristus Broun, 1909 (Figs 6E; 8F; 9O; 11O; 12C; 13J, K; 14G, L; 15D)

Type species. *Protopristus minutus* Broun, 1909

Adult diagnosis. Head, pronotum and elytra finely punctate to squamous; gular sutures united anteriorly, diverging posteriorly; neck distinctly narrower than head, delimited dorsally by nuchal groove; eyes approximately one-quarter head length (measured from frontal margin of head to nuchal groove), or shorter, or absent; left mandible with

minute ventral tooth below preapical tooth; labium bilobed with median overlapping teeth (Fig 12C, arrow); transverse submental carina absent; wingless; mesothoracic anapleural carina absent; mesoventrite not carinate; mesoventral intermesocoxal process with sharp apex not contacting carinate metaventral intermesocoxal process; tarsal formula 4-4-4; abdominal segments III–VII each with two pairs of parasclerites, VII with one parasclerite more anterior to other; sternite III with lateral carina (Fig. 14J, middle arrow) obsolete before middle of sternite; tergite IX of male forming elongate bridge in front of X (Fig. 14L); female with tergite IX either elongate and divided mid-dorsally by suture, or reduced medially to thin strip in front of tergite X, with intergonopodal sclerite (Fig. 15D, left arrow), and gonocoxites I and II articulated ipsilaterally (Fig. 15D, right arrow).

Adult material examined. *Protopristus* spp. (*Protopristus*-TAS): AUSTRALIA: 1♂, 1♀, Tasmania, Florentine Valley, 10 km NW Maydena, berlesate 233, 14.ii.1977 (*Kethley*); 3♂, 4♀, 2 sex indet. (SEM), Victoria, Tarra-Bulga National Park, Tarra Valley, near picnic area, 38°27.0′S, 146°32.0′E, 340 m, cool temperate rainforest with *Nothofagus cunninghamii*, *Dicksonia* tree ferns, etc. (site ANMT 927), leaf & log litter (berlesate; FMHD#93-89), 13.ii.1993 (*Newton, Thayer*). *Protopristus* spp. (*Protopristus*NZ): NEW ZEALAND: 1♂, 1♀, Owaka, Glenomaru Reserve, forest litter (berlesate), 18.i.1978 (*Peck, Kukalová-Peck*); 1♂, 1♀, Taupo, Kaimanawa Forest Park, Mill Road, SSE Taupo, 840 m, *Nothofagus* forest, leaf & log litter (berlesate), 3-8.iv.1980 (*Newton, Thayer*); 3♂, 3♀ (SEM), Banks Peninsula, Peraki Saddle Scenic Reserve, 500 m, hardwood–podocarp elfin forest (site ANMT 701), leaf & log litter (berlesate), 11.xii.1984-22.i.1985 (*Newton, Thayer*).

Larval diagnosis. Nuchal carina reduced, represented by aligned microsculpture (Fig. 6E, arrow); stemmata reduced in size and/or number, not protruding laterally (Fig. 6E); nasale with 6 teeth arranged into 2 crowns of 3 teeth each, medial tooth absent (Fig. 9O); ventral surface of head capsule with posterior tentorial pits located at about mid-length of head, with anteriorly divergent ridges arising from posterior tentorial pits (Fig. 8F, top arrow), and with compact group of cuticular teeth adjacent to posterior tentorial pits (Fig. 8F, bottom arrow); mesal edges of mandibles smooth; apical antennomere less than half width of penultimate antennomere, length to width ratio 0.9; antennal sensorium bulbous, with convex sides and constricted base, about as long as width of penultimate antennomere; mala small but clearly recognizable, twice as long as wide, with at least one seta; labial palpiger absent; ligula 3× as wide and about as long as basal labial palpomere, concave at apex; tibia abruptly styliform in apical half; urogomphi bottle-shaped with distal part abruptly narrowing at about middle.

Larval material examined. *Protopristus* sp. (*Protopristus*-TAS): NEW ZEALAND: 1 larva (HW = 456 mm), 1 associated ♀, 8.0 km S Arthur's Pass (town), 670 m, *Nothofagus solandri* forest, 14.iii.1980 (*Newton, Thayer*).

Schatzmayrina Koch, 1934

Type species. *Schatzmayrina oxyclypea* Koch, 1934

Adult diagnosis. Head, pronotum, and elytra coarsely punctured; gular sutures united; neck distinctly narrower than head, delimited dorsally by nuchal groove; eyes less than half head length (measured from frontal margin of head to nuchal groove); antennae 9-segmented, with large 1-segmented club; labrum with anterior edge indistinctly serrate, nearly smooth; labium with pair of membranous digitiform processes (Fig. 12B, top arrow); pronotal lateral carina absent; winged, macropterous; subcircular procoxal rests of mesoventrite present (Fig. 13E, top arrow); mesothoracic anapleural carina absent; tarsal formula 4-4-4; metacoxae with mesal edges widely separated; abdominal segments III–VII each with one pair of parasclerites; sternite III with lateral carina (Fig. 14J, middle arrow) obsolete before middle of sternite; tergite IX of male and female entire, forming thick bridge in front of X; female with gonocoxites I and II fused ipsilaterally (Fig. 15E).

Adult material examined. *Schatzmayrina oxyclypea* Koch, 1934. SOUTH AFRICA: 1♂, 1♀, E Transvaal, Kruger Park, Pretoriuskop, thorn scrub, *Ficus sycomorus* fruit litter (berlesate; FMHD#85-847; P#85-280), 13.xii.1985 (*Peck*).

Larvae. Unknown.

Tribe Fenderiini Scheerpeltz, 1974

Fenderia Hatch, 1957 (Figs 6A; 8B; 9K; 10K, L; 11B; 12K; 14D; 17B, K)

Type species. *Fenderia capizzii* Hatch, 1957

Adult diagnosis. Head (Fig. 11B), pronotum and elytra with many long setae; head expanded laterally in front of eyes, with dorsolateral carina (Fig. 11B, bottom arrow); gular sutures united posteriorly, gradually diverging anteriorly; eyes less than one-quarter head length (measured from frontal margin of head to nuchal line); condyle of first antennomere exposed dorsally (Fig. 11B, top arrow); labrum with very large teeth; labium bilobed (Fig. 11I); anteprocoxal prosternal carina and lobes absent (Fig. 12K); elytra fused to pterothorax; wingless; mesothoracic anapleural carina present, continuous with transverse carina on side of mesothorax (Fig. 13F, left arrows); mesoventrite with midlongitudinal and anterior oblique carinae (Fig. 13F, right arrows); tarsal formula 5-5-5; abdominal segments III–VII with basal transverse carina (Fig. 14F, top right arrow), without parasclerites (Fig. 14J), and each of III–VI with tergite fused to sternite to form a solid ring; lateral carina of sternite III absent, paramedial carina present (Fig. 14J, bottom left arrow); tergite IX

of male forming thick bridge in front of tergite X; female with tergite IX divided dorsally, gonocoxites I and II articulated ipsilaterally (Fig. 15D, right arrow).

Adult material examined. *Fenderia capizzii* Hatch, 1957. U.S.A.: California, Mendocino Co.: 2♂, 1♀, Mendocino, 17.vii.1954 (*Helfer*); 1♂, 3♀ (SEM), Leggett, Drive-Thru Tree Park, 39°51.5′N, 123°43.0′W, 300 m, *Sequoia–Pseudotsuga menziesii* forest with some hardwoods (site ANMT 956), leaf & log litter (berlesate; FMHD#95-54), 27.iii.1995 (*Newton, Thayer*).

Larval diagnosis. Nuchal carina present, linear; stemmata reduced in size and/or number, not protruding laterally (Fig. 6A); nasale with paramedial teeth markedly longer than remaining teeth, medial tooth absent (Fig. 9K); ventral surface of head capsule with posterior tentorial pits located at about midlength of head, without anteriorly divergent ridges (Fig. 8B); mesal edges of mandibles smooth; apical antennomere approximately half width of penultimate antennomere; length to width ratio 1.2; antennal sensorium elongate and narrow, parallel-sided along much of its length, about as long as maximum width of penultimate antennomere (Fig. 8B, left arrow); mala small but clearly recognizable, 1.5× as long as wide, with one long and one short seta; labial palpiger absent; ligula 1.5× as wide as and slightly longer than half length of basal labial palpomere, rounded at apex; tibia abruptly styliform in apical half; urogomphi bottle-shaped with distal part abruptly narrowing at about middle.

Larval material examined. *Fenderia* sp. U.S.A.: 1 larva (HW = 0.68 mm), 2 associated ♂, 1♀, Oregon, Benton Co., Marys Peak, Forest Road 30, 0.4 mi. W Parker Creek, *Tsuga-Pseudotsuga-Alnus* forest (site ANMT 853), litter, 25.vi.1988 (*Newton, Thayer*).

Tribe Stenaesthetini Bernhauer & Schubert, 1911

Agnosthaetus Bernhauer, 1939 (Figs 5D; 7E; 9G; 10C–I; 11M; 12N; 15C)

Type species. *Agnosthaetus brouni* Bernhauer, 1939

Adult diagnosis. Head, pronotum and elytra (Fig. 12N) smooth or finely microsculptured; gular sutures united; eyes large, occupying most of side of head (Fig. 11A, C); labium with pair of elongate sclerotized processes (Fig. 11M, middle arrow); lateral margin of galea with large cuticular projection (Fig. 11M, left arrow); pronotum with pair of lateral and dorsal grooves; wingless; mesothoracic anapleural carina present only posteriorly (Fig. 13D, left arrow); tarsal formula 5-5-4; metatarsus with first tarsomere longer than combined length of succeeding two tarsomeres; abdominal segments III–VII without parasclerites (Fig. 14J), III–VI each with tergite fused to sternite to form a solid ring; sternite III with lateral carina (Fig. 14J, middle arrow) reaching apex of sternite; tergite IX of male entire, elongate in front of X; female with tergite IX divided dorsally or reduced to thin strip in front of tergite X (Fig. 15C, arrow), gonocoxites I and II articulated ipsilaterally (Fig. 15D, right arrow).

Adult material examined. *Agnosthaetus* spp. NEW ZEALAND: 1♂, Nelson Lakes National Park, Lake Rotoroa, 450 m, *Nothofagus* forest, litter (berlesate), 7.ii.1978 (*Peck, Kukalová-Peck*); 1♀, Riwaka River Reserve, 20 km NW Motueka, 100 m, mixed forest litter, 28.v.1982 (*Peck, Kukalová-Peck*); 2♂, 2♀ (SEM), Waipoua State Forest, 0.8 km NW Wairau Summit, 350 m, hardwood–podocarp forest (site ANMT 689), litter (Winkler extraction), 27.xi.1984 (*Newton, Thayer*).

Larval diagnosis. Nuchal carina present, linear; stemmata fully developed, not or slightly protruding laterally (Fig. 5D); nasale with paramedial teeth markedly longer than others, without medial tooth (Fig. 9G); ventral surface of head capsule with posterior tentorial pits located at about midlength of ventral surface of head (Figs 7E; 10E, arrow), without anteriorly divergent ridges; mesal edges of mandibles smooth; apical antennomere length slightly less than width of penultimate antennomere, length to width ratio 2; antennal sensorium elongate and narrow, parallel-sided along much of its length, slightly longer than width of penultimate antennomere; mala small but clearly recognizable, 2× as long as wide, with one long apical seta (Fig. 10C, arrow); labial palpiger absent; ligula 3× as wide as basal labial palpomere, slightly longer than half length of basal labial palpomere, pointed at apex; tibia abruptly styliform in apical half; urogomphi evenly narrowed towards apices.

Larval material examined. *Agnosthaetus* sp. NEW ZEALAND: 1 larva (HW = 1.08 mm), 1 associated ♂, Mount Aspiring National Park, 12.5 km NNE Makarora, 370 m, 11-17.i.1985 (*Newton, Thayer*).

Stenaesthetus Sharp, 1874 (Figs 11A, F; 12B, F, I, M; 13D; 14E, J)

Type species. *Stenaesthetus sunioides* Sharp, 1874

Adult diagnosis. Head with gular sutures united; eyes large (Fig. 11A), more than half head length (measured from frontal margin of head to nuchal line); antennae filiform, much longer than head, antennomeres 9–11 much longer than wide; anterior margin of labrum smooth, without any teeth (Fig. 11A); labium with pair of membranous digitiform processes (Fig. 12B); pronotum with (Fig. 12F) or without medial and lateral grooves; prosternum with antero-medial callosity (Fig. 12I, top arrow), and with divided anteprocoxal carina (Fig. 12I, bottom arrow); elytral epipleural ridge present (Fig. 12M, left arrow), distinctly toothed at humerus; mesothoracic anapleural carina present only posteriorly (Fig. 13D, left arrow); tarsal formula 5-5-4; metatarsus with first tarsomere longer than combined length of succeeding two

tarsomeres; abdominal segments III–VII without parasclerites (Fig. 14J), III with suture separating tergite and sternite (Fig. 14J, top arrow), IV–VI each with tergite and sternite fused to form a solid ring; sternite III with lateral carina reaching beyond middle of sternite (Fig. 14J, middle arrow); paramedial carinae present (Fig. 14J, bottom left arrow); tergite IX of male indistinguishably fused with X (Fig. 14M); female with tergite IX completely divided dorsally or reduced to thin strip in front of X (Fig. 15A, left arrow), gonocoxites I and II articulated ipsilaterally (Fig. 15D, right arrow).

Adult material examined. *Stenaesthetus mrazi* Rambousek, 1915. BRAZIL: 1♂, 1♀, and 1♂, 3♀ (SEM), Santa Catarina, Nova Teutônia, 300–500 m, iv-v.1977 (*Plaumann*). *Stenaesthetus* spp. COLOMBIA: 1♂, 1♀, and 1♂, 1♀ (SEM), Amazones, Leticia, forest litter (B276, 27 kg), 27-28.ii.1974 (*Peck, Kukalová-Peck*); SOUTH AFRICA: 1♂, Kwazulu-Natal, Cathedral Peaks Forest Station, 75 km WSW Estcourt, Rainbow Gorge, 1500 m, podocarp forest, pantraps, 11-31.xii.1979 (*Peck, Kukalová-Peck*).

Larvae. Unknown.

Stenaesthetini: EuaAUS

Adult diagnosis. Head, pronotum and elytra smooth; gular sutures united; eyes shorter than half head length (measured from frontal margin of head to nuchal line); mandibles distinctly explanate basally; labium bilobed, with pair of membranous digitiform processes (Fig. 12D); pronotum without grooves; elytral epipleural ridge present (Fig. 12M, left arrow), continuous with ridge at base of elytron; wingless; disc of mesoventrite with paired narrowly arcuate carinae; mesothoracic anapleural carina present only posteriorly (Fig. 13D, left arrow); tarsal formula 5-5-4; metatarsus with first tarsomere longer than combined length of succeeding two tarsomeres; abdominal segments III–VII without parasclerites (Fig. 14J), III–VI each with tergite fused to sternite to form a solid ring; sternite III with lateral carina (Fig. 14J, middle arrow) nearly reaching apex of sternite; tergite IX of male indistinguishably fused with X (Fig. 14M); female with tergite IX completely divided middorsally (Fig. 15A, left arrow), gonocoxites I and II articulated ipsilaterally (Fig. 15D, right arrow).

Adult material examined. Stenaesthetini: EuaAUS. AUSTRALIA: 1♂, 1♀, and 1♀ (SEM), Victoria, Otways, Melba Gully, 38°42.0′S, 143°23.0′E, 350 m, rainforest, pyrethrum fogging, 5.xi.1997 (*Monteith*).

Larvae. Unknown.

Remarks. Puthz (1978: 118) commented on a single female specimen in the National Museum of Victoria (now Museum Victoria), which is 'distinctly different from *Stenaesthetus* Sharp, *Aulacosthaetus* Bernhauer, and *Gerhardia* Kistner'. He noted that because *Agnosthaetus* was insufficiently described, a clear decision on the generic status of that female was impossible, but that it probably represents a new genus. Based on examination of several additional specimens and comparison with all other genera of Euaesthetinae, we confirm that it belongs to an undescribed genus, which is somewhat intermediate between *Stenaesthetus* and *Agnosthaetus*, but has several autapomorphies (e.g. structure of mandibles, arcuate carinae on the mesoventrite). It is placed in the tribe Stenaesthetini based on its 5-5-4 tarsal formula and unmargined abdomen. Formal taxonomic treatment of this taxon is beyond the scope of this study, and so we do not name it formally here.

Euaesthetinae: Eua?LTAS (Figs 6B; 8C; 9F; 10J; 17G, H, J)

Larval diagnosis. Nuchal carina present, linear; stemmata fully developed, not or slightly protruding laterally (Fig. 6B); nasale with medial tooth, paramedial teeth markedly longer than others (Fig. 9F); ventral surface of head capsule with posterior tentorial pits located at about midlength of head, without anteriorly divergent ridges (Fig. 8C); mesal edges of mandibles smooth; apical antennomere less than half length of antennal sensorium, length to width ratio 1.2; antennal sensorium (Fig. 6B, arrow) elongate and narrow, parallel-sided along much of its length, about 1.5× as long as width of penultimate antennomere; mala small but clearly recognizable, as long as wide, with 3 subequal setae; labial palpiger absent; ligula half as wide as basal labial palpomere, slightly more than half length of basal labial palpomere, rounded at apex; tibia abruptly styliform in apical half; urogomphi bottle-shaped with distal part abruptly narrowing at about middle (Fig. 10J, arrow).

Larval material examined. Euaesthetinae: Eua?LTAS. AUSTRALIA: 2 larvae (HW = 0.96 mm), Tasmania, Lower Gordon River, 42°43.0′S, 145°45.0′E – 42°43.0′S, 145°50.0′E, moss, 16.ii.1978 (*Howard, Hill*).

Remarks. Our phylogenetic analysis (Fig. 2) indicates that these larvae may belong to a species of *Austroesthetus* or *Chilioesthetus*. The structure of the larval labium in Eua?LTAS, however, differs from those of larval labia occurring in both genera (cf. Fig. 8C, arrow, with Figs 8A, arrow, and 16A).

Acknowledgements

The authors thank Margaret Thayer and Al Newton (Field Museum) for the generous loan of their specimens and for providing DJC with guidance and unlimited access to their time, literature collection and countless other resources, without which this study would have been impossible. Hank Krishman generously took the habitus photos. Betty Strack provided training and invaluable support to DJC in the SEM lab at FMNH. Other colleagues and friends contributed in various ways to this project and their input is greatly appreciated: Alexey Solodovnikov, Kevin Pitz, Jim Boone,

Sarah O'Brien, Rich Leschen and John Nunn. Previous versions of the manuscript were improved greatly by comments from Margaret Thayer, Al Newton, Alexey Solodovnikov, Matt Renner, Kevin Pitz, Rolf Beutel, and two anonymous reviewers. We are particularly grateful to Rolf Beutel for clarifying some morphological structures, especially those associated with the endoskeleton. Support for this project came from NSF PEET grant no. 0118749 to Margaret Thayer and Al Newton. This research was conceived at the 19th International Meeting on Biology and Systematics of Staphylinidae, and travel assistance to DJC was provided by a Travel Award from the School of Biological Sciences, University of Illinois, at Chicago.

References

Agnarsson, I. (2004) Morphological phylogeny of cobweb spiders and their relatives (Araneae, Araneoidea, Theridiidae). *Zoological Journal of the Linnean Society*, **141**, 447–626.

Ashe, J.S. (2000) Mouthpart structure of *Stylogymnusa subantarctica* Hammond, 1975 (Coleoptera: Staphylinidae: Aleocharinae) with a reanalysis of the phylogenetic position of the genus. *Zoological Journal of the Linnean Society*, **130**, 471–498.

Ashe, J.S. (2005) Phylogeny of the tachyporine group subfamilies and 'basal' lineages of the Aleocharinae (Coleoptera: Staphylinidae) based on larval and adult characteristics. *Systematic Entomology*, **30**, 3–37.

Ashe, J.S. & Watrous, L.E. (1984) Larval chaetotaxy of Aleocharinae (Staphylinidae) based on a description of *Atheta coriaria* Kraatz. *Coleopterists Bulletin*, **38**, 165–179.

Ballard, J.W.O, Thayer, M.K., Newton, A.F. & Grismer, E.R. (1998) Data sets, partitions, and characters: philosophies and procedures for analysing multiple data sets. *Systematic Biology*, **47**, 367–396.

Bernhauer, M. (1939) Neue Staphyliniden (Coleoptera) aus Neu-Seeland. *Annals and Magazine of Natural History*, **4**, 193–216.

Bernhauer, M. & Schubert, K. (1911) Staphylinidae II. *Coleopterorum Catalogus*, **5**, 87–190.

Besuchet, C. (1970) Les *Clidicus* de Ceylan (Col. Scydmaenidae). *Mitteilungen der Schweizerischen Entomologischen Gesellschaft*, **43**, 249–257.

Beutel, R.G. & Molenda, R. (1997) Comparative morphology of selected larvae of Staphylinoidea (Coleoptera, Polyphaga) with phylogenetic implications. *Zoologischer Anzeiger*, **236**, 37–67.

Betz, O. (1996) Function and evolution of the adhesion–capture apparatus of *Stenus* species (Coleoptera, Staphylinidae). *Zoomorphology*, **116**, 15–34.

Betz, O. (1998) Comparative studies on the predatory behavior of *Stenus* spp. (Coleoptera: Staphylinidae): the significance of its specialized labial apparatus. *Journal of Zoology*, **244**, 527–544.

Betz, O. (1999) A behavioral inventory of adult *Stenus* species (Coleoptera: Staphylinidae). *Journal of Natural History*, **33**, 1691–1712.

Betz, O. (2002) Performance and adaptive value of tarsal morphology in rove beetles of the genus *Stenus* (Coleoptera, Staphylinidae). *Journal of Experimental Biology*, **205**, 1097–1113.

Betz, O. (2003) Structure of the tarsi in some *Stenus* species (Coleoptera, Staphylinidae): external morphology, ultrastructure, and tarsal secretion. *Journal of Morphology*, **255**, 24–43.

Betz, O. & Kölsch, G. (2004) The role of adhesion in prey capture and predator defense in arthropods. *Arthropod Structure and Development*, **3**, 3–30.

Blackwelder, R.E. (1936) Morphology of the coleopterous family Staphylinidae. *Smithsonian Miscellaneous Collections*, **94**, 1–102.

Bremer, K. (1988) The limits of amino acid sequence data in angiosperm phylogenetic reconstruction. *Evolution*, **42**, 795–803.

Broun, T. (1909) Descriptions of new genera and species of New-Zealand Coleoptera (continued). *Annals and Magazine of Natural History*, **3**, 223–233.

Cameron, M. (1944) Description of a new genus of Euaesthetinae (Col., Staph.). *Annals and Magazine of Natural History*, **11**, 68–70.

Caterino, M.S., Hunt, T. & Vogler, A.P. (2005) On the constitution and phylogeny of Staphyliniformia (Insecta: Coleoptera). *Molecular Phylogenetics and Evolution*, **34**, 655–672.

Coiffait, H. & Decou, V. (1970) Recherches sur les Coléoptères endogés des Carpates Roumaines. III Staphylinidae – Euaesthetinae: *Euaesthetotyphlus almajensis*, n.gen., n.sp. *Annales de Spéléologie*, **25**, 378–382.

Crowson, R.A. (1950) The classification of the families of British Coleoptera. *Entomologists Monthly Magazine*, **86**, 149–171, 274–288, 327–344.

Crowson, R.A. (1960) The phylogeny of Coleoptera. *Annual Review of Entomology*, **5**, 111–134.

Crowson, R.A. (1967) *The Natural Classification of the Families of Coleoptera*. E.W. Classey Ltd., Hampton.

Cunningham, C.W. (1997) Can three incongruence tests predict when data should be combined? *Molecular Biology and Evolution*, **14**, 733–740.

Dettner, K. (1993) Defensive secretions and exocrine glands in free-living staphylinid beetles – their bearing on phylogeny (Coleoptera: Staphylinidae). *Biochemical Systematics and Ecology*, **21**, 143–162.

Eriksson, T. (2001) *Autodecay, version 5.0*. Software program distributed by the author. Bergius Foundation, Royal Swedish Academy of Sciences, Stockholm, Sweden.

Farris, J.S., Källersjö, M., Kluge, A. & Bult, C. (1994) Testing significance of incongruence. *Cladistics*, **10**, 315–319.

Fauvel, A. (1873) Faune Gallo-Rhénane ou description des insectes qui habitent la France, la Belgique, la Hollande, les provinces Rhénanes et le Valais, avec tableaux synoptiques et planches gravées. (Suite). *Bulletin de la Société Linnéenne de Normandie*, **6**, 8–136.

Felsenstein, J. (1985) Confidence limits on phylogenies: an approach using the bootstrap. *Evolution*, **39**, 783–791.

Gravenhorst, J. (1806) *Monographia Coleopterorum Micropterorum*. H. Dieterich, Gottingae, Göttingen.

Hansen, M. (1997) Phylogeny and classification of the staphyliniform beetle families (Coleoptera). *Biologiske Skrifter, Det Kongelige Danske Videnskabernes Selskab*, **48**, 1–339.

Hatch, M.H. (1957) The beetles of the Pacific Northwest. Part II. Staphyliniformia. *University of Washington Publications in Biology*, **16**, ix–384.

Herman, L.H. (1970) Phylogeny and reclassification of the genera of the rove-beetle subfamily Oxytelinae of the world (Coleoptera, Staphylinidae). *Bulletin of the American Museum of Natural History*, **142**, 347–454.

Herman, L.H. (1975) Revision and phylogeny of the monogeneric subfamily Pseudopsinae for the world (Staphylinidae, Coleoptera). *Bulletin of the American Museum of Natural History*, **155**, 243–317.

Herman, L.H. (2001) Catalog of the Staphylinidae (Insecta: Coleoptera). 1758 to the end of the second millennium. IV. Staphylinine Group (Part 1). Euaesthetinae, Leptotyphlinae,

Megalopsidiinae, Oxyporinae, Pseudopsinae, Solieriinae, Steninae. *Bulletin of the American Museum of Natural History*, **265**, 1807–2440.

Jenkins, M.F. (1957) The morphology and anatomy of the pygidial glands of *Dianous coerulescens* Gyllenhal (Coleoptera: Staphylinidae). *Proceedings of the Royal Entomological Society of London (A)*, **32**, 159–168.

Jenkins, M.F. (1960) On the method by which *Stenus* and *Dianous* (Coleoptera: Staphylinidae) return to the banks of a pool. *Transactions of the Royal Entomological Society of London*, **112**, 1–14.

Kasule, F.K. (1966) The subfamilies of the larvae of Staphylinidae (Coleoptera) with keys to the larvae of the British genera of Steninae and Proteininae. *Transactions of the Royal Entomological Society of London*, **118**, 261–283.

Kistner, D.H. (1960) Mission zoologique de l'I.R.S.A.C. en Afrique orientale (P. Basilewsky et N. Leleup, 1957). XXXIX. Coleoptera Staphylinidae Euaesthetinae. *Annales du Musée Royal du Congo Belge, Tervuren (Série 8°, Sciences Zoologiques)*, **88**, 31–39.

Kistner, D.H. (1961) A new genus and species of Euaesthetinae from Chile (Coleoptera: Staphylinidae). *Pan-Pacific Entomologist*, **37**, 216–220.

Koch, C. (1934) Wissenschaftliche Ergebnisse der entomologischen Expeditionen seiner Durchlaucht des Fuersten Alessandro C. della Torre e Tasso nach Aegypten und auf die Halbinsel Sinai. IV. Staphylinidae (Coleoptera). *Bulletin de la Société Royale Entomologique d'Egypte*, **18**, 33–91.

Kölsch, G. & Betz, O. (1998) Ultrastructure and function of the adhesion–capture apparatus of *Stenus* species (Coleoptera, Staphylinidae). *Zoomorphology*, **118**, 263–272.

Lawrence, J.F. (1991) Order Coleoptera (general discussion, family key, various family treatments). *Immature Insects. Volume 2*. (ed. by F. W. Stehr), pp. 144–658. Kendall/Hunt Publishing Co., Dubuque, IA.

Lawrence, J.F. & Newton, A.F. Jr. (1982) Evolution and classification of beetles. *Annual Review of Ecology and Systematics*, **13**, 261–290.

Lawrence, J.F. & Newton, A.F. (1995) Families and subfamilies of Coleoptera (with selected genera, notes, references, and data on family-group names). *Biology, Phylogeny, and Classification of Coleoptera: Papers Celebrating the 80th Birthday of Roy A. Crowson* (ed. by J. Pakaluk and S. A. Ślipiński), pp.779–1006. Muzeum i Instytut Zoologii PAN, Warszawa.

Lefebvrea, F., Vincenta, B., Azarb, D. & Nel, A. (2005) The oldest beetle of the Euaesthetinae (Staphylinidae) from early Cretaceous Lebanese amber. *Cretaceous Research*, **26**, 207–211.

Leschen, R.A.B. & Newton, A.F. Jr. (2003) Larval description, adult feeding behavior, and phylogenetic placement of Megalopinus (Coleoptera: Staphylinidae). *Coleopterists Bulletin*, **57**, 469–493.

Maddison, W.P. & Maddison, D.R. (2007) *Mesquite: A Modular System for Evolutionary Analysis. Version 2.01* [WWW document]. URL http://mesquiteproject.org

Motschulsky, V. (1857) Voyages. Lettres de M. de Motschulsky à M. Ménétriés. No. 3. New York le 15 Juillet 1654 (sic). *Études Entomologiques*, **5**, 3–20.

Naomi, S.-I. (1985) The phylogeny and higher classification of the Staphylinidae and their allied groups (Coleoptera: Staphylinoidea). *Esakia*, **23**, 1–27.

Naomi, S.-I. (1987a) Comparative morphology of the Staphylinidae and the allied groups (Coleoptera, Staphylinoidea), I. Introduction, head sutures, eyes and ocelli. *Kontyû*, **55**, 450–458.

Naomi, S.-I. (1987b) Comparative morphology of the Staphylinidae and the allied groups (Coleoptera, Staphylinoidea), II. Cranial structure and tentorium. *Kontyû*, **55**, 666–675.

Naomi, S.-I. (1988a) Comparative morphology of the Staphylinidae and the allied groups (Coleoptera, Staphylinoidea), III. Antennae, labrum and mandibles. *Kontyû*, **56**, 67–77.

Naomi, S.-I. (1988b) Comparative morphology of the Staphylinidae and the allied groups (Coleoptera, Staphylinoidea), IV. Maxillae and labium. *Kontyû*, **56**, 241–250.

Naomi, S.-I. (1988c) Comparative morphology of the Staphylinidae and the allied groups (Coleoptera, Staphylinoidea), V. Cervix and prothorax. *Kontyû*, **56**, 506–513.

Naomi, S.-I. (1988d) Comparative morphology of the Staphylinidae and the allied groups (Coleoptera, Staphylinoidea), VI. Mesothorax and metathorax. *Kontyû*, **56**, 727–738.

Naomi, S.-I. (1989a) Comparative morphology of the Staphylinidae and the allied groups (Coleoptera, Staphylinoidea), VII. Metendosternite and wings. *Japanese Journal of Entomology*, **57**, 82–90.

Naomi, S.-I. (1989b) Comparative morphology of the Staphylinidae and the allied groups (Coleoptera, Staphylinoidea), VIII. Thoracic legs. *Japanese Journal of Entomology*, **57**, 269–277.

Naomi, S.-I. (1989c) Comparative morphology of the Staphylinidae and the allied groups (Coleoptera, Staphylinoidea), IX. General structure, lateral plates, stigmata and 1st to 7th segments of abdomen. *Japanese Journal of Entomology*, **57**, 517–526.

Naomi, S.-I. (1989d) Comparative morphology of the Staphylinidae and the allied groups (Coleoptera, Staphylinoidea), X. Eighth to 10th segments of abdomen. *Japanese Journal of Entomology*, **57**, 720–733.

Naomi, S.-I. (1990) Comparative morphology of the Staphylinidae and the allied groups (Coleoptera, Staphylinoidea), XI. Abdominal glands, male genitalia and female spermatheca. *Japanese Journal of Entomology*, **58**, 16–23.

Naomi, S.-I. (2006a) Taxonomic study of the genus *Stenus* Latreille, 1797 (Coleoptera, Staphylinidae, Steninae) of Japan: species group of *S. indubius* Sharp. *Japanese Journal of Systematic Entomology*, **12**, 39–120.

Naomi, S.-I. (2006b) Taxonomic revision of the genus *Stenus* Latreille, 1797 (Coleoptera, Staphylinidae, Steninae) of Japan: species group of *S. (Hypostenus) rufescens* Sharp. *Natural History Research, Special Issue*, **9**, 1–81.

Newton, A.F. (1982a) Redefinition, revised phylogeny and relationships of Pseudopsinae (Coleoptera: Staphylinidae). *American Museum Novitates*, **2743**, 1–13.

Newton, A.F. (1982b) A new genus and species of Oxytelinae from Australia, with a description of its larva, systematic position, and phylogenetic relationships (Coleoptera, Staphylinidae). *American Museum Novitates*, **2744**, 1–24.

Newton, A.F. (1985) South Temperate Staphylinoidea (Coleoptera): their potential for biogeographic analysis of austral disjunctions. *Taxonomy, Phylogeny and Zoogeography of Beetles and Ants* (ed. by G. E. Ball), pp. 180–220. Dr. W. Junk Publishers, Dordrecht.

Newton, A.F. (1990a) Larvae of Staphyliniformia (Coleoptera): where do we stand? *Coleopterists Bulletin*, **44**, 205–210.

Newton, A.F. Jr. (1990b) Insecta: Coleoptera, Staphylinidae adults and larvae. *Soil Biology Guide* (ed. by D. L. Dindal), pp. 1137–1174. J. Wiley and Sons, New York.

Newton, A.F. & Thayer, M. K. (1988) A critique on Naomi's phylogeny and higher classification of Staphylinidae and allies (Coleoptera). *Entomologica Generalis*, **14**, 63–72.

Newton, A. F. & Thayer, M. K. (1992) Current classification and family-group names in Staphyliniformia (Coleoptera). *Fieldiana: Zoology*, **67**, 1–92.

Newton, A.F. & Thayer, M.K. (1995) Protopselaphinae new subfamily for *Protopselaphus* new genus from Malaysia, with a

phylogenetic analysis and review of the Omaliine group of Staphylinidae including Pselaphidae (Coleoptera). *Biology, Phylogeny, and Classification of Coleoptera: Papers Celebrating the 80th Birthday of Roy A. Crowson* (ed. by J. Pakaluk and S. A. Ślipiński), pp. 219–320. Muzeum i Instytut Zoologii PAN, Warszawa.

Nixon, K.C. (2002) *WinClada (BETA), version 1.00.08*. Published by the author, Ithaca, NY.

Nixon, K.C. & Davis, J.I. (1991) Polymorphic taxa, missing values and cladistic analysis. *Cladistics*, **7**, 233–241.

Oke, C. (1933) Australian Staphylinidae. *Proceedings of the Royal Society of Victoria*, **45**, 101–136.

Orousset, J, (1987) Un nouveau genre d'Euaesthetinae africain: *Macroturellus pulcher* n. gen., n. sp. *Bulletin de la Société Entomologique de France*, **91**, 219–227.

Orousset, J. (1988) Insectes, Coléoptères, Staphylinidae, Euaesthetinae. *Faune de Madagascar*, **71**. Muséum national d'Histoire naturelle, Paris.

Orousset, J. (1990) Révision des Euaesthetinae néotropicaux du genre *Stenaesthetus* Sharp (Coleoptera, Staphylinidae). *Mémoires du Muséum National d'Histoire Naturelle (A: Zoologie)*, **147**, 9–55.

Page, R.D.M. (2001a) *NDE: NEXUS Data Editor, 0.5.0*. University of Glasgow, U.K. [WWW document]. URL http://taxonomy.zoology.gla.ac.uk/rod/rod.html.

Page, R.D.M. (2001b) *TreeView, 1.6.6*. University of Glasgow, U.K. [WWW document]. URL http://taxonomy.zoology.gla.ac.uk/rod/rod.html.

Prendini, L. (2001) Species or supraspecific taxa as terminals in cladistic analysis? Groundplans versus exemplars revisited. *Systematic Biology*, **50**, 290–300.

Puthz, V. (1970) Revision of the Australian species of the genus *Stenus* Latreille (Coleoptera; Staphylinidae). *Memoirs of the National Museum of Victoria*, **31**, 55–80.

Puthz, V. (1971) Revision of the *Stenus*-species of New Guinea. Part I (Coleoptera: Staphylinidae). *Pacific Insects*, **13**, 447–469.

Puthz, V. (1972) Revision of the *Stenus*-species of New Guinea. Part II. (Coleoptera: Staphylinidae). *Pacific Insects*, **14**, 475–527.

Puthz, V. (1973) On some neotropical Euaesthetinae. *Studies on the Neotropical Fauna*, **8**, 51–73.

Puthz, V. (1978) Revision of the Australian Euaesthetinae (Coleoptera: Staphylinidae). *Memoirs of the National Museum of Victoria*, **39**, 117–133.

Puthz, V. (1980) Über einige Euaesthetinen-Gattungen und -Arten (Coleoptera, Staphylinidae). *Entomologische Blätter für Biologie und Systematik der Käfer*, **76**, 15–32.

Puthz, V. (1995) Sexualität mit dem Lasso? - oder: Revalidierung der Gattung *Gerhardia* Kistner, 1960 (Coleoptera, Staphylinidae). 74. Beitrag zur Kenntnis der Euaesthetinen. *Entomologische Blätter für Biologie und Systematik der Käfer*, **91**, 119–125.

Puthz, V. (2000) The genus *Dianous* Leach in China (Coleoptera, Staphylinidae). 261. Contribution to the knowledge of Steninae. *Revue Suisse de Zoologie*, **107**, 419–559.

Puthz, V. (2006a) Description of new species and notes on some Neotropical Euaesthetinae (Coleoptera: Staphylinidae) (93th Contribution to the knowledge of Euaesthetinae). *Dugesiana*, **13**, 25–38.

Puthz, V. (2006b) The ventralis group of *Edaphus*: Neotropical Euaesthetines with special abdominal characters (Coleoptera, Staphylinidae) (95th Contribution to the knowledge of Euaesthetinae). *Dugesiana*, **13**, 77–90.

Puthz, V. (2006c) New southern African species and distribution records of the genus *Octavius* Fauvel (Coleoptera: Staphylinidae). *Annals of the Transvaal Museum*, **43**, 1–28.

Puthz, V. (2006d) On the genus *Stenus* Latreille, mostly from southern Africa, with a revision of the *Stenus mendicus* species-group (Coleoptera: Staphylinidae). *Annals of the Transvaal Museum*, **43**, 29–67.

Puthz, V. (2008) *Kiwiaesthetus*, a new genus of Euaesthetinae from New Zealand (Coleoptera, Staphylinidae). 100th contribution to the knowledge of Euaesthetinae. *Zeitschrift der Arbeitsgemeinschaft Österreichischer Entomologen*, **60**, 59–69.

Sáiz, F. (1968) *Chilioesthetus*, nuevo genero de la subfamilia Euaesthetinae (Col. Staphylinidae). *Revista Chilena de Entomología*, **6**, 73–79.

Sáiz, F. (1970) *Nothoesthetus* nouveau genre humicole et endoge des Euaesthetinae chiliens (Col. Staphylinidae). *Bulletin de la Société d'Histoire Naturelle de Toulouse*, **105**, 295–310.

Scheerpeltz, O. (1974) Coleoptera: Staphylinidae. *South African Animal Life* (ed. by B. P. B. Hanström, P. Brinck and G. Rudebeck), Vol. 15, pp. 43–394. Swedish Natural Science Research Council, Stockholm.

Sharp, D.S. (1874) The Staphylinidae of Japan. *Transactions of the Entomological Society of London*, **1874**, 1–101.

Snodgrass, R.E. (1935) *Principles of Insect Morphology*. McGraw-Hill Book Company, Inc, London.

Solodovnikov, A.Yu. (2007) Larval chaetotaxy of Coleoptera (Insecta) as a tool for evolutionary research and systematics: less confusion, more clarity. *Journal of Zoological Systematics and Evolutionary Research*, **45**, 120–127.

Solodovnikov, A.Yu. & Newton, A.F. (2005) Phylogenetic placement of Arrowinini trib. n. within the subfamily Staphylininae (Coleoptera: Staphylinidae), with revision of the relict South African genus *Arrowinus* and description of its larva. *Systematic Entomology*, **30**, 398–441.

Steel, W.O (1970) The larvae of the genera of the Omaliinae (Coleoptera: Staphylinidae) with particular reference to the British fauna. *Transactions of the Royal Entomological Society of London*, **122**, 1–47.

Swofford, D.L. (2002) *PAUP*. Phylogenetic Analysis Using Parsimony (*and Other Methods) Version 4.0b10 for 32-bit Microsoft Windows*. Sinauer Associates, Sunderland, MA.

Thayer, M.K. (2005) 11.7. Staphylinidae. *Handbook of Zoology, Coleoptera, Vol. 1: Evolution and Systematics, Archostemata, Adephaga, Myxophaga, Staphyliniformia, Scarabaeiformia, Elateriformia* (ed. by R. G. Beutel and R. A. B. Leschen), pp. 296–344. De Gruyter, Berlin.

Thomson, C. G. (1859) *Skandinaviens Coleoptera, Synoptiskt Bearbetade. I*. Berlingska Boktryckeriet, Lund.

Weinreich, E. (1968) Über den Klebfangapparat der Imagines von *Stenus* Latr. (Coleopt., Staphylinidae) mit einem Beitrag zur Kenntnis der Jugendstadien dieser Gattung. *Zeitschrift für Morphologie der Tiere*, **62**, 162–210.

Welch, R.C. (1966) A description of the pupa and third instar larva of *Stenus canaliculatus* Gyll. (Col., Staphylinidae). *Entomologist's Monthly Magazine*, **101**, 246–250.

Wilkinson, M. (1995) A comparison of two methods of character construction. *Cladistics*, **11**, 297–308.

Accepted 27 October 2008

Table 1. Morphological data matrix for characters 1–167.

Subfamily (-nae) or Tribe (-ini)		0000000000 0000000000 0000000000 0000000000 0000000000 0000000000 0000000000 0000000000 0000000000 0000000000 0000000000 00000
		0000000001 1111111112 2222222223 3333333334 4444444445 5555555556 6666666667 7777777778 88888
		1234567890 1234567890 1234567890 1234567890 1234567890 1234567890 1234567890 1234567890 12345
PIESTINAE	*Siagonium*	1000001002 0000000000 0000000000 0010000100 0100010000 0000000000 0001000000 0000000000 00000
OXYPORINAE	*Oxyporus*	0000000001 0000000000 0000000000 0000000100 0000000020 0000000000 0000010001 0000000000 31000
MEGALOPSIDIINAE	*Megalopinus*	0000000011 0001100000 0000000001 1010000100 0000010000 0000100011 0001010100 0000a00001 01100
PSEUDOPSINAE	*Pseudopsis*	0000001002 0110000000 0001000100 0010000000 0000000000 0010000000 000a101110 0000000000 20000
PSEUDOPSINAE	*Nanobius*	0000001002 0110000000 0001000110 0010000000 0000000000 0010000101 0011101110 0000100000 00000
STENINAE	*Stenus*	1100011111 0001110000 0001111111 1001011111 0000120111 0110101111 0011010111 0000000211 10000
STENINAE	*Dianous*	1100011111 0001110000 0001111111 1001011110 0000020110 0010101111 0011010111 0000000211 10000
STENINAE	SteNovAUS1W	1100011111 0111100000 0001111111 1001011111 0010120111 1110101111 0011010111 0001000211 10000
STENINAE	SteNovAUS2F	1000011111 0111100000 0001111111 1001011111 0010120111 1110101111 0011010111 0001000211 10000
ALZADAESTHETINI	*Alzadaesthetus chilensis*	1001101000 1111200100 1001110111 1101011110 1000010110 0011100001 0111010111 0000001111 00111
ALZADAESTHETINI	*Alzadaesthetus furcillatus*	1001101000 1111200100 1001110111 1101011110 1000010110 0010100001 0011010111 0010001111 00111
AUSTROESTHETINI	*Austroesthetus*	1001101000 0111201100 1001110111 1001011110 1100010110 0011100001 0111010111 0000001111 00111
AUSTROESTHETINI	*Chiltoesthetus*	1001101000 0111201100 1001110111 1001011110 ?1000010110 0011100001 0111010111 0000000111 00111
AUSTROESTHETINI	*Mesoaesthetus*	1001101000 1111200100 1001110111 1001011110 1100010110 0011100001 0111010111 0000001111 00111
AUSTROESTHETINI	*Nothoesthetus*	1001101000 0111200100 1001110111 1001011110 0100011110 0011100001 0111010111 1000001111 00111
AUSTROESTHETINI	*Tasmanosthetus*	1001101000 1111200100 1001110111 1001011110 0100011110 0011100001 0111010111 1000001211 00111
AUSTROESTHETINI	*Kiwiaesthetus*	1001101000 1111200100 1001110111 1001011110 0100010110 0011100001 0111010111 0000001111 00111
EUAESTHETINI	*Edaphus*	1000001000 0111200100 1001111111 1001011110 0000011110 0010110001 0011010111 0100111101 00101
EUAESTHETINI	*Euaesthetus*	1001001000 1111200100 1001111111 1001011110 0000011110 0010100001 0011010111 0100111101 00101
EUAESTHETINI	*Octavius*SA	1001101100 0111200101 1111110111 1001011110 0100011110 0010100001 0011010111 0000111101 00121
EUAESTHETINI	*Octavius*PAN	1001101102 0111200101 1111110111 1001011110 0100011110 0010100001 0011010111 0000111101 00121
EUAESTHETINI	*Protopristus*NZ	1001201100 0111200100 1011110111 1000111??0 0101011110 0010100101 0111010111 0000001211 00121
EUAESTHETINI	*Protopristus*TAS	1001201100 0111200100 1011110111 1000111??0 0101011110 0010100101 0111010111 0000001211 00121
FENDERIINI	*Fenderia*	1011101110 1111210100 1001110111 1000011110 0100011110 0011100001 0001010111 0000111101 00121
FENDERIINI	*Stictocranius*	1001101000 1111200100 1001110111 1001011110 0000010110 0011100001 0111010111 0000001111 00101
STENAESTHETINI	*Agnosthaetus*	1011101001 1111200100 1001110111 1101011110 1100010110 0011100001 0111010111 0000001111 00111
STENAESTHETINI	*Gerhardia*	1011101002 1111200110 0001110111 1001011110 1000010110 0011100001 1211010110 0000001111 00111
STENAESTHETINI	*Stenaesthetus*	1011101002 1111200110 0001110111 1001011110 1000010110 0011100001 1211010110 0000001111 00111
STENAESTHETINI	EuaAUS	1011101002 1111200100 1001110111 1001011110 1100010110 0011100001 0111010110 0000001111 00111
?	EuaL?TAS	?????????? ?????????? ?????????? ?????????? ?????????? ?????????? ?????????? ?????????? ?????

Table 1. Continued.

Subfamily (-nae) or Tribe (-ini)		0000000000 0000111111 1111111111 1111111111 1111111111 1111111111 1111111111 1111111111 11 8888999999 9999000000 0000111111 1111222222 2222333333 3333444444 4444555555 5555666666 66 6789012345 6789012345 6789012345 6789012345 6789012345 6789012345 6789012345 6789012345 67
PIESTINAE	*Siagonium*	0000000000 0000000000 0100000010 0100000000 0000001000 0000010000 0000000000 0000000000 00
OXYPORINAE	*Oxyporus*	0000000000 0000100000 0000000000 0000000000 0000000000 0000010000 0000010000 0000000020 01
MEGALOPSIDIINAE	*Megalopinus*	0001010000 0100100001 0000000110 0000000001 0000000101 0101010001 0000010000 0000000000 01
PSEUDOPSINAE	*Pseudopsis*	0000010000 0000000011 0000000000 0010101011 0a1010100a 0211101110 0001100010 0020001020 11
PSEUDOPSINAE	*Nanobius*	0000010000 0000100001 0001000110 0000002011 0110101000 0211101110 0001100010 0020001020 00
STENINAE	*Stenus*	1111010000 1010211101 12a1000111 01bcbc3101 0010101a01 1220111100 1111110010 1120111111 10
STENINAE	*Dianous*	1111010000 1010211101 1211000111 0110103101 0010101001 1220101110 1111110010 1120111111 10
STENINAE	SteNovAUS1W	1111110000 1010211101 1211100111 0110103101 0010101001 ?????????? ?????????? ?????????? ??
STENINAE	SteNovAUS2F	1111110000 1010211101 1211100111 0110103101 0010101001 ?????????? ?????????? ?????????? ??
ALZADAESTHETINI	*Alzadaesthetus chilensis*	1111010000 1010301011 1211101111 0110103001 0110001011 ?????????? ?????????? ?????????? ??
ALZADAESTHETINI	*Alzadaesthetus furcillatus*	1111010111 1010301011 1211101111 0122223001 0110001011 0211101111 0011101111 0111201110 11
AUSTROESTHETINI	*Austroesthetus*	1111010111 1010301011 1211001111 0110223001 1111001011 0221101111 0011101111 0111201110 11
AUSTROESTHETINI	*Chilioesthetus*	1111010111 1010301011 1211001111 0110223001 1111001011 0221101111 0011101111 0111201110 11
AUSTROESTHETINI	*Mesoaesthetus*	1111010111 1010301011 1211001111 0121213001 0100001011 ?????????? ?????????? ?????????? ??
AUSTROESTHETINI	*Nothoesthetus*	1111010111 1010301011 1211001111 0110103001 0110001011 0211101111 0011101111 0111201110 11
AUSTROESTHETINI	*Tasmanosthetus*	1111010111 1010301011 1211001111 0122223001 0110001011 ?????????? ?????????? ?????????? ??
AUSTROESTHETINI	*Kiwiaesthetus*	1111010111 1010301011 1211001111 0121213001 0110001011 ?????????? ?????????? ?????????? ??
EUAESTHETINI	*Edaphus*	1111010111 1010301111 1201001111 0110102001 0110101111 0210111101 0010111111 0111101110 11
EUAESTHETINI	*Euaesthetus*	1111010111 1010301011 1201001111 0110103001 0110101111 0221101111 0010111111 0111201110 11
EUAESTHETINI	*Octavius*SA	1101011111 1010301011 0211011111 1100001001 1110100011 0221101111 0010101111 0111201110 11
EUAESTHETINI	*Octavius*PAN	1101010111 1010301011 0211011111 1100001001 1110100011 0221101111 0010101111 0111201110 11
EUAESTHETINI	*Protopristus*NZ	1101011111 1010301011 0211011111 0100001001 0110110011 0211101111 0010101111 0111201110 11
EUAESTHETINI	*Protopristus*TAS	1101011111 1010301011 0211011111 0100001001 0110000011 ?????????? ?????????? ?????????? ??
FENDERIINI	*Fenderia*	1101011000 1010411011 0001001110 1122223001 0110001011 0211101111 0011101111 0111201110 11
FENDERIINI	*Stictocranius*	1111010000 1010301111 1211001111 0110223001 0110001111 ?????????? ?????????? ?????????? ??
STENAESTHETINI	*Agnosthaetus*	1111010001 1011301011 1211001111 0122223001 0110001011 0211101111 0011101111 0111201110 11
STENAESTHETINI	*Gerhardia*	1111010001 1011301011 1211001111 1121223001 1110001011 ?????????? ?????????? ?????????? ??
STENAESTHETINI	*Stenaesthetus*	1111010001 1011301011 1211001111 1121223001 1110001011 ?????????? ?????????? ?????????? ??
STENAESTHETINI	EuaAUS	1101010001 1011301011 1211001111 0122223001 1110001011 ?????????? ?????????? ?????????? ??
?	EuaL?TAS	?????????? ?????????? ?????????? ?????????? ?????????? 0221101111 0011101111 0111201110 11

Characters 1–167 described in text; a, polymorphism 0,1; b, polymorphism 1,2; c, polymorphism 0,2.

Appendix 1. List of characters and discussion

Adults

Head capsule.

1. *Epistomal (frontoclypeal) suture* (Leschen & Newton, 2003: character 3): (0) present (e.g. Naomi, 1987a: fig 1B); (1) absent.
2. *Location of antennal insertion* (Leschen & Newton, 2003: character 2: antennal insertion in dorsal view [0] at front of head under shelf concealing insertion, or [1] on frons, more or less exposed): (0) near frontal margin of head, anterior to eye (Fig. 11A–D); (1) on frons between eyes (Fig. 11E).

Character 2 in Leschen & Newton's analysis contributed to the conflict in the placement of Steninae with respect to the euaesthetines they analysed. However, they assigned *Euaesthetus* and *Octavius* state (1) for that character, whereas following their state delimitations, we would assign those taxa state (0) and the character would have been uninformative for their analysis. We redefine their character 2 to emphasize only the location of the antennal insertion with respect to the frontal margin of the head capsule.

3. *Dorsolateral carina of head*: (0) absent (Fig. 11C–E); (1) present at least anteriorly (Fig. 11A, arrow, B, bottom arrow).
4. *Postoccipital nuchal region*: (0) absent; (1) present (see Orousset, 1987: fig. 4).

This character describes a subtriangular region posterior to a transverse internal carina in the nuchal region and is intersected medially by the dorsomedian nuchal phragma (character 11).

5. *Gular sutures* (Leschen & Newton, 2003: character 7, states: 0 = completely separate, 1 = largely fused to one another): (0) separate; (1) united along most of length; (2) united anteriorly only.

Although *Euaesthetus* has state (0) the sutures are only very narrowly separated. Because of interspecific variability in degree of separation we did not define different states within 'completely separate' (e.g. narrowly versus broadly separate). In many cases, SEM analysis is required to interpret this character correctly.

6. *Apodemes arising from interantennal pits*: (0) absent; (1) present.

Two interantennal pits located between the antennae in stenines (Fig. 11E, arrow) each have an apodeme extending internally that is not continuous with any part of the tentorium in cleared specimens. *Oxyporus* has two pairs of apodemes extending internally from the epistomal ridge; the more mesial of these pairs is situated in approximately the same location as the interantennal apodemes in Steninae, but because these apodemes arise from the epistomal suture and do not appear to be associated with an external pit we consider these non-homologous to the interantennal pits in stenines.

Note for characters 7–10: see Naomi (1987b: fig 2A) for a complete schematic illustration of the tentorium. We agree with Newton & Thayer (1995), and follow Snodgrass (1935) for terminology of tentorial structures. Thus we use 'tentorial bridge' for Naomi's 'corpotentorium', and 'corporotentorium' for Naomi's 'laminatentorium'.

7. *Dorsal tentorial arms*: (0) not fused with cranium; (1) fused with cranium.

In cleared specimens of taxa assigned state (0) the dorsal tentorial arms do not contact the roof of the cranium; however, the apices of these arms may have fibrillae or other connective tissue connecting them to the cranial wall. In taxa assigned state (1) the dorsal tentorial arms are fully contacting the roof of the cranium and in most cases external dorsal tentorial pits are also present where the arms fuse with the cranial wall.

8. *Tentorial bridge* ('corpotentorium' or 'corpotentorial arm' of Naomi, 1987b): (0) present; (1) absent.
9. *Tentorial loop*: (0) absent; (1) present.

In referring to the 'corpotentorial [sic] arm [= tentorial bridge in this study]' in Steninae, Naomi (1987b: 675) states that it 'arises from the base of the dorsal tentorial arm'. We describe this distinctive structure in Steninae (also present in Megalopsidiinae, and *Fenderia*) as the 'tentorial loop' and distinguish it from the 'tentorial bridge' (character 8) because of the topographical difference between these two structures: the tentorial bridge arises from the base of the posterior tentorial walls – at the back of the head – in contrast to the tentorial loop which arises from near the base of the posterior tentorial arms at the front of the head, proximad of the junction of the anterior and dorsal tentorial arms. In contrast to the tentorial bridge, which arches dorsally in a transverse plane, the tentorial loop arches posteriorly and lies in a frontal plane. Although there seems to be some variation in the location of the tentorial bridge along the posterior tentorial walls in other members of the Staphylinine group (A. Newton, personal communication), apparently both the tentorial bridge and our tentorial loop are present in Megalopsidiinae (fused posterodorsally). This latter observation combined with the topographical difference provides justification for our assessment that these two structures are non-homologous.

10. *Corporotentorium* (Newton & Thayer, 1995: character 24; laminatentorium of Naomi, 1987b): (0) split; (1) absent; (2) fused.

The corporotentorium arises from between the posterior tentorial arms.

11. *Dorsomedian nuchal phragma*: (0) absent; (1) present.

This character refers to an internal median sclerotized plate near the posterior margin of the head capsule, which divides the nuchal region usually along its entire length. It is generally easily visible as a darker line externally and is probably a muscle attachment site. The development (length and depth) of this structure varies considerably among genera, but seems more or less constant within genera.

12. *Ommatidia structure*: (0) facets hexagonal and flat; eye surface smooth; (1) facets round and strongly convex; eye surface botryoidal (Fig. 11F).

Protopristus and *Tasmanosthetus* include eyeless species, which we regard as independent secondary losses.

13. *Long interfacetal ocular setae* (Thayer, 2005: 311): (0) absent; (1) present (Fig. 11F).

This character refers specifically to the long setae dispersed among individual ommatidia. *Nanobius* (coded as state 1) has distinctly clubbed setae. Steninae and all outgroups except Pseudopsinae have minute projections (setae?), barely projecting above the eye surface.

Antennae.

14. *Antennal club* (Leschen & Newton, 2003: character 1, reworded): (0) absent; (1) present (Fig. 11G).
15. *Number of antennomeres in antennal club*: (0) zero, club absent; (1) three; (2) two.
16. *Condyle of first antennomere in dorsal view*: (0) concealed (Fig. 11A, C–E); (1) exposed (Fig. 11B, top arrow).
17. *Apex of antennomere 10* (Newton, 1985: 205, reworded): (0) not concave to receive antennomere 11; (1) concave to receive antennomere 11.
18. *Differentiated setae on antennomere 10*: (0) absent; (1) present (Fig. 11G, H, arrows).

These setae are modified in the same way in different taxa assigned state (1), and are probably used for identical or related functions. They have characteristically acuminate apices, are distinctly thicker, and generally more parallel-sided than typical antennal setae. They are closely situated in a group positioned on the anterior side of the antennomere, and are sometimes also present on antennomere 9.

19. *Length of antennomeres 9–11*: (0) each less than 3× maximum width (Fig. 11G); (1) each greater than 3× maximum width.
20. *Antennomeres 10 and 11*: (0) separated by antennal stem; (1) partly fused, antennal stem absent (Fig. 11G).

Mouthparts.

21. *Anterior margin of labrum*: (0) smooth (Fig. 11A); (1) denticulate or serrate (Fig. 11C, I, M).

Although the exact form of serration differs among some taxa (e.g. some with truncate, others with pointed serrations), observations of intermediate states both within and among taxa (and specimens) suggest that these different states are homologous.

22. *Surface of epipharynx*: (0) flat, without furrows; (1) distinctly longitudinally furrowed (Fig. 11I, J, left arrow).
23. *Epipharyngeal marginal setae*: (0) absent; (1) present (Fig. 11J, right arrow).
24. *Frontoclypeal–labral junction*: (0) not visible in dorsal view, labral attachment concealed beneath frontoclypeal margin; (1) visible in dorsal view, labrum attached to frontoclypeal margin (Fig. 11A, C, E).
25. *Mandibular structure*: (0) robust; (1) slender, falciform (Fig. 11L).

Hansen (1997: 128) regards the slender falciform mandibles, each with a single mesal preapical tooth, to be a synapomorphy uniting Steninae + Euaesthetinae.

26. *Mandibles when closed*: (0) tips fully exposed; (1) tips concealed beneath labrum (Fig. 11K).

This character refers specifically to the position of the mandibles when at rest and is independent of mandible length but related to the distance between the cranio-mandibular articulations. Taxa assigned state (0) cannot fully close their mandibles, which remain crossed at rest. Taxa assigned state (1) can completely close their mandibles such that the apices are concealed in dorsal view; at least one mandible usually has a groove on the outer side to receive the other mandible when closed and the mandibles thus become interlocked.

27. *Inner edge of mandibles posterior to preapical tooth*: (0) smooth; (1) serrated (Fig. 11L).
28. *Preapical mandibular teeth* (Newton & Thayer, 1995: character 31, reworded): (0) asymmetrical in number; (1) symmetrical in number (Fig. 11L).

This character refers to the general symmetry in number of homologous teeth on both the left and right mandibles in all taxa assigned state (1) and is independent of the total number of teeth present on each mandible. As such, this character refers to the observation of mandibular symmetry itself as a hypothesis of homology in that it is inferred that there is a genetic and/or developmental basis controlling the formation of the same number of teeth in similar locations on each mandible. All euaesthetines and stenines examined have a single preapical tooth on each mandible. Note: some *Edaphus* species appear to have secondarily lost the preapical tooth on the inner edge of the mandibles, and in others it is reduced. But in all observed cases the teeth are reduced or absent on both mandibles, thus still satisfying the key observation of symmetry.

29. *Maximum number of preapical teeth on inner margin of mandibles* (Newton & Thayer, 1995: character 32): (0) two; (1) one.

In taxa assigned state (1) there is only a single tooth on each mandible; in taxa assigned state (0) there can be more than one tooth. See note under previous character.

30. *Mandibular prostheca* (Leschen & Newton, 2003: character 4, reworded): (0) present; (1) absent.
31. *Mandibular molar lobe* (Leschen & Newton, 2003: character 5): (0) present; (1) absent.
32. *Spine on lateral edge of galea*: (0) absent (Fig. 12B); (1) present (Fig. 11M, left arrow).
33. *Apical unarticulated spine of lacinia* (Newton & Thayer, 1995: character 38, reworded): (0) absent; (1) present.
34. *Cluster of digitiform sensilla on outer side of maxillary palpomere 3*: (0) absent; (1) present (Fig. 11N, arrow).

In *Austroesthetus*, *Chilioesthetus* and SteNovAUS these sensilla are nearer to the apex than to the middle of palpomere 3.

35. *Pair of papillate sensilla at apex of maxillary palpomere 3*: (0) absent; (1) present (Fig. 11O, arrow).

In *Protopristus* these sensilla are similar to those described and figured for *Euaesthetotyphlus almajensis* by Coiffait & Decou (1970: 378).

36. *Setation of maxillary palpomere 3*: (0) glabrous except for few scattered macrosetae; (1) very densely setose and without macrosetae (Fig. 11N).

Within the ingroup, state (1) appears to be correlated with the distinctly fusiform shape of the palpomere, which is also very elongate and much longer than palpomere 2.

37. *Maxillary palpomere 4* (Leschen & Newton, 2003: character 6, reworded): (0) well developed, fully sclerotized; (1) minute, hyaline (Fig. 11N, O).

It is worth pointing out here that the genus *Coiffaitia* Kistner & Shower (not analysed here) has the 4th palpomere setose and much larger than in other euaesthetines (see Orousset, 1988: 59, fig. 71). Orousset's (1988) descriptions and figures of *Coiffaitia* and *Neocoiffaitia* cast doubt on the placement of those genera in Euaesthetinae, or even in the stenine group.

Note for characters 38–41: these characters refer to labial structures that pose considerable problems for primary homology assessment. The terms 'glossae', 'paraglossae', 'ligula' and 'labium' are not used consistently among staphylinid workers, and even Snodgrass (1935: 146) notes that, 'Unfortunately the current terms given to the parts of the labium cannot be made to fit consistently with the morphology of the organ'. We avoid using the terms 'glossae' and 'paraglossae' for structures apparently corresponding with those structures labelled as such by Snodgrass (1935). R. Beutel (personal communication) points out that all (so far examined) beetles lack muscles primarily associated with the glossae and paraglossae, like most endopterygote insects, and he considers typical glossae and paraglossae to never be present. If this is true, the homology of various labial structures in Euaesthetinae, Steninae and other staphylinids is more difficult to assess. In the absence of detailed musculature and fine structural studies judgments must be made on external similarity and positional criteria alone. Using these criteria it is necessary to divide the various observable structures into multiple characters, as we have done for characters 38, 40 and 41. Combining these structures into a single multistate character (and into one column of the data matrix) assumes that these very different structures positioned on different parts of the labium are all homologous, which we feel is an assumption that is not justified by standard criteria for assessing primary homology.

38. *Medial lobes of labium*: (0) present (see Herman, 1975: fig. 8); (1) absent.

This character applies specifically to the long paired finger-like membranous processes at the middle of the anterior labial margin of *Pseudopsis* and *Nanobius*. Unlike the structures described by character 41, these structures are contiguous basally.

39. *Two pairs of setae on anterior margin of labium*: (0) absent; (1) present (Figs 11I, M, right arrow; 12A, right arrow, B).

Betz (1996: 19) refers to the four (two pairs of) conspicuous sense-spines at the anterior labial margin of *Stenus* as 'glossae', and describes these as sense-spines. These setae do not correspond to the morphological glossae (sensu Snodgrass, 1935). They have various arrangements among taxa, including: pairs closely and evenly spaced in a line along the anterior margin of the labium; pairs variably widely separated by a medial emargination of the anterior labial margin (e.g. Fig. 11M); pairs forming a cluster situated on a medial prominence at the front of the labium (as in SteNovAUS, Fig. 12A, right arrow; see also character 43).

40. *Adhesive cushions of labium*: (0) absent; (1) present (Figs 11L, right arrow; 12A, left arrow).
41. *Digitiform processes of labium*: (0) absent; (1) present (Fig. 12B, top arrow; D, left arrow).

These processes were not visible in available material of *Chilioesthetus*, so this taxon is assigned a question mark for this character. In *Agnosthaetus* (Fig. 11M) these processes are sclerotized. In all other terminals assigned state (1) these processes are membranous.

42. *Mesal notch in apex of labium*: (0) absent; (1) present (Fig. 11I, M).
43. *Mesal mound at apex of labium*: (0) absent; (1) present (Fig. 12A, right arrow).
44. *Median overlapping teeth of ligula (anteromedial labial margin)*: (0) absent; (1) present (Fig. 12C, arrow); the more derived ligula of *Protopristus* (Puthz, 1980; Newton, 1985: 205) with two median overlapping teeth is evidently a unique autapomorphy of this genus.
45. *Lateral rows or combs of setae on hypopharynx*: (0) present (Fig. 12D, right arrow); (1) absent.
46. *Insertion location and proximity of labial palps*: (0) more or less contiguous and nearer to base than to apex of labium; (1) widely separated at sides of labium (Figs 11 I, M; 12B, C); (2) almost contiguous and nearer to medial apex than to sides of labium (Fig. 12A).
47. *Labial palpomere 1*: (0) elongate, half as long as, to slightly longer than, palpomere 2 (Figs 11M; 12A, B); (1) much shorter than half length of palpomere 2 (the latter sessile to subsessile) (Figs 11I; 12C).
48. *Labial palpomere 2*: (0) unmodified, similar in shape to palpomere 1; (1) strongly expanded, subglobular or subfusiform (Figs 11I, M; 12A-C).
49. *Labial palpomere 3*: (0) well developed, fully sclerotized; (1) acicular, hyaline (Figs 11I, M; 12A, C); (2) moderately to strongly expanded apically, subtriangular (after Thayer, 2005: 330, autapomorphic for Oxyporinae).

50. *Prementum*: (0) normal (e.g. Figs 11I, M; 12B, C); (1) modified, elongated into eversible rod-like structure (Fig. 11L).
51. *Mentum*: (0) entire surface in same plane (Figs 11I; 12B); (1) transversely divided near middle by a ridge, with anterior half deflected vertically (Fig. 11L, left arrow).
52. *Lateral palpomere rests on mentum divided by medial longitudinal carina*: (0) absent; (1) present (Fig. 11K, arrow).
53. *Submentum and gula*: (0) separated by suture located significantly anterior to posterior tentorial pits; (1) fused.

This character may refer to the same structure as Newton & Thayer's (1995) character 20 (gular sutures with or without external transverse connection at level of tentorial pits).

54. *Submental transverse carina*: (0) absent; (1) present (Fig. 12B, bottom arrow).

Thorax and legs.

55. *Cervical sclerites* (Leschen & Newton, 2003: character 8): (0) large; (1) small and very slender.
56. *Anterior margin of prosternum*: (0) smooth; (1) deeply notched (Fig. 12E, top arrow; an autapomorphy of *Edaphus*).
57. *Pronotal marginal carina*: (0) not meeting pronotosternal suture, reaching anterolateral prothoracic margin (Fig. 12F, arrow); (1) meeting pronotosternal suture anterolaterally (Fig. 12G, left arrow), not reaching anterior prothoracic margin.

In stenines the prosternum is fused to the pronotum and the pronotosternal suture is consequently absent. However, the location of the suture is assumed to be evident as a faint indistinct line extending arcuately from the procoxal cavities to the anterolateral prothoracic margin (Fig. 12G, right arrow). Therefore, in state (1) the pronotal marginal carina (or line), when present, is interrupted from reaching the anterolateral prothoracic margin (as in state 0) by the more arcuate location of the remnant pronotosternal suture in stenines. (The point in adult development at which this suture is obliterated is unknown. There is no internal phragma visible where this line is situated.)

58. *Ventral hypomeral marginal carina*: (0) present (Fig. 12 E, bottom arrow); (1) absent.
59. *Pronotosternal suture* (Leschen & Newton, 2003: character 9): (0) present and complete (Fig. 12E, middle arrow); (1) absent or very incomplete and evident only posteriorly near coxal cavity (Fig. 12H; see note under character 57).
60. *Protrochantin* (Leschen & Newton, 2003: character 10): (0) exposed; (1) concealed.
61. *Prosternal callosity (usually depigmented)*: (0) absent; (1) present (Fig. 12I, top arrow).
62. *Anteprocoxal carina*: (0) absent (Fig. 12E, H, K); (1) present, transversely arcuate (Fig. 12J, left arrow); (2) present and divided, with each side directed anteroobliquely (Fig. 12I, bottom arrow).
63. *Anteprocoxal lobes*: (0) absent (Fig. 12K); (1) present (Fig. 12J, right arrow).

These lobes are cuticular prosternal projections usually appressed against the coxae. In *Fenderia* (state 0) the anterolateral margins of the procoxal cavities are deflected beneath the hypomeron (Fig. 12K).

64. *Procoxal mesial surface* (Leschen & Newton, 2003: character 11, reworded): (0) without carina-delimited groove; (1) with carina-delimited groove (Fig. 12K, arrow).

State definitions as per Newton (1982a: character 32, reworded). Our polymorphic coding for *Pseudopsis* agrees with Newton (1982a).

65. *Longitudinal carinae or costae on pronotum and elytra* (Thayer, 2005: 329, reworded): (0) absent; (1) present (Thayer, 2005 lists state 1 as an apomorphy for Pseudopsinae).
66. *Mesothoracic spiracles in ventral view* (Thayer, 2005: 329): (0) exposed; (1) concealed by pronotum.
67. *Antemesoventral sclerite or sclerites* (Newton, 1982a: character 33; Thayer, 2005: 330): (0) absent; (1) present (one or two sclerites are positioned ventrally in the membrane between pro- and mesothorax, and are separated from the mesothoracic spiracles).
68. *Scutellum* (sensu Blackwelder, 1936: fig. 4A, C): (0) mostly visible in dorsal view; (1) mostly to entirely concealed by the posterior pronotal edge (Fig. 12L).
69. *Elytral striae* (Leschen & Newton, 2003: character 22, reworded): (0) present; (1) absent.

Note: *Siagonium*, *Oxyporus* and *Megalopinus* (all state 0) have rows of punctures disposed longitudinally in grooves (striae). *Nanobius* also has punctures arranged in longitudinal rows, but these are separated by low longitudinal ridges; we infer that they are not homologous to those rows of punctures in the aforementioned taxa and assign *Nanobius* state 1.

70. *Elytral epipleural keel* (Leschen & Newton, 2003: character 23): (0) present (Fig. 12M, left arrow); (1) absent.

The lateral elytral region is highly variable among euaesthetine genera. SEM analyses reveal that some 'epipleural ridges' present in different taxa are probably not homologous to the epipleural keel of common usage. Naomi (1989a: 86) describes the epipleural ridge as lying on the same level as the upper surface of the elytron, or somewhat below it, but for most taxa we studied the demarcation between disc and epipleura is vague. Within our taxon sample the elytral epipleural region is variably demarcated from the discal region, and the elytron is either completely smooth from suture to edge (Fig. 12O), or there are one (Fig. 12N, arrow) or two (Fig. 12M, arrows) distinct lateral elytral ridges. Leschen & Newton (2003: 491) note that 'for *Agnosthaetus* (coded as present) this structure [epipleural keel] is a small fold that is not a distinct carina that originates at the humeral

callus as it does in *Megalopinus*', but in taxa with only one ridge (as in *Agnosthaetus*; Fig. 12N) we hypothesize that this ridge is actually a thickened marginal ridge, not an epipleural keel, because it occurs anteriorly below the humeral callus. A comparison of *Agnosthaetus* (Fig. 12N) and *Stenaesthetus* (Fig. 12M) suggests that the ridge in *Agnosthaetus* is homologous to the marginal ridge of *Stenaesthetus* (Fig. 12M, middle arrow) based on positional criteria. We therefore code *Agnosthaetus* as absent (state 1) for this character.

71. *Elytral epipleural fold*: (0) absent; (1) present (Fig. 13A, arrow).

This character may be homologous to the marginal ridge, rather than to the epipleural keel (see previous character), or represent an entirely different structure. Newton (1985: 205) notes that the 'epipleural fold' of *Nothoesthetus* and *Tasmanosthetus* (each with only one ridge laterally, e.g. Fig. 13A) is derived 'since other Euaesthetinae and related subfamilies have a very reduced fold'. We treat the lateral fold in these taxa as a separate character because these taxa do not match any others that we examined in the structure of the epipleural region (and have only one ridge), and in both of these the elytra are unusually thickened laterally.

72. *Basal spine of elytral marginal ridge*: (0) absent; (1) present (Fig. 13B, arrow).
73. *Underside of elytra*: (0) smooth; (1) densely tuberculate (Fig. 13C; an autapomorphy of *Alzadaesthetus furcillatus*).
74. *Procoxal rests of mesoventrite*: (0) absent; (1) present (Fig. 13E, top arrow).
75. *Midlongitudinal carina of mesoventrite* (Newton, 1982a: character 34, reworded): (0) absent; (1) present (Fig. 13 F, middle arrow).

Megalopinus is coded as polymorphic for this character.

76. *Oblique carina of mesoventrite*: (0) absent; (1) present Fig. 13F, right arrow).
77. *Mesothoracic pleural suture*: (0) present (Fig. 13E, left arrow); (1) absent, (Fig. 13D, F).

When present this suture is visible externally as an oblique ridge or narrow groove. In the euaesthetines that we examined an internal oblique phragma is usually visible in cleared specimens but the suture is never indicated externally (except *Chilioesthetus*).

78. *Mesothoracic anapleural suture* (Leschen & Newton, 2003: character 13, reworded): (0) present at both anterior and posterior ends; (1) present only posteriorly (Fig. 13D, left arrow, F, bottom left arrow); (2) absent (Fig. 13E).

In all outgroups this suture is clearly present as a suture at least along part of its length. However, within Euaesthetine it is not present as a membranous suture. There is an external carina (mesothoracic anapleural carina, as used in descriptive part), reaching from the mesocoxal cavities anteriorly to about half the length of the mesoventrite, which we interpret as the anapleural suture, although in euaesthetines it does not continue to the anterior margin of the prosternum. In some this carina is continuous with the transverse carina on the side of the mesothorax (character 79; Fig. 13F, left arrows). Based on our interpretation, we would have assigned *Agnosthaetus*, *Euaesthetus* and *Octavius* state (0) in Leschen & Newton's matrix; the absence of the suture then would have been an autapomorphy of Steninae, and hence uninformative for their analysis.

79. *Transverse carina on side of mesothorax*: (0) present (Fig. 13F, top left arrow); (1) absent.
80. *Mesotrochantin* (Leschen & Newton, 2003: character 12): (0) exposed; (1) concealed.
81. *Intermesocoxal process of mesoventrite*: (0) overlapping intermesocoxal process of metaventrite ventrally (Fig. 13 D, middle arrow, F); (1) with apex abutting apex of intermesocoxal process of metaventrite (Fig. 13E, bottom arrow); (2) cariniform, reduced; (3) absent (coxae widely separated by anterior part of metaventrite).

Note for characters 82–85: the 'mesothoracic apodeme' is an ental projection arising from the anterior region of the mesocoxal cavity (e.g. see Orousset, 1988: fig. 299). These processes vary among taxa in their apical structure and points of fusion with regions of the mesothorax, as described in the following four characters.

82. *Mesothoracic apodemes*: (0) projecting anteriorly, free from pleural phragma (e.g. see Orousset, 1988: fig. 299); (1) projecting anterodorsally, partly fused to pleural phragma.
83. *Shape of mesothoracic apodemes*: (0) elbowed; (1) straight (e.g. see Orousset, 1988: fig. 299).
84. *Fusion of mesothoracic apodemes with mesoventrite*: (0) completely free from mesoventrite after basal point of attachment to mesoventrite; (1) partly fused anteriorly to mesoventrite; (2) fused to mesoventrite along entire length.
85. *Apical muscle disc of mesothoracic apodemes*: (0) absent; (1) present (e.g. see Orousset, 1988: fig. 299).
86. *Meso-metaventral suture*: (0) present dorsal to mesocoxae (or between mesocoxae, as in *Oxyporus*); (1) absent dorsal to mesocoxae.

Among species of *Pseudopsis* there is a varying degree of fusion of the meso- and metaventrites and consequently variation in the development of this suture. In *P. arrowi* it has almost totally fused; in *Megalopinus* the suture is very faint, but evident.

87. *Mesal posterior lobes of metaventrite*: (0) absent; (1) present.

These 'lobes' consist of medial extensions of the metaventrite. In *Stenus*, *Dianous* and *Stictocranius* these intercoxal lobes form a pair of large explanate plates; they are variously reduced in other ingroup terminals.

88. *Stem of metendosternite* (Leschen & Newton, 2003: character 14): (0) present; (1) absent.
89. *Tibial apical spurs* (Thayer, 2005: 329): (0) well developed (Fig. 13G, right arrow); (1) reduced (Fig. 13H, right arrows).

Tibial apical spurs are mostly indistinguishable in slide material of Megalopsidiinae, Steninae and Euaesthetinae, but SEM reveals that they are present but much reduced.

90. *Protibia*: (0) normal, rounded; (1) distinctly expanded and concave ventrally (Fig. 13I, arrow).
91. *Protibial external spines* (Thayer, 2005: 324): (0) present (Fig. 13G, top arrow); (1) absent.
92. *Modified setae on protarsomeres 1 and 2 of males*: (0) absent; (1) present (Fig. 13K, arrow). In *Fenderia* these setae are also present on the mesotarsi.

Note for characters 93–95 (tarsomere formula, redefined as three characters): numerous euaesthetine genera have the tarsomere formula 4-4-4; others have 5-5-4. Tarsomere formula is a composite character, which implies non-independence among legs and a common mechanism for reduction in tarsomere number on each leg (e.g. fusion of the same two tarsomeres, or loss of the same tarsomere among legs). Ashe (2000: 478) used the distribution of sensory pores and setae as 'landmarks' to identify individual labial palpomeres that had become fused in the aleocharine genus *Stylogymnusa* Hammond. Using a similar approach we identified serially homologous lateroventral spines present on each tarsomere of the euaesthetines we examined. By using these spines as 'landmarks' we conclude that 5-5-4 and 4-4-4 tarsomere formulae have occurred universally by fusion of the basal two tarsomeres, not by tarsomere loss. This fusion is associated with a duplication of the number of spines on the basal tarsomere (e.g. Fig. 13J: arrows indicate duplicated spines on the basal tarsomere). Moreover, a constriction in the basal tarsomere is sometimes evident, further supporting our interpretation (i.e. this part is not a 'pseudoarticle', sensu Herman (1970: 349), as spines occur proximal to the constriction). Thus, in Euaesthetinae a uniform mechanism might indeed explain tarsomere reduction. Nonetheless, we assume a priori that fusion of the basal two tarsomeres of one pair of legs is independent of the same transformation occurring on other legs, and divide the character tarsomere formula (Leschen & Newton, 2003: character 24) into three reductive characters. We were also motivated to treat this character reductively because of spurious transformations in this character when treating tarsomere formula as a composite character in Leschen & Newton's (2003) study, in which the tarsal formula 5-5-4 is optimized as a derived state of *Agnosthaetus* (see their Table 2), whereas this transformation obscures at least one instance of a reversal (from 4 to 5 tarsomeres on the pro- and mesolegs) and is uninformative with respect to the number of metatarsomeres (4). Because euaesthetines with tarsal formula 4-4-4 or 5-5-4 have all five tarsomeres in each tarsus we contrast the character states for the basal two tarsomeres as 'fused' versus 'articulated'.

93. *Protarsomeres 1 and 2*: (0) articulated (Fig. 13L, arrow); (1) fused (Fig. 13H, left arrow).
94. *Mesotarsomeres 1 and 2*: (0) articulated; (1) fused.
95. *Metatarsomeres 1 and 2*: (0) articulated; (1) fused.
96. *Ventral process projecting over empodium*: (0) absent (Fig. 13N, right arrow); (1) present (Fig. 13M, arrow).
97. *Tarsal claws*: (0) smooth (Fig. 13G, M); (1) serrate basoventrally (Fig. 13N, top arrow; an autapomorphy of Megalopsidiinae).
98. *Empodial setae*: (0) present (Fig. 13G, left arrow, N, middle arrow); (1) absent (Fig. 13M).
99. *Mesocoxal mesial surface*: (0) without carina-delimited groove; (1) with carina-delimited groove (Fig. 13D, right arrow).

Note for characters 100–103 (metacoxae): the structure of the pleurocoxal articulation and the lateral part of the metacoxae are characteristic in both Steninae and Euaesthetinae, and each of these subfamilies differs significantly from outgroup taxa. These characters require more detailed analyses than was possible here.

100. *Metacoxae*: (0) strongly expanded laterally and posteriorly; with posterolateral edge reaching and contiguous with dorsal edge of metepimeron (Fig. 13O, arrow); (1) strongly expanded laterally but not posteriorly; with posterior edge contiguous with posterior margin of metepimeron (Fig. 14A, arrow); (2) not strongly expanded laterally; subtriangular to subconical, length subequal to greatest width; posterior face more or less rounded, not forming distinct edge (Fig. 14B, arrow); (3) moderately expanded posterolaterally; subtriangular to subconical with posterolateral edge forming sharpened flange laterally (Fig. 14C, E, upper left arrow), reaching and contiguous with posterior margin of metepimeron (Fig. 14C, right arrow); (4) expanded posteriorly, coxae much wider than long; subtriangular to distinctly conical, with posterolateral edge not forming sharpened flange laterally (Fig. 14D, arrow).
101. *Posterior face of metacoxae* (Leschen & Newton, 2003: character 16): (0) oblique (Figs 13O; 14A, C); (1) vertical (Fig. 14B, arrow, D, arrow).

This character refers to the 'femoral plate of hind coxa' (Crowson, 1967: 32), and for some taxa it is difficult to determine if the posterior face is oblique or vertical, and indeed whether some taxa have a 'plate' or not as the metacoxae are variably reduced within Euaesthetinae. We have coded taxa as state (0) only when the posterior or posterolateral faces of the metacoxae are perpendicular to the horizontal plane, and the femoral plate is therefore completely absent. We therefore assign *Agnosthaetus* and *Octavius* state (0), which would have rendered this character an autapomorphy of Steninae and therefore uninformative for Leschen & Newton's analysis.

102. *Mesal articulations of metacoxae*: (0) approximate, close to mesal edges of metacoxae; (1) widely separated and on ventral side of metacoxae.
103. *Proximity of mesal edges of metacoxae*: (0) contiguous or only very narrowly separated anteriorly (Fig. 14E, right arrow); (1) widely separated anteriorly, usually by a distance of more than half the length of the metacoxae.

104. *Line of macrosetae on posterolateral edges of metacoxae*: (0) absent; (1) present (Fig. 14C, left arrow, E, bottom arrow).

Abdomen (excluding genital segment and genitalia)

105. *Wing-folding microtrichia patches on tergite IV* (Leschen & Newton, 2003: character 18, reworded): (0) present (Fig. 14F, middle arrow); (1) absent.
106. *Attachment of abdominal intersegmental membrane to preceding segment* (Leschen & Newton, 2003: character 20): (0) apical (Fig. 14G, I); (1) preapical (Fig. 14H, J).
107. *Shape of intersegmental membrane sclerites*: (0) quadrangular; (1) irregular; (2) hexagonal.

Solodovnikov & Newton (2005: character 55) define states similar to ours. The intersegmental membrane sclerites in *Fenderia* form a distinct pattern with a few rows of large rectangular sclerites anteriorly and much smaller sclerites posterior to these. One difference between states (0) and (2) is that the sclerites usually form a brick-wall pattern in state (2), whereas the sclerites are usually placed in semi-regular rows in state (0).

108. *Anterior transverse basal carina of abdominal tergites IV–VII* (Solodovnikov & Newton, 2005: characters 46–50, reworded): (0) present (Fig. 14F, top arrow); (1) absent.

This character is the same as the 'sinuous transverse fold or suture' of Blackwelder (1936: 45, fig. 9A 'ts'), and the 'transverse basal suture' of Naomi (1989c); see Solodovnikov & Newton (2005) for discussion. Some euaesthetines have a variably developed basal carina on tergite III but no carina on other segments. In *Octavius*SA (coded as state 1) the carina is well developed on tergite III, weakly developed on tergite IV and more or less effaced on tergites V–VII. *Stenus* is coded as polymorphic for this character.

109. *Basolateral ridges of abdominal tergites* (Newton, 1982a: character 37): (0) present (Fig. 14F, left arrow); (1) absent.
110. *Deep arcuate carinae at base of abdominal tergites*: (0) absent; (1) present (Fig. 14H, right arrow).
111. *Apicolateral spines of abdominal tergites III–VI*: (0) absent; (1) present (Fig. 14I, arrow).

The abdominal intersegmental membranes of *Octavius* and *Protopristus* are attached apically, but the sides of the tergites are produced into minute spines projecting over the membrane.

112. *Spiracles of abdominal segment I* (Leschen & Newton, 2003: character 17, reworded): (0) placed in membrane beside tergite I; (1) placed in tergite I.
113. *Spiracles of abdominal segment II*: (0) placed in membrane beside tergite II; (1) placed in tergite II.

In *Oxyporus*, the spiracle is more inset into the edge of the tergum but still surrounded by membrane.

114. *Intercoxal carina of sternites II/III* (Leschen & Newton, 2003: character 21): (0) absent; (1) present (Fig. 14 J, right arrow).
115. *Longitudinal carina at sides of sternite III*: (0) absent; (1) present (Fig. 14J, middle arrow).

The development of this character is variable. In *Edaphus*, it extends to the apex of the sternite; in most other examined genera it extends only part way to the apex of the sternite. In *Megalopinus*, the sternites have serially homologous arch-like ridges connecting to the transverse basal carinae that are structurally dissimilar, and therefore probably not homologous to the lateral carinae in euaesthetines and stenines.

116. *Paramedial carinae of sternite III*: (0) absent; (1) present (Fig. 14J, bottom left arrow).

Note for characters 117–122: the abdomen is commonly referred to as 'margined' when the abdominal terga and sterna articulate laterally with parasclerites (either one or two pairs). Leschen & Newton (2003) used 'pairs of abdominal parasclerites per segment III–VI' (their character 19), which combines variation from those segments and is therefore a composite character (appropriate for their taxon sample). According to observed variation within our taxon sample, we parse out the variation into six reductive characters as below. *Stenus* is coded as polymorphic for characters 118–121.

117. *Parasclerites on each side of segment II*: (0) one present (Fig. 14F, top left arrow); (1) absent.

In state (0) only one parasclerite is apparent, although there could be two that have become fused. State (1) conceals four possibilities for an interpretation of 'absence': (a) parasclerite completely absent, secondarily lost; (b) parasclerite fused to tergum II; (c) parasclerite fused to sternum II and/or III; (d) parasclerite II fused to parasclerite(s) of segment III. We could not distinguish among these possibilities, although we know of no reason to suspect intersegmental fusion (alternatives c and d). In *Megalopinus*, parasclerites are visible on segment II, and are at least partly fused to sternum II. In *Siagonium* there is a small transverse sclerite of uncertain homology situated in front of the inner parasclerite of segment II.

118. *Parasclerites on each side of segment III*: (0) two present (Fig. 14F); (1) one present (Fig. 14H, arrow); (2) absent (Fig. 14J).
119. *Tergum and sternum of segment III*: (0) separated by parasclerites (Fig. 14F, H, I); (1) separated by suture (Fig. 14J, top arrow); (2) fused into solid ring.
120. *Parasclerites on each side of segments IV–VI*: (0) two present (Fig. 14F); (1) one present; (2) absent (Fig. 14J).
121. *Tergum and sternum of segments IV–VI*: (0) separated by parasclerites (Fig. 14F); (1) separated by suture; (2) fused into solid ring.
122. *Parasclerites on each side of segment VII*: (0) two present, longitudinally separated; (1) two present, one more anterior to other (Fig. 14G, arrows); (2) one present; (3) absent.

In state (3) the tergum and sternum articulate only at the base of the segment. In *Siagonium*, abdominal segments

III–VI have two parasclerites on each side of the abdomen. The outermost and thinner parasclerite of each segment has a single macroseta, and the innermost and wider parasclerite has a continuation of the anterior transverse basal carina (character 108). On segment VIII *Siagonium* has a single visible parasclerite with both a single macroseta and a continuation of the anterior transverse basal carina. Based on the presence of both of these serially homologous characters on this parasclerite we infer that in *Siagonium* the single visible parasclerite is a result of fusion of inner and outer parasclerites, and we assign state (0) to this taxon. *Oxyporus* has two longitudinally separated parasclerites on each side of segment VII, but in cleared specimens of the two species that we examined a third sclerite is also visible anteriorly to the others. Homology of this sclerite is unknown.

123. *Paired pygidial defence glands opening into rectum*: (0) absent; (1) present.

Stenus and *Dianous* possess two pairs of secretory glands near the apex of the abdomen. This character refers to the much larger, more elongate pair, which opens into the rectum and which in some *Stenus* species secretes the compound stenusin. They are also found in SteNovAUS1W and SteNovAUS2F. The structure of these glands is described by Dettner (1993) and in detail for *Dianous* by Jenkins (1957). They were searched for but not discovered in any euaesthetines examined here, but they could be reduced and undetectable.

Genitalia.

124. *Stridulatory file of tergite IX* (Newton (1982a: figs 1, 2: character 43): (0) absent; (1) present (Newton, 1982a records state 1 as a unique autapomorphy of Pseudopsinae).
125. *Tergite IX in male* (Leschen & Newton, 2003: character 25): (0) divided (Fig. 14K, arrow); (1) entire (Fig. 14L).

We assign state 1 to those taxa in our sample that (a) have tergites IX and X present and separated by a membranous suture (Fig. 14L, arrow), and (b) do not have tergites IX and X separated by a suture (i.e. they are probably fused, Fig. 14M), although we are assuming that other transformations have not taken place (see next character).

126. *Tergite IX in male*: (0) separated from tergite X at least laterally (Fig. 14K, L); (1) fused to tergite X, or absent (Fig. 14M).

There are four alternative possibilities potentially hidden within state (1): (a) tergite IX; or (b) X has been lost altogether; (c) tergite IX has fused with X without first becoming divided dorsally; (d) tergite IX has become completely divided dorsally and then the lateral parts have fused with tergite X. Because complete tergite loss seems unlikely, and because it is impossible to distinguish between alternatives (c) and (d), it is most appropriate to code those taxa without definite tergites IX and X as our state (1).

127. *Apex of sternite IX in male*: (0) truncate or emarginate, not acutely produced (Fig. 14N, arrow); (1) acutely produced into medial spine (Fig. 14O, arrow).

Pseudopsis is coded as polymorphic for this character.

128. *Aedeagus when retracted in abdomen*: (0) with median foramen left lateral; (1) with median foramen dorsal.
129. *Parameres*: (0) normal, unilobed; (1) bilobed.

Newton (1985: 205) notes the unique aedeagal structure with bilobed parameres present in species of *Austroesthetus* and *Chilioesthetus*. At least one species of *Mesoaesthetus* does not have parameres, which we regard as independent secondary loss or fusion to the median lobe.

130. *Tergite IX in female* (Leschen & Newton, 2003: character 26, reworded and Hansen, 1997: character 84, reworded): (0) completely divided by tergite X, or connected at most by thread-like cuticular or membranous strip (Fig. 15A, arrow); (1) not divided by, and forming elongate bridge in front of, tergite X (Fig. 15B).

Leschen & Newton assign their state (1) (i.e. tergite IX entire) to *Agnosthaetus*, but we assign *Agnosthaetus* state (0) (see Fig. 15C). A number of the euaesthetines that we examined (plus *Megalopinus* and *Oxyporus*) have tergite IX in females more or less completely divided dorsally but with what appears to be an extremely thin cuticular or membranous connection (in *Siagonium*, *Stenaesthetus* and EuaAUS the tergite is completely divided).

131. *Longitudinal suture dividing tergite IX in female*: (0) absent; (1) present (similar to Solodovnikov & Newton's (2005) character 60, state 2, and is here an autapomorphy of *Protopristus*NZ).
132. *Female intergonopodal sclerite* (Newton, 1982a: character 52): (0) present (Fig. 15D, left arrow); (1) absent.
133. *First and second gonocoxites* (Leschen & Newton, 2003: character 28, reworded): (0) distinctly separated by suture (Fig. 15D, right arrow); (1) fused ipsilaterally (Thayer, 2005) (Fig. 15E).

Stenus is coded as polymorphic for this character.

134. *Mesal edge of second gonocoxite*: (0) not produced into spine (Fig. 15E, arrow); (1) produced into spine (Fig. 15A, right arrow).

In some species of *Stenus* the lateral edge of the gonocoxite is produced into a spine, and the edge mesal to this spine is lined with small teeth in many species (e.g. Naomi, 2006a, b) and the most mesal of these is frequently larger than the others. However, our character 134 refers to the whole structure of the second gonocoxite (in as much as it terminates apically in a mesal spine), which is very different from that in any *Stenus* species we have seen.

135. *Gonostyle* (Leschen & Newton, 2003: character 27): (0) present (Fig. 15F, arrow); (1) absent.

Newton (1982a) used two characters (55 and 56) to describe the form (elongate versus reduced, knob-like) and

presence/absence of the gonostyle. Although Leschen & Newton (2003) coded *Pseudopsis* as absent, our coding (0/1) agrees with Newton (1982a).

Larvae
Head capsule.

136. *Variation in length and width of setae on cranium and tergites*: (0) not differentiated into long and thick versus short and thin setae (Figs 16A, E; 17G, H); (1) differentiated into long and thick versus short and thin setae (Figs 5A; 17A, E, F).
137. *Labrum* (Leschen & Newton, 2003: character 30, reworded): (0) separated from head capsule by distinct suture; (1) fused to head capsule mesally, separated at least laterally; (2) indistinguishably fused to head capsule to form nasale.

We add a second state (1) to this character to account for the state in *Megalopinus*, which we think can be coded neither as state (0) nor as state (2).

138. *Anterior edge of labrum or nasale* (Leschen & Newton, 2003: character 31, reworded): (0) without spines or teeth (Fig. 9A); (1) with an even number of spines or teeth, without central tooth; (2) with an odd number of spines or teeth, with distinct central tooth (Figs 9B, C; 16A, bottom arrow, E, F).

We split Leschen & Newton's state (1) into two separate states to account for the distinct central tooth of the nasale present in some taxa but absent in others.

139. *Nuchal carina* (Leschen & Newton, 2003: character 40): (0) absent; (1) present (Fig. 5B, bottom arrow).
140. *Coronal suture*: (0) shorter than half length of head capsule; (1) as long as or longer than half length of head capsule (Fig. 5A, bottom arrow).
141. *Location of posterior tentorial pits*: (0) at or near middle of ventral surface of head capsule (Fig. 7C, arrow); (1) at posterior edge of ventral surface of head capsule adjacent to occipital foramen (Fig. 7D, left arrow).
142. *Submentum* (Leschen & Newton, 2003: character 36): (0) free; (1) fused to head capsule.
143. *Maxillary foramen* (Leschen & Newton, 2003: character 39, [0] open, [1] partially closed, [2] completely closed): (0) open mesially and anteriorly; (1) closed completely or closed at least anteriorly.

We combine their states (1) and (2) because of a lack of discrete variability in our taxon sample.

144. *Stem of ventral ecdysial lines* (Leschen & Newton, 2003: character 41, reworded): (0) absent (Figs 7A, D; 10A); (1) present (Fig. 7B, arrow).

Although we employ the same terminology as Leschen & Newton (2003) for this character, it is not clear to us whether these lines are true ecdysial lines or gular sutures; Beutel & Molenda (1997) refer to apparently homologous lines as gular sutures.

145. *Attachment of antennae*: (0) directly to antennifer-like projection of cranium (Fig. 5A, middle arrow); (1) to markedly developed membranous ring (Fig. 16A, bottom arrow).
146. *Antennomere 1* (Solodovnikov & Newton, 2005: character 76, reworded): (0) not constricted or separated by membrane, antennae clearly 3-segmented (Fig. 16A); (1) constricted transversely in basal part, antennae appearing 4-segmented (Fig. 5A, top arrow).

Thayer (2005: 330) noted that besides Steninae, some other Staphylinidae larvae have seemingly 4-segmented antennae (e.g. apparently all Paederinae and Staphylininae). Membranous areas of the basal antennomeres in Steninae are, however, differently shaped and in a different location from those in Paederinae and Staphylininae, thus suggesting that membranous regions are not homologous and possibly reflecting the need for increased antennal flexion in these different subfamilies. Thus we avoid describing this character as antennae 3- or 4-segmented (Solodovnikov & Newton, 2005: 15, character 76) and instead rephrase it to make it specific for Steninae larvae.

147. *Antennomeres 1 and 2*: (0) of regular length (e.g. Fig. 5B–F); (1) markedly elongate (Fig. 5A).
148. *Position of antennal sensorium on antenna* (Leschen & Newton, 2003: character 29, [0] anterior, [1] posterior, [2] dorsal): (0) anterior; (1) not anterior, moved markedly dorsad (Fig. 16C, right arrow, D, arrow).
149. *Shape of antennal sensorium* (Solodovnikov & Newton, 2005: character 78, reworded): (0) more or less bulbous, with convex sides and constricted base (Fig. 16C, right arrow); (1) elongate and narrow, parallel-sided along much of its length (Fig. 16D, arrow).
150. *Mandibles* (Leschen & Newton, 2003: character 32, [0] apically bifid, [1] subapically blade-like, [2] falcate): (0) with one or more preapical teeth (e.g. Fig. 9A, arrow); (1) falcate, without preapical teeth (e.g. Fig. 5 A–F).

We code only two states for this character and thereby hypothesize that the blade-like 'guillotine' tooth of *Megalopinus* (Fig. 9A) is homologous to subapical teeth in other taxa assigned state (0).

151. *Inner edge of mandibles*: (0) smooth (e.g. Fig. 5D–F); (1) serrate (Figs 5A–C; 9A–C, arrows).
152. *Mala* (Leschen & Newton, 2003: character 33, [0] normal in size, [1] reduced in size but fixed, [2] reduced and finger-like, articulated at base): (0) of normal size or slightly enlarged (Figs 10B, arrow; 16G, right arrow); (1) markedly reduced in size or apparently absent (Fig. 10C, arrow).

We redefine this character based on the qualitative assessment that the mala is more or less strongly reduced and almost invisible in Euaesthetinae, whereas in other taxa the mala is large (either longer or shorter than the basal

labial palpomere) and obvious. We do not compare mala length with the first labial palpomere because the length of the latter structure varies among our terminal taxa.

153. *Cardo*: (0) about as wide as base of stipes (Fig. 16G, bottom arrow); (1) reduced in size, much narrower than base of stipes (Fig. 7D–F).
154. *Ventral surface of cardo*: (0) subdivided by sclerotized ridge; (1) not subdivided by ridge.
155. *Shape of stipes (not including mala)*: (0) parallel-sided along its whole length (Fig. 16G); (1) markedly narrowed distally (Fig. 7C–F).
156. *Maxillary palpomere 2*: (0) straight and not more than 4× as long as wide (Fig. 7C–F); (1) markedly bent and at least 5× as long as wide (Fig. 16G, top arrow).
157. *Labial palpomere 2*: (0) rigid and rather wide, maximum 5× as long as its basal width (Fig. 7A); (1) very narrow and elongate, more than 5× as long as its basal width (Fig. 16B, arrow).
158. *Mentum*: (0) with triangular or subquadrate sclerite bearing two pairs of setae; (1) mainly membranous with narrow transverse bisetose sclerite (Fig. 10F, arrow); (2) absent or indistinguishable (Fig. 16B).

Thorax and legs.

159. *Location of longest seta on legs*: (0) trochanters (Fig. 16 I, arrow); (1) tibia (Fig. 16H, arrow).
160. *Tibial form* (Leschen & Newton, 2003: character 46, reworded): (0) normal (fairly stout); (1) entirely styliform (Fig. 16I); (2) abruptly styliform in apical half (Fig. 16H).
161. *Tibia*: (0) without 4–6 apical setae exceeding the length of claw (Fig. 16H); (1) with 4–6 apical setae exceeding the length of claw (Fig. 16I, J, arrow).

Abdomen.

162. *Sub-basal carinae on abdominal tergites II–VIII* (Leschen & Newton, 2003: character 43, [0] present on T2-3 and A1-8, [1] present on T2-3 and A1 only, [2] absent): (0) present; (1) absent.

We redefine this character specifically for the abdominal tergites.

163. *Spiracular openings*: (0) flat or only slightly elevated; (1) located on apices of tube-like projections (Fig. 17 A, B, arrows, G, arrow, I, top arrow).
164. *Maximal number of abdominal parasclerites on each side* (Leschen & Newton, 2003: character 44, reworded): (0) zero; (1) one (Fig. 17K, arrow); (2) two.
165. *Abdominal segment IX*: (0) without latero-ventral projection on each side (Fig. 17J); (1) with latero-ventral projection on each side (Fig. 17I, top right arrow).
166. *Urogomphal segments* (Leschen & Newton, 2003: character 47, reworded): (0) two; (1) one (Figs 10J, K; 17I, bottom arrow, J, arrow, K).
167 *Urogomphi*: (0) about twice as long as tergum IX (Fig. 17I, bottom arrow); (1) about as long as tergum IX (Fig. 17J, arrow).